Woods Hole Oceanographic Institution

COASTAL SEDIMENT TRANSPORT
POPPONESSET BEACH, MA

by

David G. Aubrey and Margaret R. Goud

August 1983

TECHNICAL REPORT

Funding was provided
by the Alcoa Foundation

WOODS HOLE, MASSACHUSETTS 02543

WHOI -83-26

COASTAL SEDIMENT TRANSPORT
POPPONESSET BEACH, MA

by

David G. Aubrey and Margaret R. Goud

WOODS HOLE OCEANOGRAPHIC INSTITUTION
Woods Hole, Massachusetts 02543

August 1983

TECHNICAL REPORT

Funding was provided
by the Alcoa Foundation

This report should be cited as:
Woods Hole Oceanog. Inst. Tech. Rept. WHOI-83-26.

Approved for Distribution: R. P. Von Herzen

Richard P. von Herzen, Chairman
Department of Geology and Geophysics

TABLE OF CONTENTS

TABLE OF CONTENTS

TABLES

FIGURES

SUMMARY

Pathways and rates of near-bed sediment transport near Popponesset Beach, MA., were calculated using several distinct techniques. For the nearshore platform, sand transport in the form of sand waves was determined from vertical aerial photography spanning periods of four decades. In addition, calculations based on theoretical and empirical equations for near-bed sediment transport were made using field measurements of wind waves and tidal currents. Net sediment transport to the southwest inferred from these two techniques differed by about a factor of five. The higher net transport rate predicted in the aerial photographic method is a result of lack of wave measurements during storm conditions. Storm waves increase the net transport through a local increase in bed shear stress. Net transport to the southwest across the platform is between 700 and 3300 m^3/yr.

Littoral sand transport along Popponesset Beach was calculated from one month of directional wave measurements, extrapolated to a yearly value using long-term meteorological observations. Littoral transport from these calculations is 10,000 m^3/yr to the northeast, opposite the sense of alongshore transport in the shallow nearshore.

Patterns of shoreline change are discussed from a historical perspective, and using the transport calculations discussed above. Several management alternatives for coping with predicted shoreline change are presented for consideration by the Town of Mashpee.

COASTAL SEDIMENT TRANSPORT

POPPONESSET BEACH, MA

by

D.G. Aubrey and M.R. Goud

INTRODUCTION

The Problem

Waves, currents and winds have caused substantial changes in the beaches of Mashpee, MA in recent years. Most notable was the loss of 1 km of the barrier beach sheltering the entrance to Popponesset Bay (figures 1 and 2), a small, shallow harbor on the southern side of Cape Cod, of considerable recreational value to the area. In a recent study, Aubrey and Gaines (1982a) analyzed historical charts and aerial photographs to assess the modes and rates of beach changes at Popponesset. The present study combines those results with aerial photographic evidence of bedform migration and field observations of waves, currents, and offshore bedforms. These are used to define pathways and estimate rates of nearshore sediment transport so that predictions of the response of beaches to natural forces can be made.

The practical value of understanding the dynamics of the beach and nearshore zones lies in use of the information to make a rational coastal management plan. Local waves and currents, and the sediment's response to them, control the effectiveness of a coastal structure at protecting the shoreline, the life expectancy of a dredged channel, and the most practical response to storm damage. The purpose of this study is to provide the basis upon which sound management decisions can be made for the Mashpee coastal region.

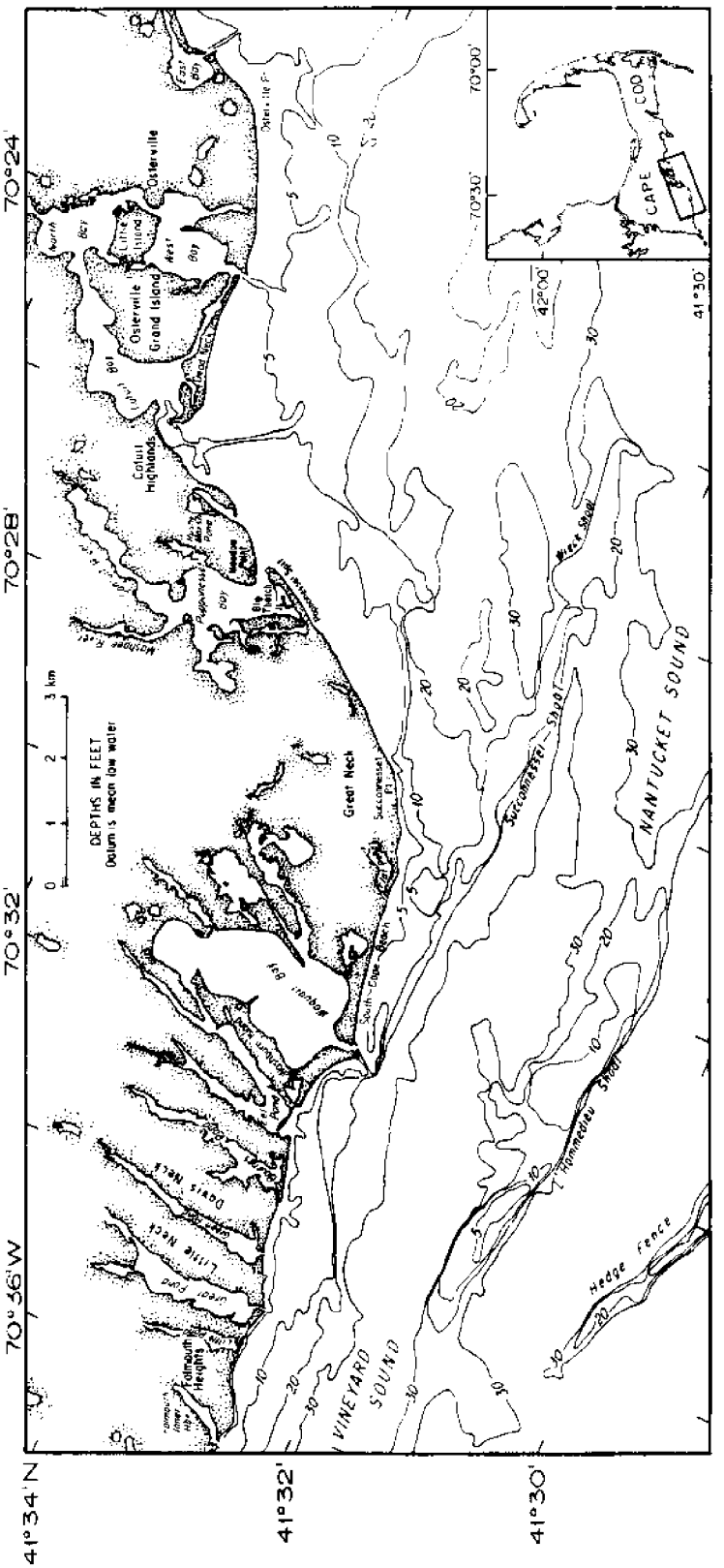

Figure 1. The Popponesset barrier beach setting. Cape Cod, Massachusetts.

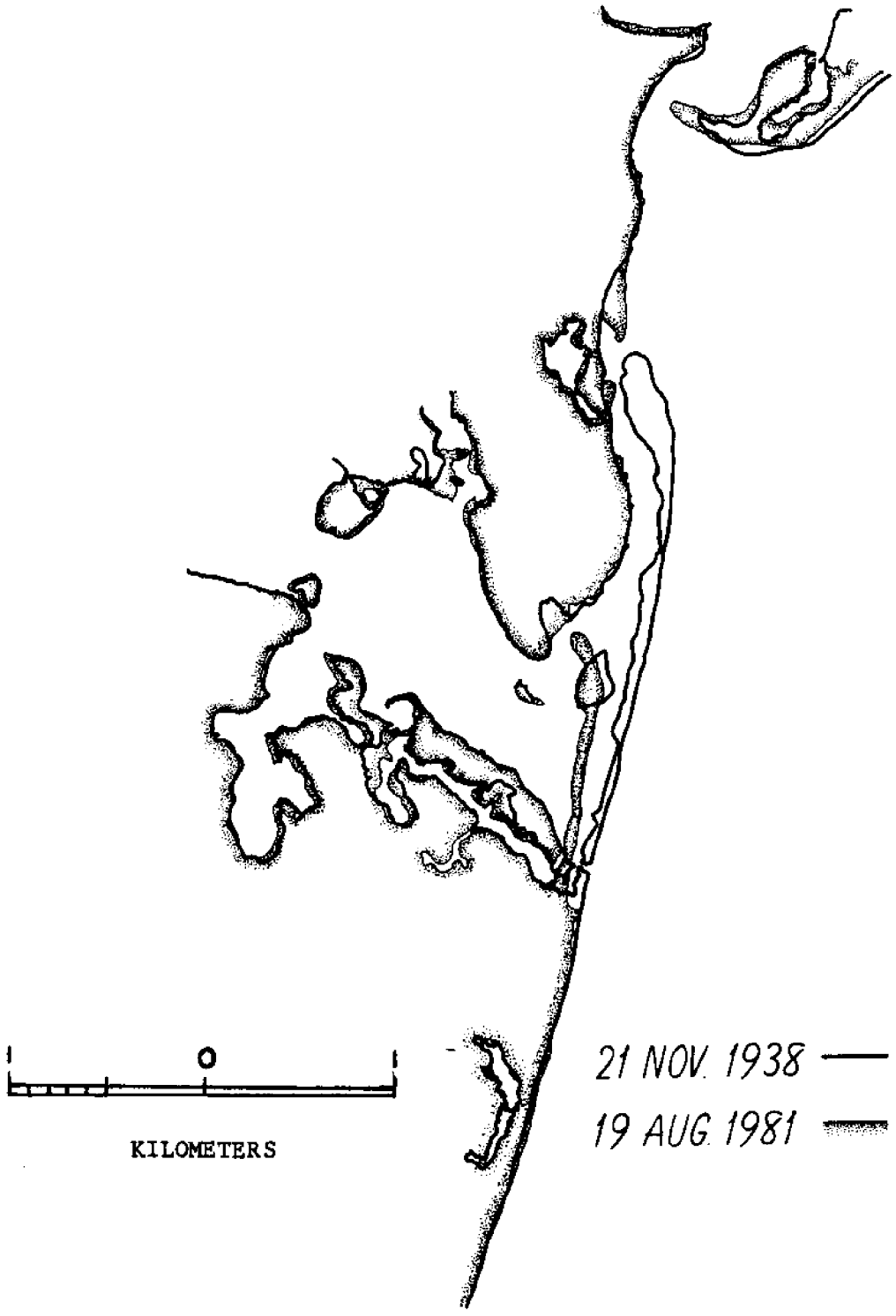

Figure 2. Net shoreline changes at Popponesset Spit, 1938-1981, based on outlines of vertical aerial photographs.

Several complementary analyses were made on the sand transport question. Aerial photographs showed sand waves on the shallow platform off Popponesset Beach, whose migration rates on time scales of 1 year and 10 years provided estimates of net volumetric sand transport rates. Wave and current measurements used with empirical bottom shear stress and bedload formulas, gave gross sediment transport estimates for comparison with the sand wave migration results. Grain size distributions, both onshore and offshore, were analyzed for systematic patterns. All coastal engineering structures were examined, and an assessment made of each one's effect on the nearby shoreline. These varied analyses were combined to make a model of the pathways and rates of nearshore sediment transport and the effect of the transport on the beaches.

Finally, elements of a coastal management plan were formulated on the basis of the present study. Because of the physical limits of the study area, these management elements emphasize the beaches and nearshore regions, with less concentration on Popponesset Bay.

DESCRIPTION OF AREA AND PREVIOUS WORK

The study area (figure 1) extends for 12 km along the shoreline from Waquoit Inlet to West Bay. Its offshore extent is limited by Succonnesset Shoal to the southeast, and includes a shallow platform 2-3 km wide, extending from Succonnesset Point to West Bay; the shoal is separated from the platform by a channel up to 11 m deep.

Like all of Cape Cod, the Popponesset area is glacial in origin. Features within the study area originated during two distinct episodes within the Cape's Pleistocene glacial history (Oldale, 1975). Low sea cliffs (<15 m) composed of poorly consolidated glacial sediment extend from Succonnesset Point to the southern limit of Popponesset Spit, and from Meadow Point to Cotuit Highlands.

The origins of the two sets of cliffs are different. The more northerly cliffs were formed as glacial outwash and are part of the Mashpee Pitted Plain Deposit. The more prominent southern cliffs, older and coarser grained, formed as ice contact deposits, perhaps in an intermediate stand of the glacier during its retreat from Martha's Vineyard/Nantucket (Oldale, 1975). Low sand dunes and beaches, originating from the glacial deposits and reworked by wind and waves, cover the remainder of the shoreline, except where coastal marshes and bogs have formed.

The dominant natural physical processes responsible for sediment transport off Mashpee are tidally-generated currents and wind-generated waves (we did not consider direct wind transport of sand on the shoreline). Human impact is significant, particularly as a result of dredging operations. Monomoy Island, Nantucket and Martha's Vineyard block incoming deep ocean waves, and the irregular intermediate shoals scatter substantial wave energy. Wave patterns, therefore, are controlled by local winds.

Because of the bathymetry and nature of the tides, tidal currents vary widely in Vineyard and Nantucket Sounds (Redfield, 1980). Before this study, the only current measurements in the vicinity were located in deeper water (>10 m) 2-3 km beyond Succonnesset Shoal (figure 3). Velocities of over 85 cm/sec (>1.5 kt) (Bumpus et al., 1971) suggested a potential for high sediment transport rates in the nearshore. Both the location and duration of these measurements, however, precluded extrapolation of these results to our specific area of interest for sand transport purposes.

Littoral sediment transport, caused by waves breaking obliquely to a beach, is generally important for beach stability. Since littoral sediment transport is difficult to measure, direction and rate are often estimated from such indirect evidence as orientation and growth rate of barrier spits, sediment prisms (fillets) captured by groins and jetties, or rates of filling

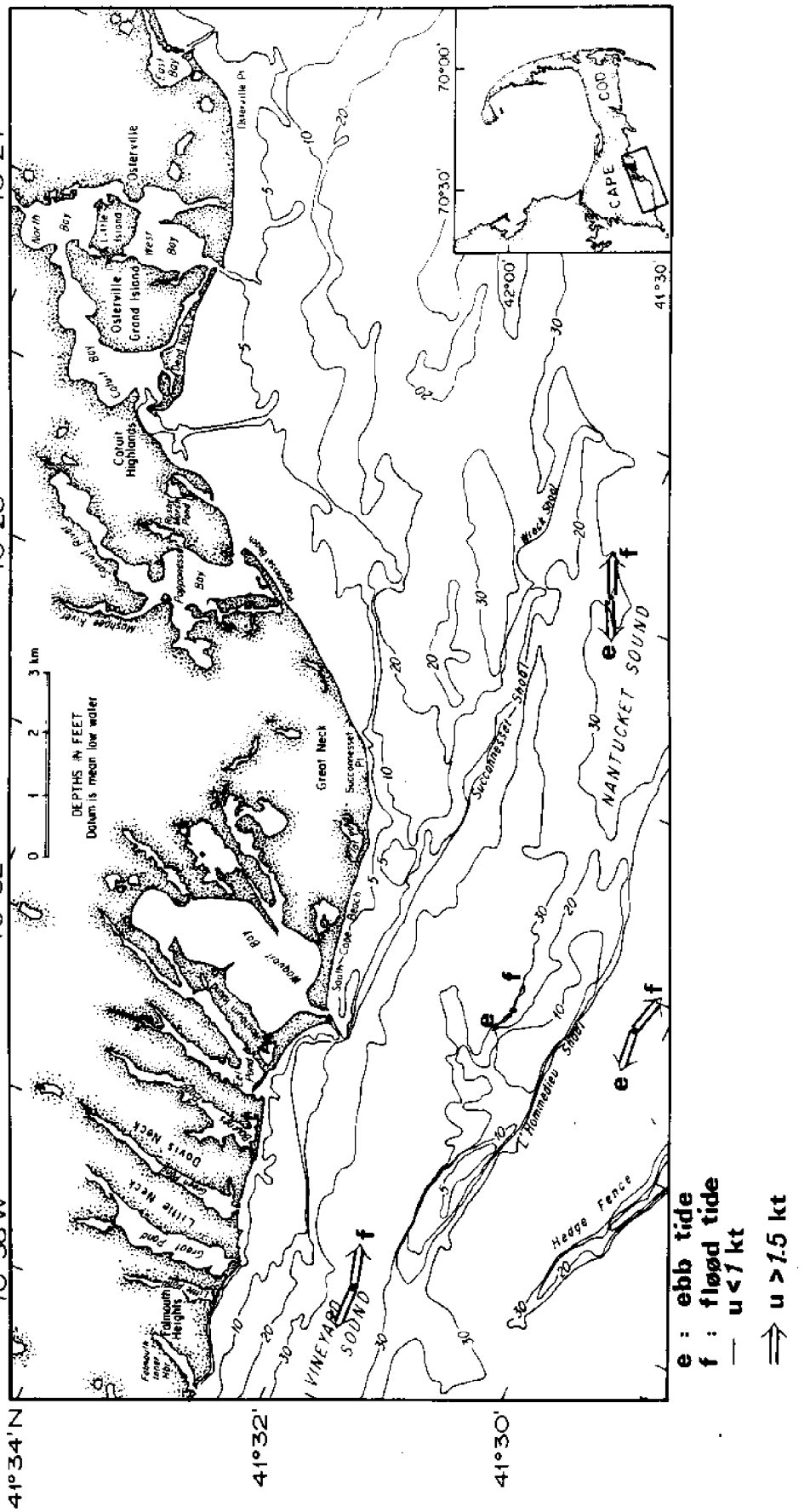

Figure 3. Tidal currents in the Popponesset Spit study area (from Haight, 1938 and Bumpus et al., 1971).

of dredged channels. Such indicators can be misleading, however, as documented by Aubrey and Gaines (1982a, b) in their discussion of the Popponesset Spit area.

Using spit orientation, with support from other observations, net longshore transport in this area has been inferred as northeastward along Popponesset Beach and westward along Dead Neck in Osterville, with a convergence near the mouth of Cotuit Bay (Woodworth and Wigglesworth, 1934; Brownlow, 1979). This assumption led recent researchers to conclude that the attrition of the northeast limb of Popponesset Spit in the late 1950's was due to loss of longshore sand input after a series of groins was constructed just southwest of the spit (Benoit and Donahoe, 1980). Close examination of the history of the area and the sand prisms trapped by the groins, however, led Aubrey and Gaines (1982a) to conclude that there was not sufficient littoral transport to cause the drastic change in the length and orientation of the spit. They proposed an alternative mechanism for building and eroding the spit which depended on Nantucket Sound as a sand source (Aubrey and Gaines, 1982b).

RESULTS

The ten tasks discussed in detail below were outlined in the project proposal based on a preliminary study of the coastal problems facing Mashpee. Some tasks were modified as field work progressed to more fully explore the sediment transport problems along the Mashpee coastline.

A) Historical Shoreline Changes

While the general configuration of the shoreline in this area has remained stable, the details of beach width and barrier beach orientation have undergone continuous change. The record of change was documented in charts from 1787 to 1938 and in aerial photographs from 1938 to the present. Results of an examination of these records were presented and discussed by Aubrey and Gaines (1982a).

The most striking evolution, and the one which first raised public concern, is that of Popponesset Spit. The attrition of nearly one-half of the barrier beach between 1954 and the present (figure 2) led to speculation that the remainder of the spit might also erode away. This impression was reinforced by the suggestion a recently completed groin field caused the loss of the northeast limb; if the spit was dependent on longshore transport for its stability, then the remainder of the spit would soon be eroding.

As discussed by Aubrey and Gaines (1982a), however, the present spit length, reaching just to Meadow Point, has been historically the stable configuration. Only in about 1860 did the spit begin to grow past Meadow Point (figure 4-7), a trend which continued until a series of hurricanes in 1954 breached the spit near the present inlet location. Because the new breach created a more efficient path into the bay than the former elongated channel, it became the primary inlet channel. The northeast limb was slowly transported onshore and to the north. It was this chain of events, not groin construction, which led to the loss of the spit (for a more complete discussion consult Aubrey and Gaines, 1982a).

Changes in beach width fronting the seacliffs were also examined over the 42-year period for which aerial photographs were available. Two sets of four stations (one set approximately halfway between Succonnesset Point and the southeast end of the spit, the other on either side of the Waquoit Bay entrance) were measured. The more northerly set showed high stability, with even a slight widening of the beach over the study period. The Waquoit stations were more variable. They showed little or no net change, although as much as 30-40 m of fluctuation in width occurred at various times. No seasonal correlations were apparent.

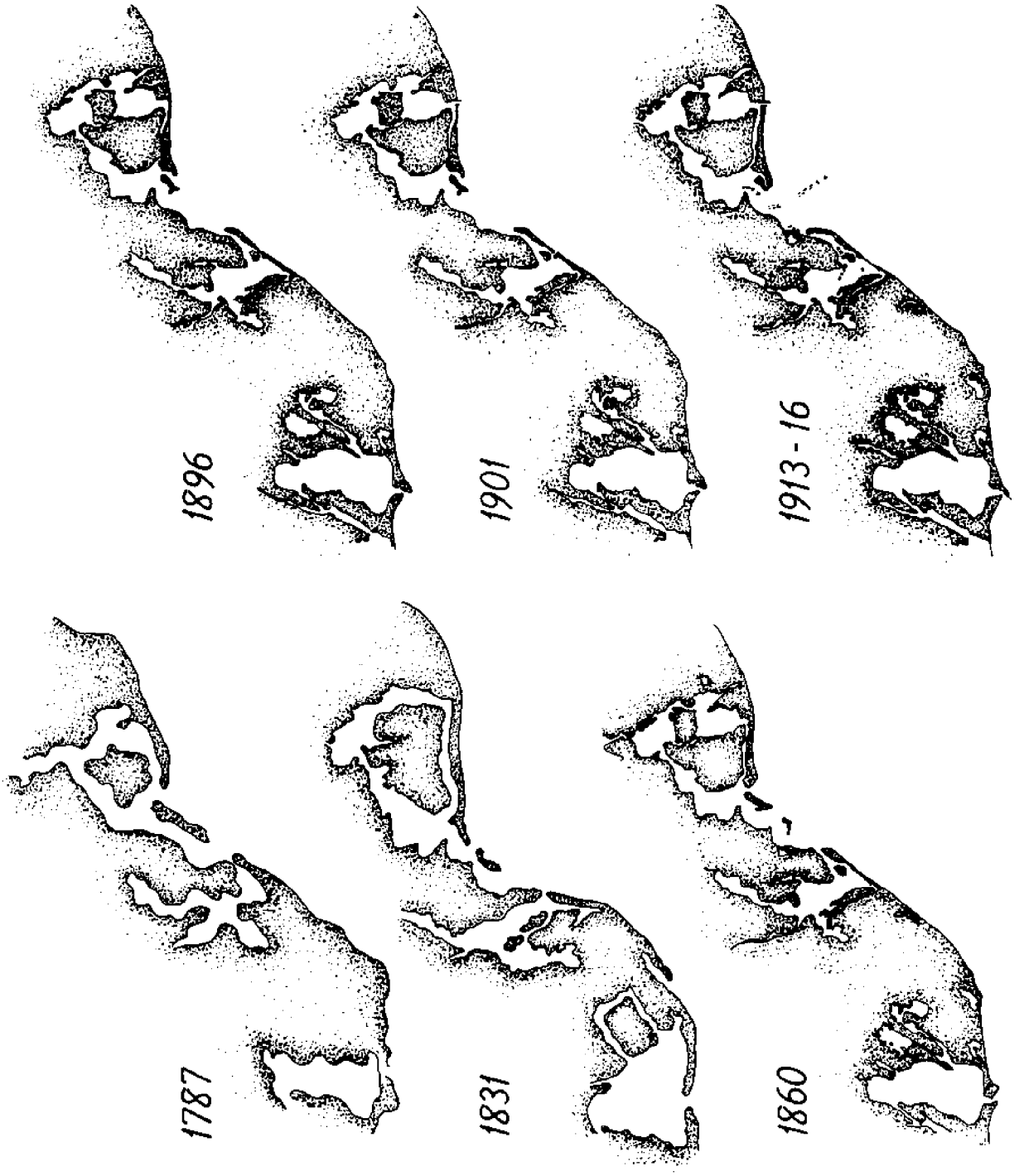

Figure 4. Outlines of selected historical charts and maps illustrating stages of shoreline evolution in the Popponesset Spit study area, 1787-1916.

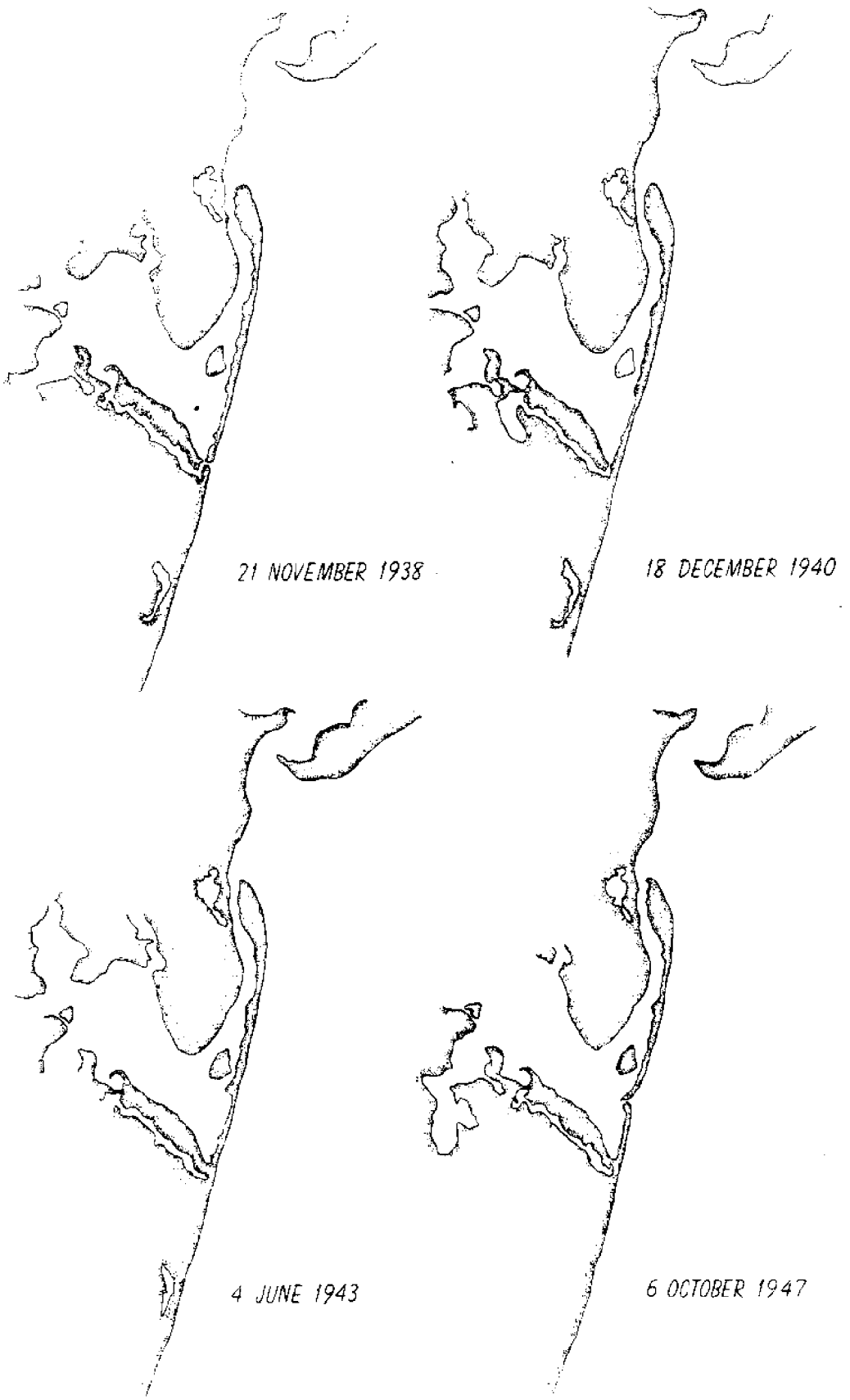

Figure 5. Outlines of selected vertical aerial photographs illustrating stages of shoreline evolution in the Popponesset Spit study area, 1938-1947.

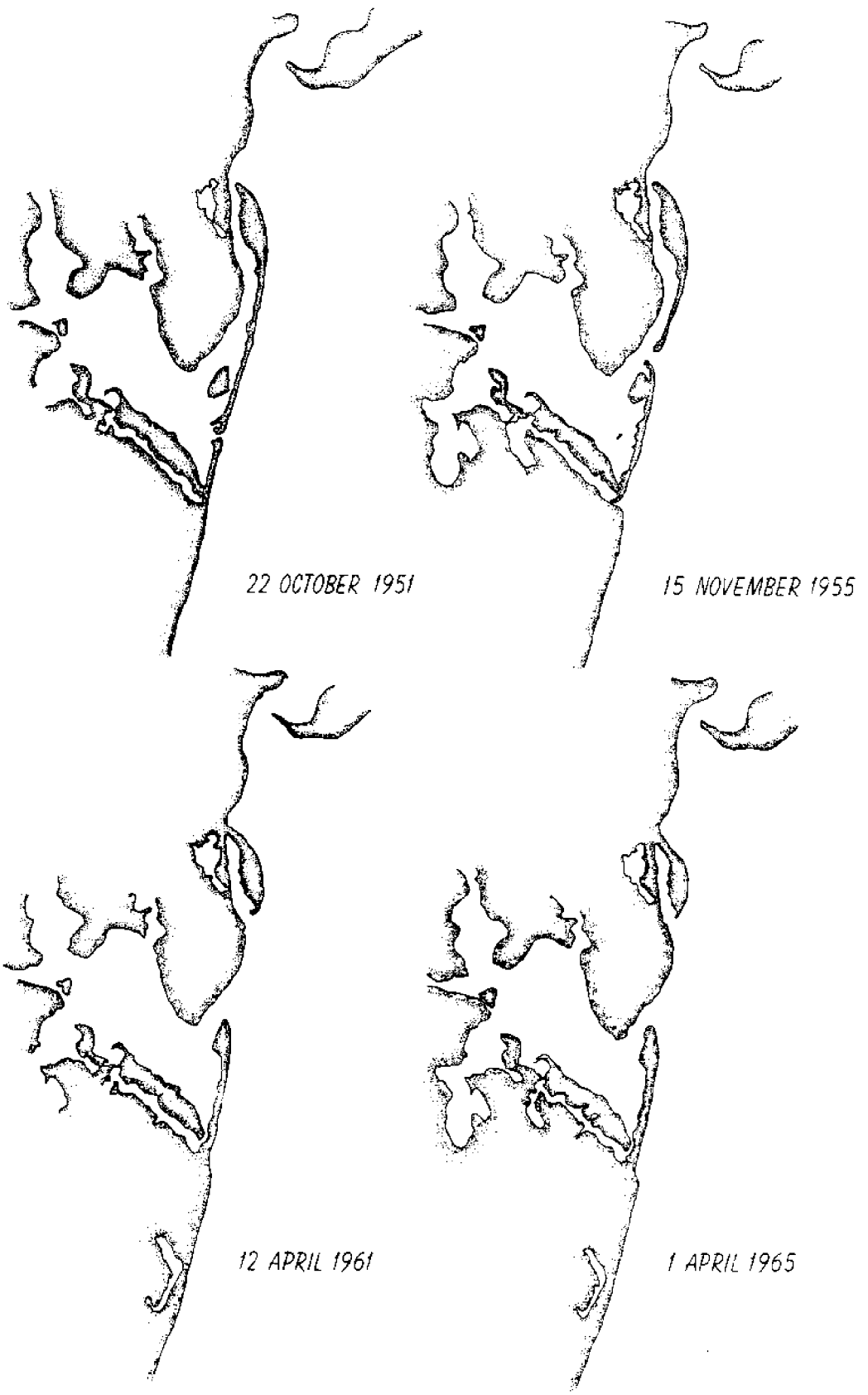

Figure 6. Outlines of selected vertical aerial photographs illustrating stages of shoreline evolution in the Popponesset Spit study area, 1951-1965.

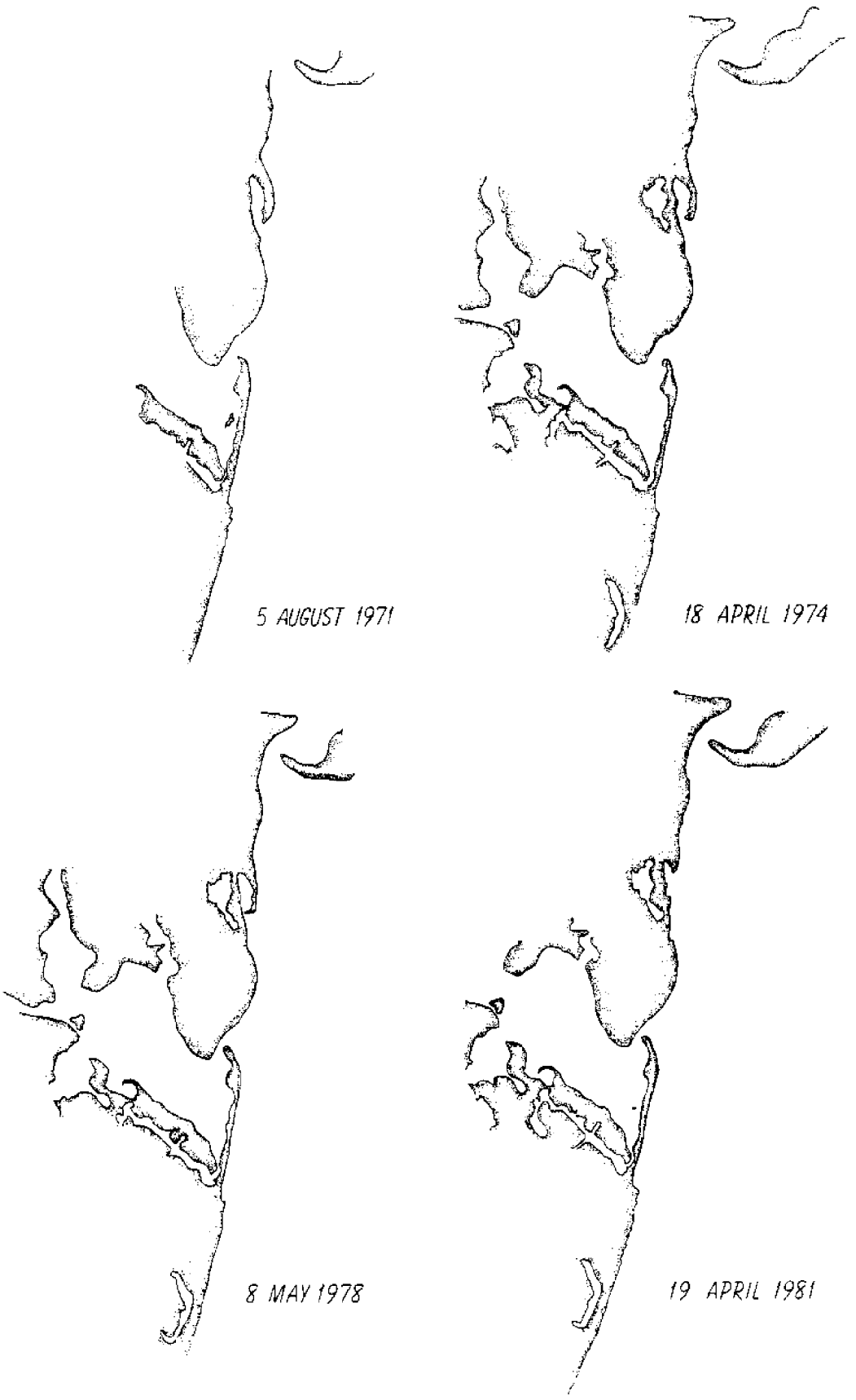

Figure 7. Outlines of selected vertical aerial photographs illustrating stages of shoreline evolution in the Popponesset Spit study area, 1971-1981.

The shoreline segment most affected by attrition of the spit extended from Meadow Point to Rushy Marsh Pond. The Meadow Point beaches lost their protection from wave attack; as a result all low cliffs now are reinforced with seawalls and groins (see structural section, below). Without these structures the cliff would be subject to erosion. Beaches farther north (near Rushy Marsh Pond) have been enhanced by onshore migration of sand from the north limb of the spit.

B) Benchmarks

For purposes of offshore navigation and precise determination of changes in shoreline configuration, three benchmarks were surveyed and marked with permanent brass monuments. The three locations span approximately 7 km of shoreline (figure 8). The most southerly is located near Succonnesset Point on an 8.9 m bluff off of Triton Way. The middle benchmark was placed on a low dune (3.26 m) at the southwest end of Popponesset Spit. The most northerly is in Cotuit Highlands, on a 9.4 m cliff. Field notes for the survey and more complete descriptions of the benchmark locations are in Appendix I.

C) Bathymetric Chart

225 km of soundings (figure 9) were run from June through October of 1982. Sounding profiles were digitized and used to produce a contour chart of the field area, showing, in detail, the prominent features of the area (figure 10): the shallow platform, the channel floor, and the Succonnesset Shoal. Bathymetry was acquired using a 200 kHz Raytheon DE719C precision echo-sounder, corrected for tides as measured at the time of the surveys. Navigation was performed with a Del Norte Trisponder microwave navigation system. Three shore transponders provided range information to a master unit on the ship. Shore transponders were usually located on the previously described benchmarks. Navigation precision is within 5 m (root-mean-square error) when all three transponders were operational.

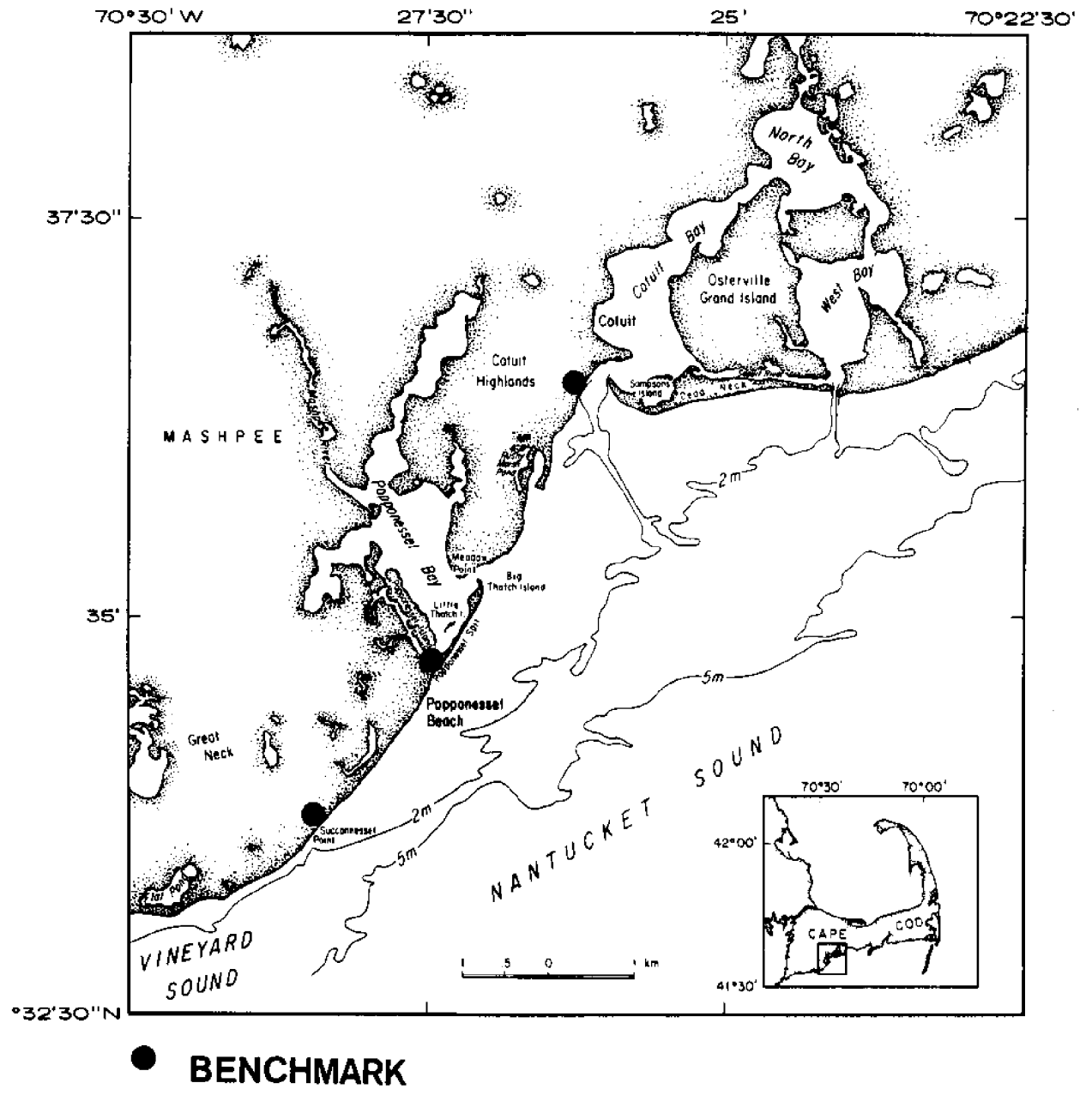

Figure 8. The Popponesset Spit study area, indicating locations of benchmarks surveyed in as part of this study. The Cotuit tide gage was located near the Cotuit benchmark.

Figure 9. Tracklines of bathymetric data collected in the Popponesset Beach study area.

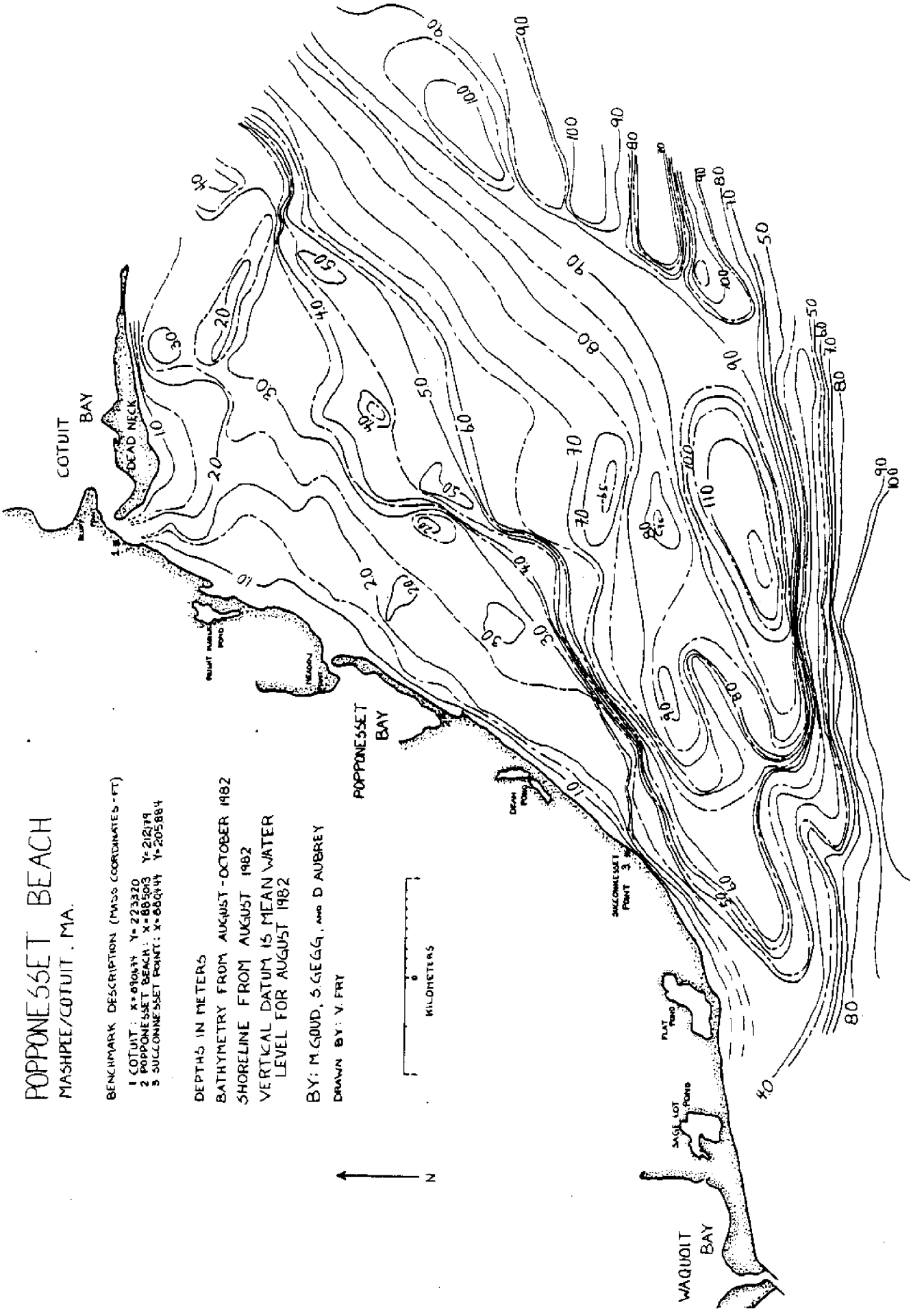

Figure 10. Bathymetry of study area as determined from tracklines in fig. 9. Contour interval 0.5 m.

D) Sediment Textures

Surface sediment samples were collected and grain size characteristics determined at 17 onshore locations, from Popponesset Spit to South Cape Beach and 27 offshore sites on the platform. Three short cores and four surface grab samples were taken in the deeper waters of the channel (figure 11). Three to five samples were taken at each onshore station, one each from the intertidal area, foreshore, berm, backshore, and dune and/or bluff (figure 12), though in some cases, the beach profile did not include one or another of these elements. If surface sediments were primarily pebbles and cobbles, no sample was taken.

Grain size analyses were performed using an electronic settling tube (Schlee, 1966), and statistics for each sample were determined by computer based on graphic moments (Inman, 1952). Parameters which were calculated for each sample include mean and median grain size, dispersion (sorting), skewness and kurtosis. Median grain sizes and dispersion for each sample are listed in Table 1; median grain sizes for the offshore stations are plotted in Figure 13. The other statistical parameters provide no additional pertinent information, and will not be presented.

The onshore samples were all combinations of coarse-to-fine sands with cobbles and pebbles; the only clay or silt size grains were found in the cliff sediments. Median grain sizes ranged from 0.23 to 1.1 mm, most often between 0.2 and 0.8 mm. Cross-beach grain size trends are predictable: very coarse near the water line, often dominated by cobbles with diameters up to 15 cm, growing finer towards the backshore where wave energy wanes. Where a seacliff is present, more fine material is introduced onto the beach. All samples with median grain size less than 0.3 mm were either in or adjacent to cliffs. On the spits where there is no direct input from cliff erosion, median grain sizes are generally higher and more uniform across the beach.

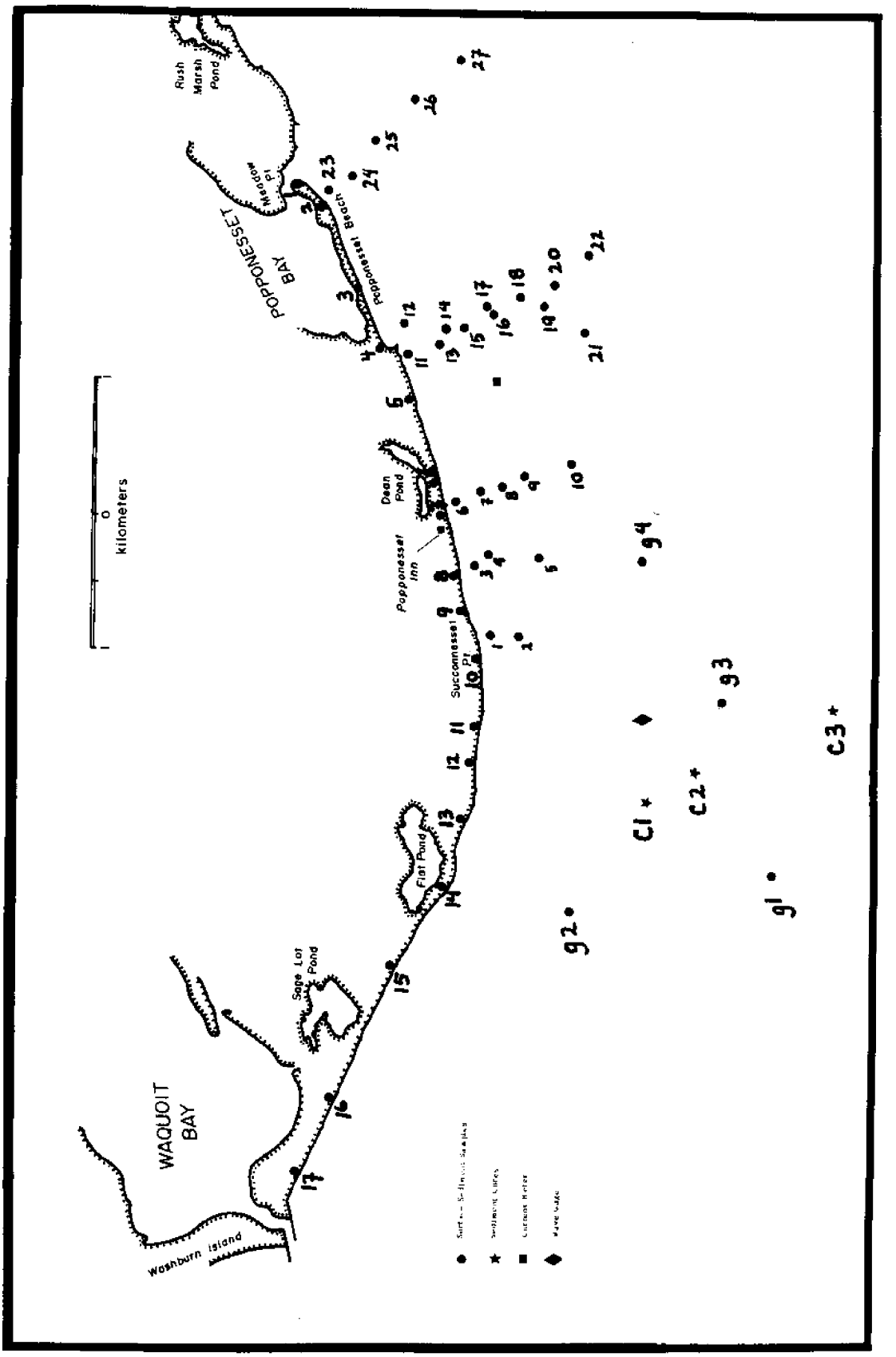

Figure 11. Locations of surface sediment samples analyzed for grain size characteristics. Sample numbers as referred to in tables 1 and 2 are labelled. Refer to Fig. 1 for location.

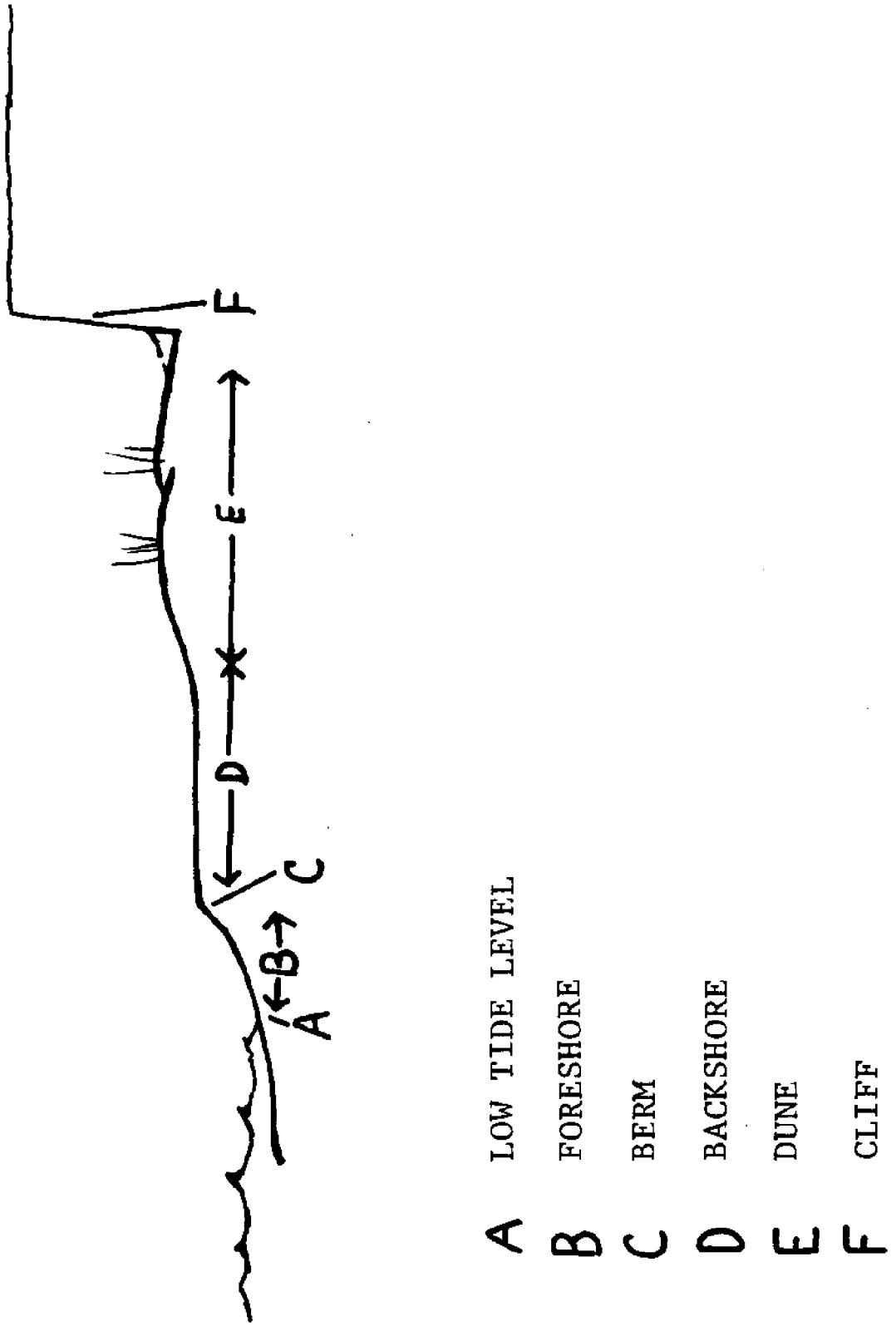

Figure 12. Typical beach profile, indicating locations of sediment samples as referred to in text and in table 1.

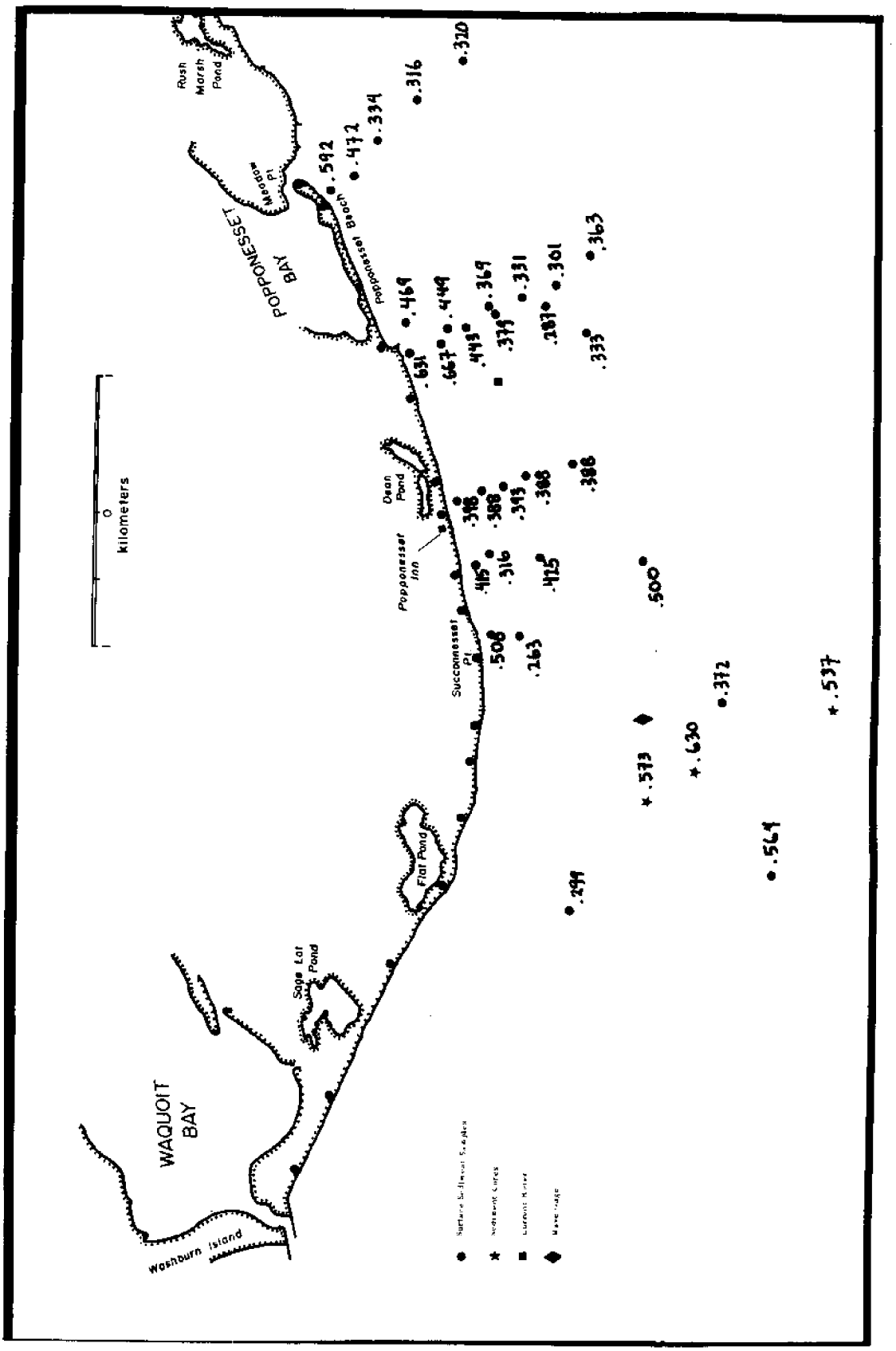

Figure 13. Median grain sizes, in millimeters, of offshore surface sediment samples in the Popponesset study area. Refer to Fig. 1 for location.

TABLE 1 GRAIN SIZE PARAMETERS ONSHORE SAMPLES

Station No.	Low Tide Level		Foreshore		Berm		Backshore		Dune		Cliff	
	Median	Dispersion	Median	Dispersion	Median	Dispersion	Median	Dispersion	Median	Dispersion	Median	Dispersion
1	635	.583	629	.595	467	.620	632	.631	637	.679		
2	1101	.385	635	.500	464	.588			474	.516		
3	897	.363	791	.639	371	.582			724	.621		
4	cobbles		640	.733	587	.631					250	1.014
5	gravel and sand		782	.410	567	.391			550	.421	595	.894
6	gravel		490	.416	506	.700	603	.737	459	.542		
7	gravel and cobbles		563	.595	500	.690					fine cliff seds	
8	gravel and cobbles		572	.721	250	.548					397	.940
9	cobbles		382	.654					290	.575	273	.850
10	cobbles		309	.503	276	.545			358	.625	284	.942
11	cobbles		1000	.564	426	.586					291	.917
12	cobbles		412	.627	437	.699			273	.764	380	.944
13	1137	1.487	1009	.702	656	.903	316	.466	231	.952		
14	1000	.970	681	.660	462	.621	375	.693	337	.563		
15	cobbles and sand		bad RSA run		787	.456	801	.703	540	.585		
16	986	.505	864	.294	794	.351	800	.416	798	.353		
17	1030	.444	794	.370	581	.573	737	.422	797	.483	___	
Mean	969		954		530		658		504		309	

Longshore trends in grain size in some cases can indicate source and transport directions of the beach sands. No general trends are evident at Popponesset, however, and only at one location along the beach do grain size patterns provide a clue to offshore processes. This is seen at stations 13 and 14, the only non-spit locations where sand is prevalent all the way across the beach, including the low tide terrace. At this spot an arm of Succonnesset Shoal meets the shore (see figure 10), and either serves as a sand source or a wave buffer for the beach in this location. One core (C1) taken near the crest of the shoal about 1.3 km offshore, shows median grain sizes of 0.53 to 1.04 mm, and a core from the flanks of the shoal (C2) displays a coarse median grain size (0.6 mm) in its near-surface sediments. These results suggest that the coarse sand found on the beach could be the product of exchange with the shoal.

Sands in the offshore samples are also medium-to-coarse grained, with median grain sizes ranging from 0.26 to 0.67 mm (figure 13 and table 2), but are less variable in both size and sorting. On the platform, a general pattern of coarsening shoreward is evident, reflecting the higher wave energy in the shallower nearshore area. Longshore trends are not pronounced, but there is a slight coarsening of nearshore grain sizes to the northeast, probably reflecting the increased width of the platform and the decrease in influence of fine, cliff-derived sediments. The variability in median grain size seen in closely-spaced samples 11 through 15 may be due to variability across a sand wave; no cross sections of waves were systematically sampled to firmly establish trends, however.

Another statistical technique for deriving information from grain size distributions is multivariate factor analysis, or eigenfunction analysis. The data is represented as a matrix of discrete phi size classes, each element of which is the percentage of sample within that size class. Eigenfunctions are

TABLE 2 GRAIN SIZE PARAMETERS OFFSHORE SAMPLES

Offshore	Median	Dispersion	$e_1(x)$	$e_2(x)$	$e_3(x)$
1	500	0.792	.1459	-.102	.008
2	263	0.672	.1315	.178	.126
3	406	0.854	.1421	-.019	-.007
4	316	0.894	.1350	.060	.092
5	425	0.570	.1757	.014	-.189
6	398	0.724	.1549	.030	-.033
7	388	0.679	.1587	.034	-.044
8	393	0.654	.1607	.031	-.065
9	388	0.516	.1738	.092	-.067
10	338	0.594	.1593	.139	.040
11	---	-----	.1508	-.166	.081
12	353	0.778	.1460	.012	.040
13	667	0.747	.1306	-.192	.209
14	375/448	0.772/.730	.1541	-.043	-.104
15	444	0.680	.1594	-.024	-.009
16	379	0.384	.1845	.171	.010
17	369	0.629	.1671	.070	-.077
18	330	0.609	.1569	.146	.057
19	258	0.443	.1353	.258	.244
20	301	0.521	.1582	.215	.149
21	372	0.554	.1692	.104	.002
22	363	0.598	.1678	.087	-.042
23	591	0.768	.1351	-.179	-.030
24	472	0.659	.1592	-.055	-.136
25	334	0.833	.1367	.084	.114
26	316	0.633	.1534	.147	-.081
27	320	0.457	.1688	.232	.135

TABLE 2 (continued) GRAIN SIZE PARAMETERS OFFSHORE SAMPLES

Offshore	Median	Dispersion	$e_1(x)$	$e_2(x)$	$e_3(x)$
Core 1 0-1 cm	573	0.684	.1450	-.159	-.0611
5-7 cm	1000	0.518	.1070	-.3024	.3295
17-19 cm	533	0.497	.1767	-.1318	-.3307
33-35 cm	1039	0.376	.0596	-.3519	.4718
43-45 cm	628	0.681	.1328	-.2062	-.0218
Core 2 0-2 cm	630	0.719	.1279	-.1773	.1175
6-8 cm	667	0.812	.1182	-.1967	.0766
20-22 cm	263	0.831	.1199	.1261	.1417
Core 3 1-3 cm	537	0.583	.1558	-.1481	-.1071
6.5-8.5 cm	429	0.867	.1394	-.0524	-.0397
14-16 cm	480	1.054	.1234	-.0570	.0693
22-24 cm	669	0.895	.1136	-.1796	.1240
g 1	564	0.781	.1360	-.1442	-.0927
g 2	299	0.467	.1621	.2475	.1753
g 3	372	0.732	.1530	.0361	.0191
g 4	500	0.519	.1772	-.0377	-.2430

derived from the data, and each function represents a certain amount of the mean square value of the data. The eigenfunction associated with the largest eigenvalue represents the data best, and most of the information in the set can usually be represented by three or four eigenfunctions.

The eigenvalues and eigenfunctions were calculated for the offshore stations and determined a mean grain size centered at 1.5ø (The phi scale is a base two logarithmic grain size scale, where 0ø corresponds to 1 mm, 1.5ø equals approximately 0.35 mm). No consistent pattern of variability was found on the platform (other than fining offshore), suggesting that the flow patterns or source differences do not cause subtle distinctions in grain size distributions. These results, as well as a description of methodology, are described in Appendix II.

E) Side-Scan Sonar and Sub-bottom Profiling

In the channel between the platform and Succonnesset Shoal, bedform orientation is more difficult to determine, since sand waves are not visible on aerial photos at depths greater than about 2.5 m. To clarify sand wave patterns for the channel and the slopes leading to it, 30 km of side-scan sonar data were collected (figure 14). In the same survey, a 3.5 KHz high-resolution seismic profiling system was employed, both for bathymetry and to provide an indication of the sediment thickness and sub-surface geological structure. This survey covered very little of the platform, since at such shallow depths the side-scan swath is very narrow, and seismic multiples obscure nearly all sub-bottom features. The latter condition effectively precludes determination of the structural control and geologic history of the platform using the seismic system.

The side-scan sonar's 43 m-wide swaths reveal an irregular pattern of sand waves in the channel with heights up to 2 m. In contrast to the long, low waves found on the platform, the channel slope and bottom displayed patches of bedforms with wavelengths of 20 to 80 m, interspersed with a flat or hummocky

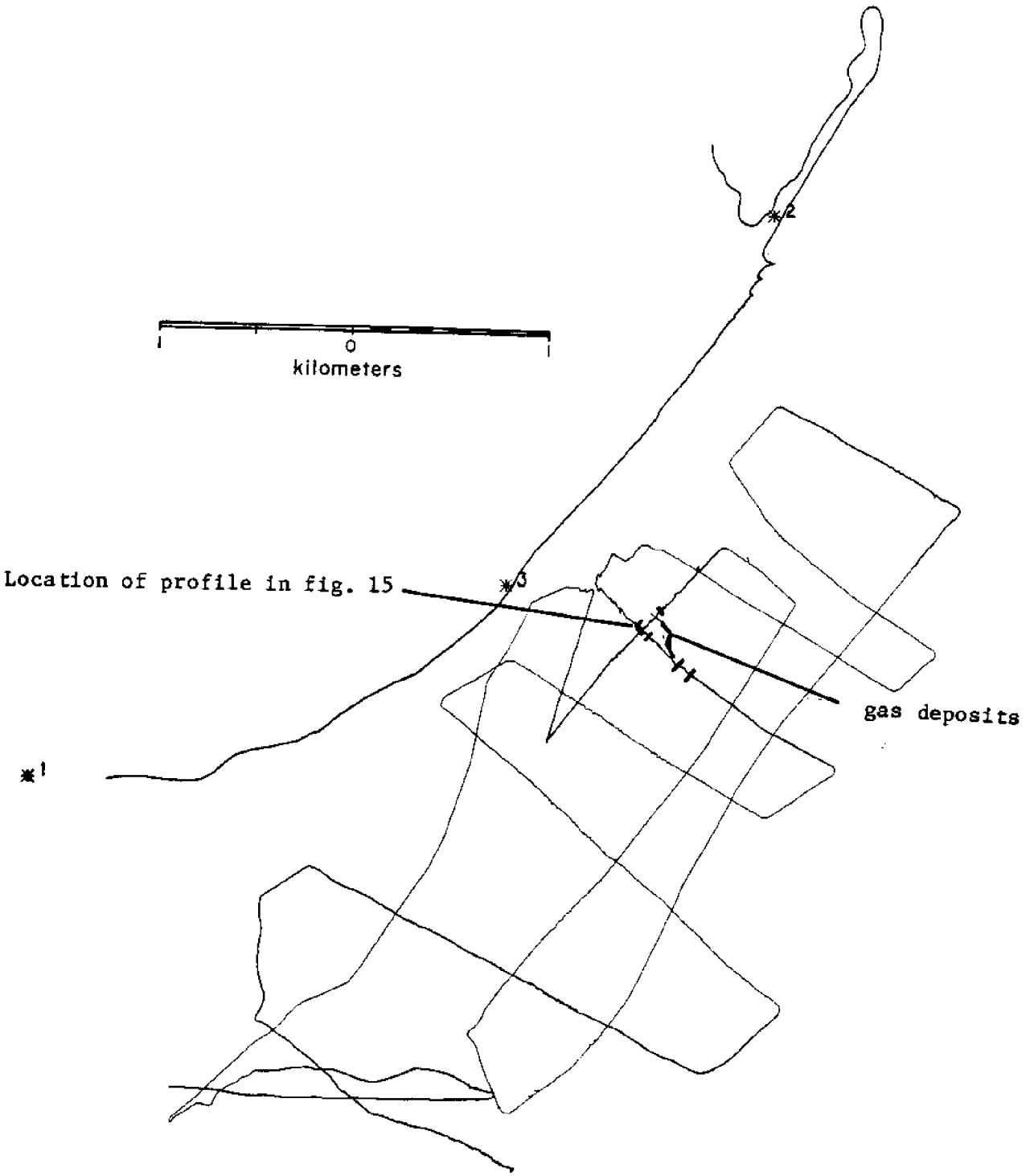

Figure 14. Tracklines of seismic data (3.5 kz and sidescan sonar) collected in the Popponesset study area.

bottom surface. Wave crests in the channel occurred at oblique angles to the shoreline, approximately perpendicular to the direction of tidal flow. They sometimes stretched across the width of the sonar record; at other locations they were laterally discontinuous. Large waves (2-2.5 m) were consistently found on the channel slopes leading up to Succonnesset Shoal, oriented with their crests sub-parallel to the shoal and lee sides downslope.

Sub-bottom profiles displayed a hummocky subsurface, broken in spots by filled paleo-channels. In some places, highly reflective layers approached the surface; in others, the acoustic basement was as much as 20 μ sec two-way travel time (approximately 15 m) deep. No correlation between depth to acoustic basement and location of bedforms was found. The ancient channels, relics of post-glacial periods when sea level was lower than it is at present, are as deep as 10 m, and in some places the seismic record shows deposits of gas (figures 14 and 15). The gas appears on the record as a wide, distinct reflector which truncates other horizons and displays no seismic multiple deeper in the record. The gas deposits are no deeper than 4 m, and may have seeped into overlying sediments. Experience in other locations has shown such deposits to be methane gas (R. Oldale, pers. comm., 1983). The deposits are neither of economic value nor harmful (they are too shallow to be under pressure). They could be unpleasant if they were dredged, however, and a beach replenishment program relying on dredge spoils from the offshore should take the presence of gas into account.

F) Bedform Migration

Sand wave patterns in shallow water (depth <2.5 m) from Succonnesset Point to West Bay are easily defined on all of the recent color photos and many of the earlier sets (figure 16). Patterns of wave crests are distinctive, and consistent from year to year, so that the migration of individual bedforms can

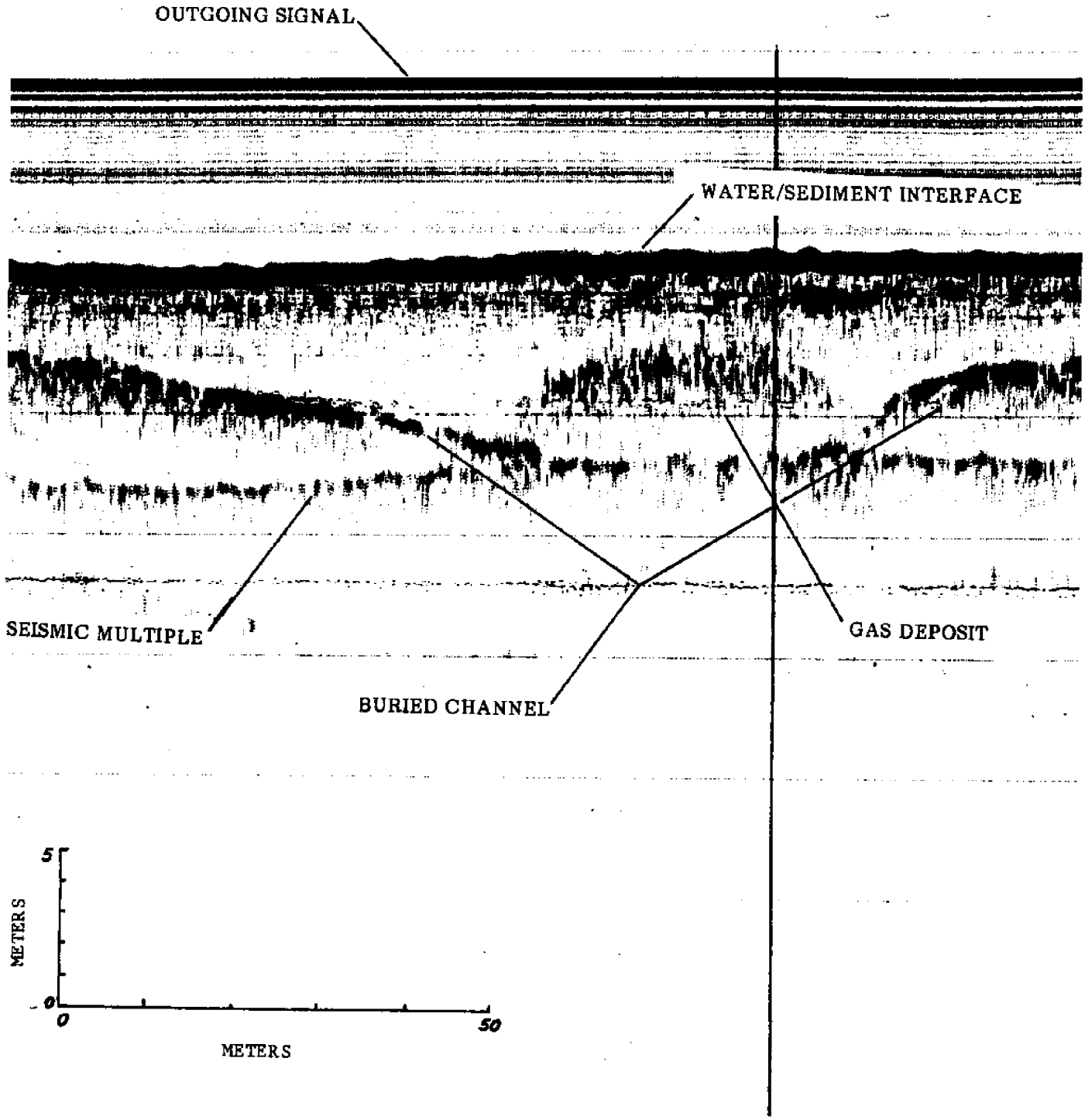

Figure 15. 3.5 kz seismic record from the offshore channel in the Popponesset study area, showing gas deposits in buried channel. Location is shown in figure 14.

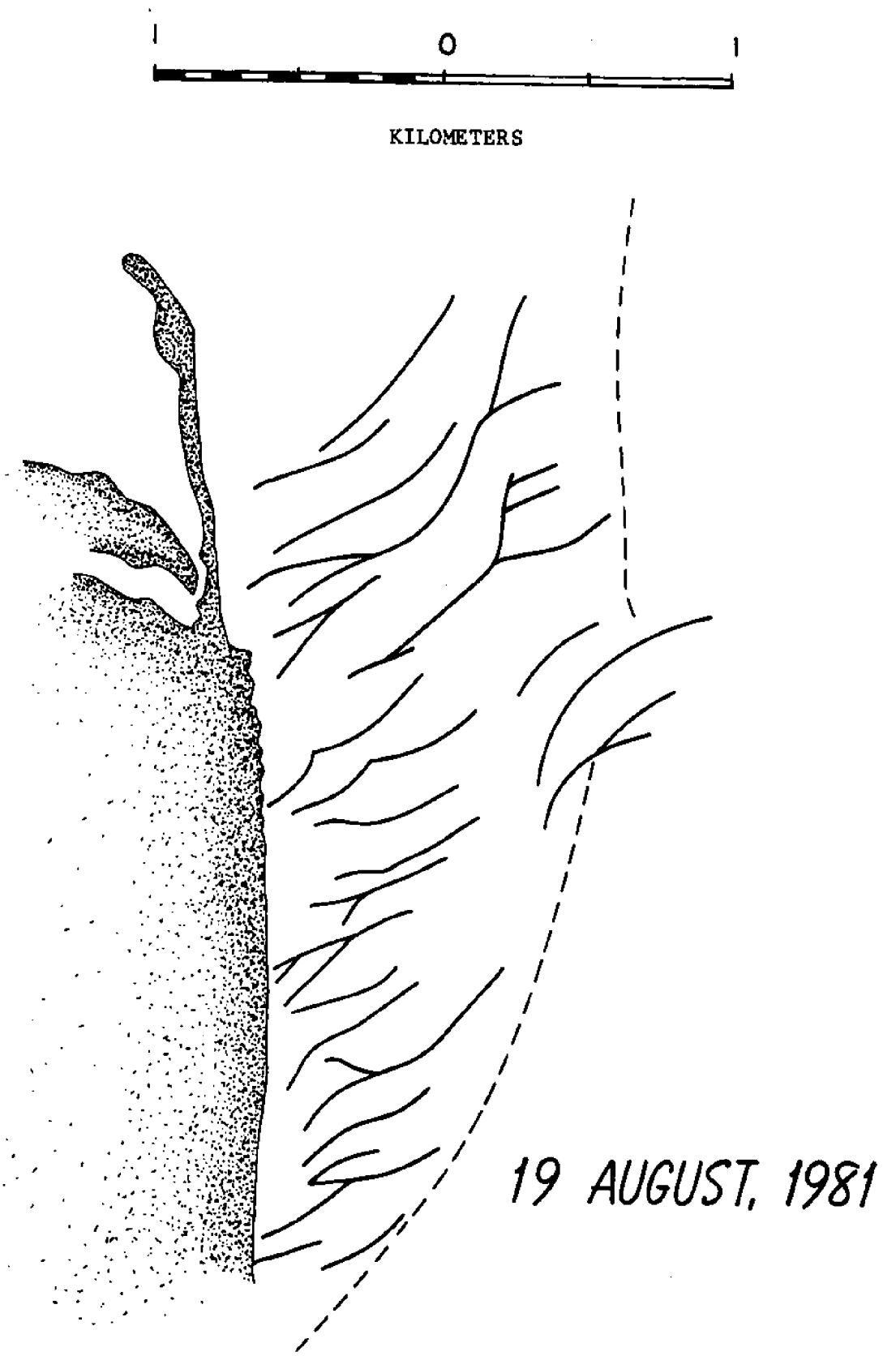

Figure 16. Sand wave crests in the Popponesset Spit study area. The dotted line indicates the approximate position of the 2 m isobath.

be traced using the photos. This has been done for the years 1981-1982 and 1971-1981. Although good photographs with easily resolved sand wave crests were available for the early 1950's, correlation with sand waves of later years was uncertain, so migration over time scales greater than 10 years was not quantified.

Volumetric estimates of sediment transported as sand waves across the platform were made by combining photographic data with bathymetric surveys. Bedform patterns were traced and adjusted to a single scale. Individual sand waves were identified, and migration distance determined for each one, both for one-year and 10-year periods. The height and wavelength of the bedforms were measured from bathymetric profiles and a detailed survey was run over a couple of waves to define their lateral variability in height and length. Because there were only minor differences in sand wave heights on the platform, a typical volume per unit length of wave crest per wavelength was defined using the detailed survey, and applied to a subsample of the sand waves. This method gave a typical sand volume of 10.1 m^3/m of wave crest/wavelength.

Sand wave migration is consistently to the southwest (figures 17 and 18); distances range up to 35 m over one year, and up to 200 m over ten years (table 3). Volume migration of sand in each wave was calculated using the average volume derived above and the formulas and methods presented in Part C of the discussion section.

G) Nearshore Circulation

As one element of the experimental design to determine sediment transport rates on the shallow platform off Popponesset Spit, water motions were observed for periods of nearly a month at three locations in the Popponesset region. Estimates of tidal range, tidal circulation and net (or mean) drift over the period of study within the channel separating Succonnesset Shoal from

Figure 17. Sand wave migration patterns in the Popponesset study area for the period 1971-1981. Sand wave labels are as referred to in table 3.

Figure 18. Sand wave migration patterns in the Popponesset study area for the period 1981-1982. Sand wave labels are as referred to in table 3.

TABLE 3 SAND WAVE MIGRATION DISTANCES (meters)
(see Figs. 17, 18)

WAVE	1981-1982	1971-1981
A	20	90-145
B	18-22	70-180
C	10-20	65-110
D	0-25	30-90
E	10-20	120-200
F	20-30	120-160
G	20-35	120-145
H	20	110-180
I	20-25	135-180
J	0-22	125-180
K	0-22	80-160
L	20	55-70
M	22	72

the shallow platform, were derived from a wave/tide gage. Second, tidal velocities on the platform were measured with a two-axis acoustic current meter. Finally, estimates of astronomical tidal constituents for Cotuit Highlands (from which future tides may be predicted) were derived from 30 days of pressure sensor information. Each of these measurements is discussed in detail below; instrument locations are shown in Figure 11 while deployment information is listed as Table 4.

1) Tidal Flows in the Channel: The Sea Data 635-12 wave gage has capabilities for measuring not only directional wave characteristics (see section H), but also mean water levels and mean currents. The instrument consists of a two-axis electromagnetic current sensor and a precise quartz oscillator pressure sensor, internally recording. It is similar to the instrument described by Aubrey (1980).

The instrument was deployed from 2 November through 30 November, 1982. It acquired data for 21 days before using up its available cassette tape storage capacity. It was located in the channel separating Succonnesset Shoal from the platform, in a mean water depth of 6.5 meters. Over the period of study, the instrument showed tidal flows to be strictly rectilinear, flowing toward a direction of approximately 45°TN on flood tide, and towards 225° during ebb tide (Appendix III). Tidal flows showed little deviation from these mean directions. The root-mean-square amplitude of the tidal flows was about 41 cm/sec, reversing approximately every six hours.

The mean flow (averaged over the twenty-two day duration of the study) was 0.07 m/sec to the southwest (about 225°TN). This mean flow superimposed on the tidal flows is probably a result of tidal rectification in this area of complex bathymetry. The result of this mean flow is a net near-bed transport

TABLE 4 SUMMARY OF INSTRUMENT DEPLOYMENTS

POPPONESSET BEACH, MA

	SEA DATA 635-12	NEIL BROWN ACM-2	SEA DATA TDR1-A
DEPLOYMENT DATE	2 Nov. 1982	22 Oct. 1982	13 July 1982
RETRIEVAL DATA	30 Nov. 1982	9 Nov. 1982	13 August 1982
BURST SAMPLE INTERVAL	4 HOURS	----	----
BURST DURATION	2064 SECONDS	----	----
BURST SAMPLE RATE	1 SECOND	----	----
CONTINUOUS SAMPLE RATE	30 MINUTES	10 SECONDS	10 MINUTES
INTERNAL AVERAGING	YES	NO	YES
DATA QUALITY	EXCELLENT	EXCELLENT	EXCELLENT

of sediment towards the southwest, to the western end of Succonnesset Shoal where water depths are very small, suggesting accumulation at that point. Surface geometry of the shoal support this suggestion, forming well-defined tidal hyperbolae indicating direction of net flow.

Tidal and mean velocities at this location cannot be easily extrapolated to other areas nearby because of complex bottom topography. Orientation of sand waves on the southern side of Succonnesset Shoal suggest that mean flows along the south margin of Succonnesset Shoal in fact may be to the east, which would help maintain the integrity of the shoal. Such circulation patterns have been observed elsewhere on shoals in nearby Vineyard Sound, as well as at other more-distant locations.

Finally, flow patterns within the vicinity of Succonnesset Shoal do not appear to respond strongly to local winds of 10 meters per second or less. The local circulation around this feature appears to be almost entirely tidally-driven.

2) Tidal flows on the platform: A Neil Brown two-axis acoustic current meter (Model ACM 2) was deployed on the shallow nearshore platform from 22 October 1982 through 9 November 1982, in a water depth of about 2.5 m. It sampled at an interval of 10 seconds, measuring two horizontal axes of water flow. The sensor head was positioned 1.5 m above the sand bed.

As expected, tidal velocities (positive to the northeast, negative to the southwest) are distinctly semi-diurnal (a period of 12.4 hours), with a modulation over a two-week period imposed by interaction of various tidal constituents. Normal tidal currents were distorted during the period of 25-26 October when local winds exceeded 7.5 m/sec for approximately 36 hours (figure 19). This relatively heavy wind from the NNE (20-50°TN) induced a quasi-steady circulation on the platform to the southwest, producing the

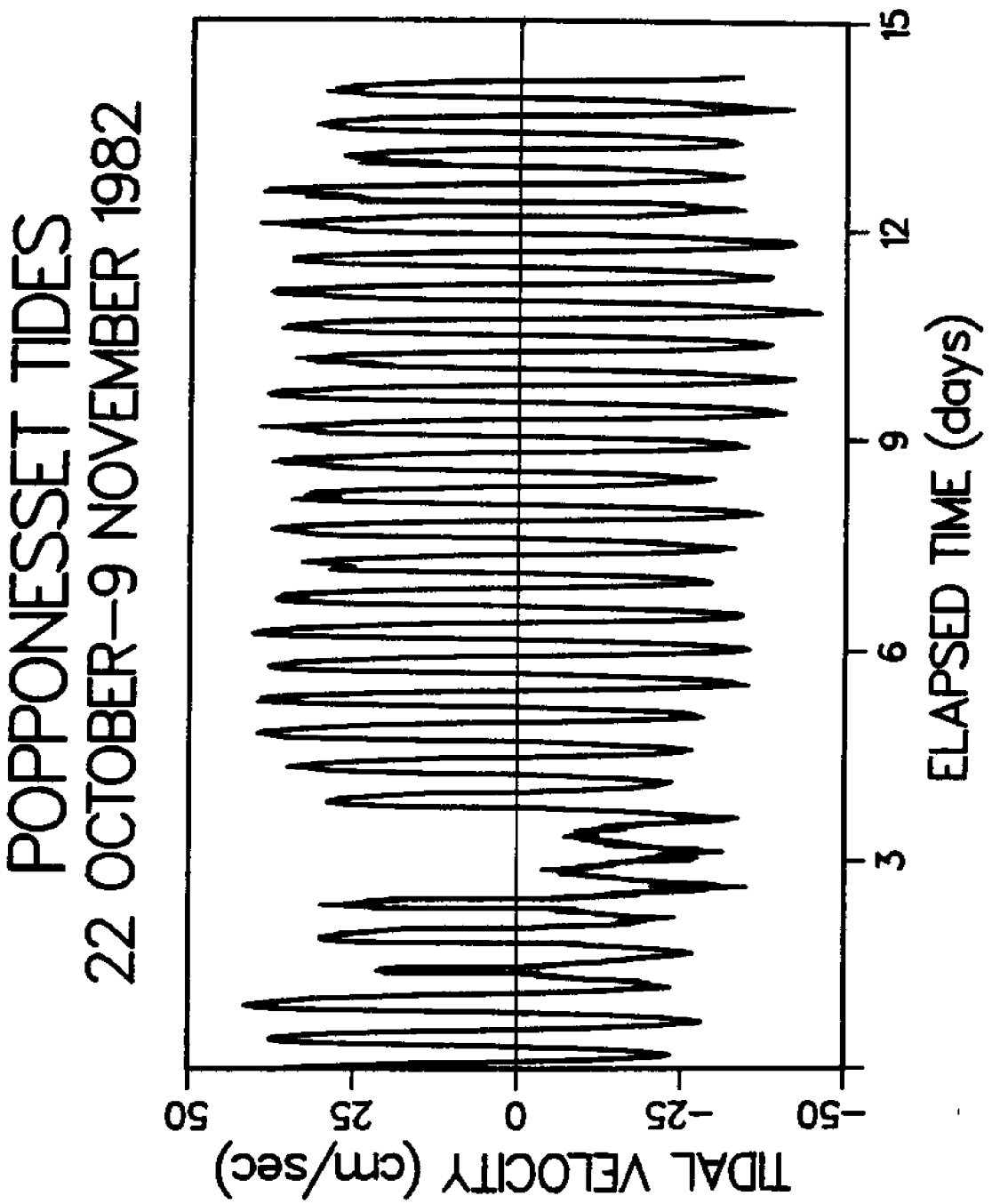

Figure 19. Time series of Neil Brown current meter data from the shallow platform near Popponesset Beach. Positive speeds are to the northeast, negative to the southwest.

offset seen in the tidal velocity record during 25-26 October. No other wind events occurred during the remainder of the period of measurement which would enable us to evaluate the consistency of this shelf response to northeast winds.

Because the velocity record was less than twenty-nine days in length, tidal harmonic analysis could not be applied conveniently to this data set. Instead, the data were analyzed using a rotary component spectral analysis technique which separates the major frequencies of velocity variation, at the same time providing an estimate of the shape of the tidal ellipse (Gonella, 1972). Results of this analysis show the primary tidal components are semi-diurnal, with a contribution from diurnal, quarter-diurnal and sexadiurnal components (figure 20). The ellipse orientation for each of these components is parallel to the coast (217°TN), with practically no flow perpendicular to the coast. Mean flow over the 18-day current meter record at this location averages 0.06 m/sec to the southwest - this estimate, of course, is affected by the 25-26 October 1982 northeast wind event. Spectral estimates for this rotary component analysis have 8 degrees of freedom, consisting of four ensembles of nearly four-day records (91 hrs), for a total length of 15.2 days. The frequency resolution of these spectral estimates is 0.0110 cycles per hour.

A histogram of current measurements at this location was constructed from 8 minute averages of tidal current data (figure 21). The modal (most frequent) speed observed is in the range of 0.25 to 0.30 m/sec. Flows above 0.35 m/sec are rarely observed (less than 10 percent of the time), while flows above 0.40 m/sec are observed less than 2 percent of the time.

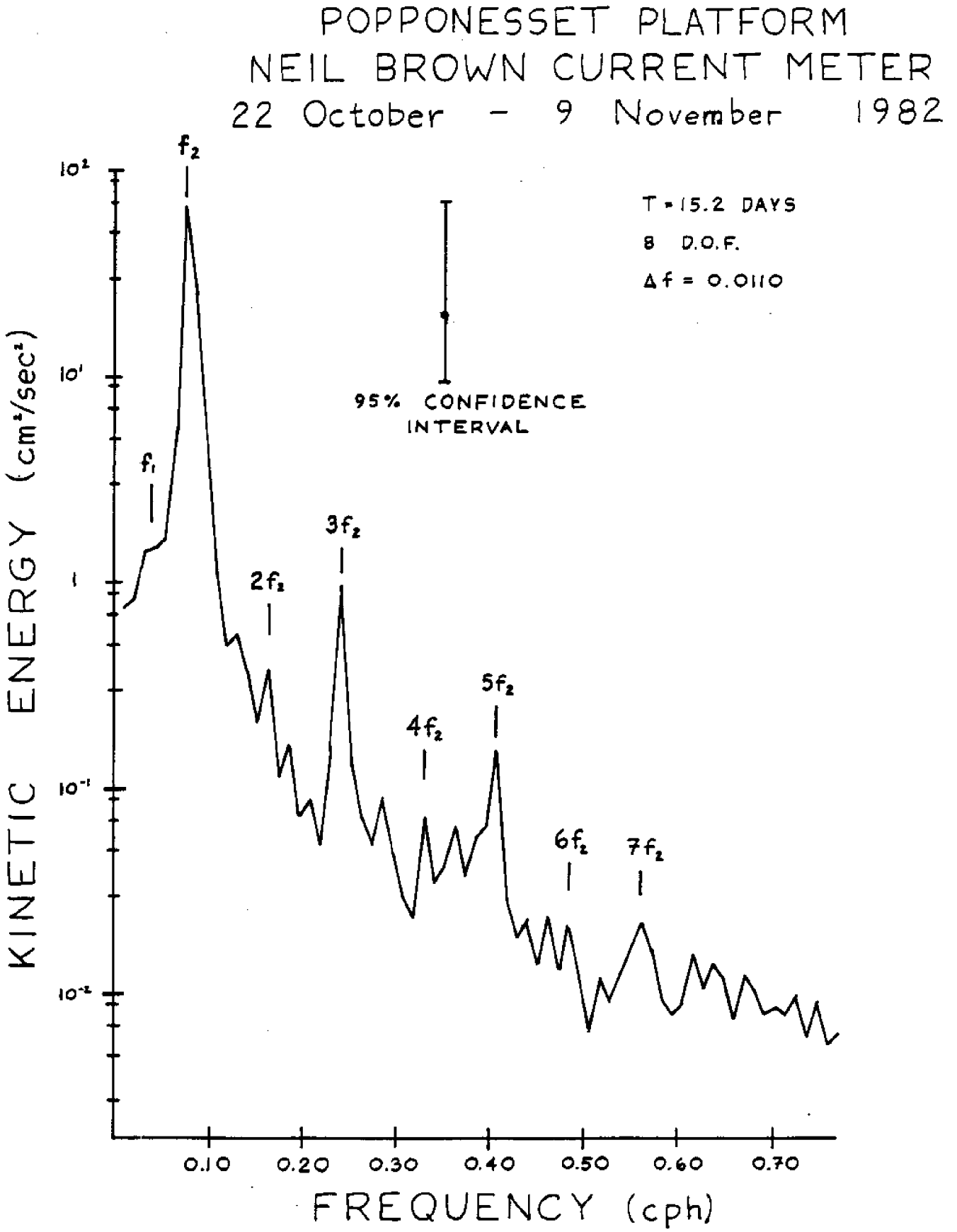

Figure 20. Plot of rotary component spectrum (total spectrum) for Neil Brown current meter data for Popponesset Beach.

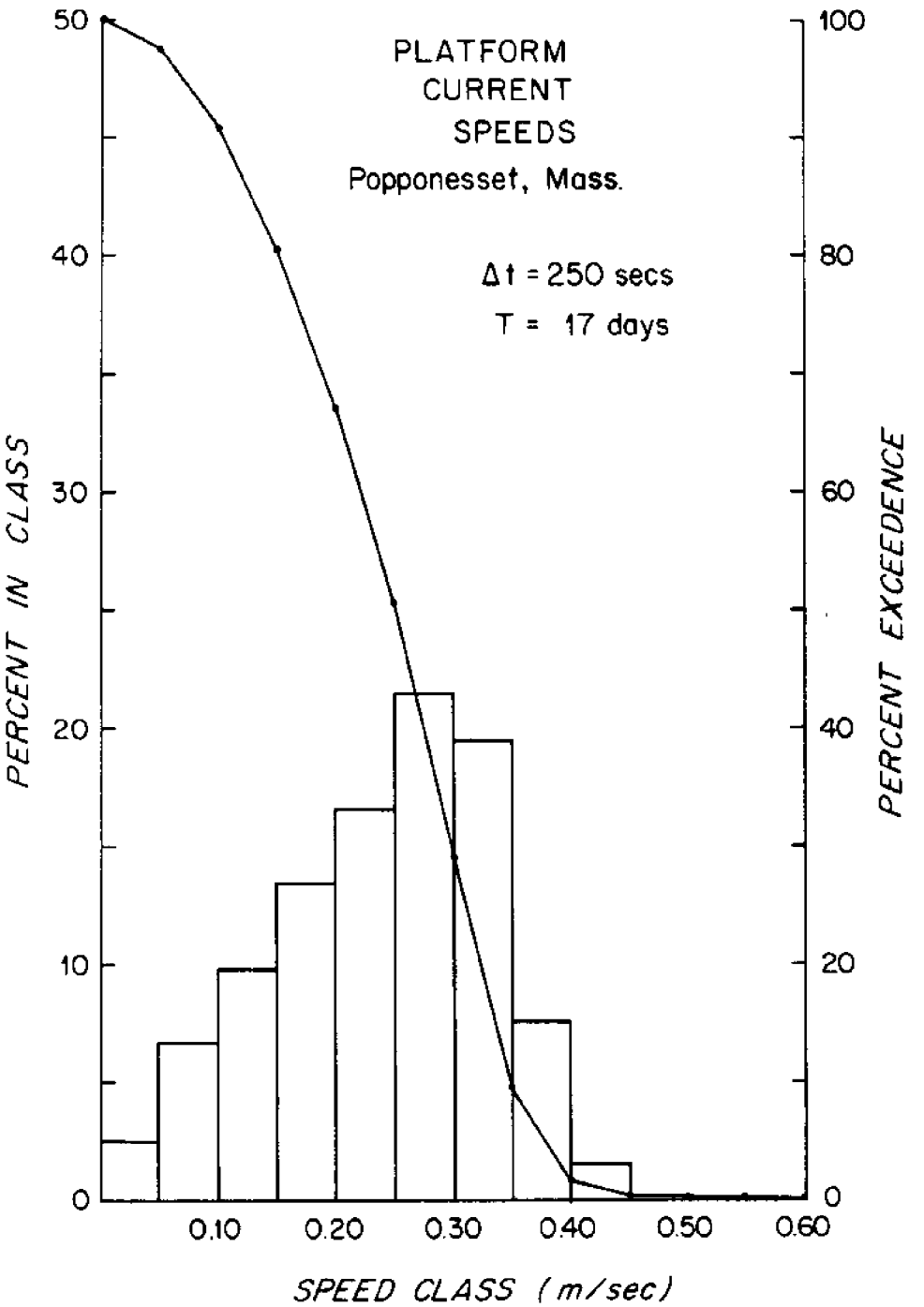

Figure 21. Histogram of speeds of tidal currents for Neil Brown deployment at Popponesset Beach, MA. Data was sampled at a 10 second rate in the field. Histogram is for a smoothed data set resampled at 640 seconds.

The root-mean-square amplitude of the velocity at this location was 34 cm/sec, at a level of 1.5 m above the bed. This amplitude is representative of the period of our measurements, and should be close to the yearly average value.

3) Tidal elevation at Cotuit Highlands: A pressure sensor was located off a pier at Cotuit Highlands for the period 13 July 1982 through 13 August 1982. The pressure sensor measures water level above it, providing a convenient means of observing surface tides. The instrument (a Sea Data Corporation TDR 1-A), measured both pressure and temperature at increments of 10 minutes. An internal electronic averaging capability assures that tide measurements are uncontaminated by surface wind waves.

The tidal signal at this location shows the dominant semi-diurnal character of local tides, with the superimposed fortnightly cycle (figure 22). Sea surface variability shows a clear diurnal inequality, with higher high tide always followed by lower low tide, imparting a definite velocity asymmetry to the southwest (or ebb) direction. This condition leads to a predominant southwest direction of sediment transport.

Because the tide record spanned more than 29 days, a harmonic analysis of the surface tide was performed (Schureman, 1971; Dennis and Long, 1971; Aubrey and Speer, 1983). This analysis separates the tide into 25 constituents primarily generated from astronomical gravitational influence. For Cotuit Highlands, the analysis shows the lunar semi-diurnal tide (M_2) to be the dominant local tide (figure 23 and table 5). Other constituents are also important, including diurnal and semi-diurnal elements. In addition, the M_4 and M_6 overtides (or harmonics) of the M_2 tide contribute to the total tide. The relatively large ratios of M_4/M_2 and M_6/M_2 mirror the asymmetry in the

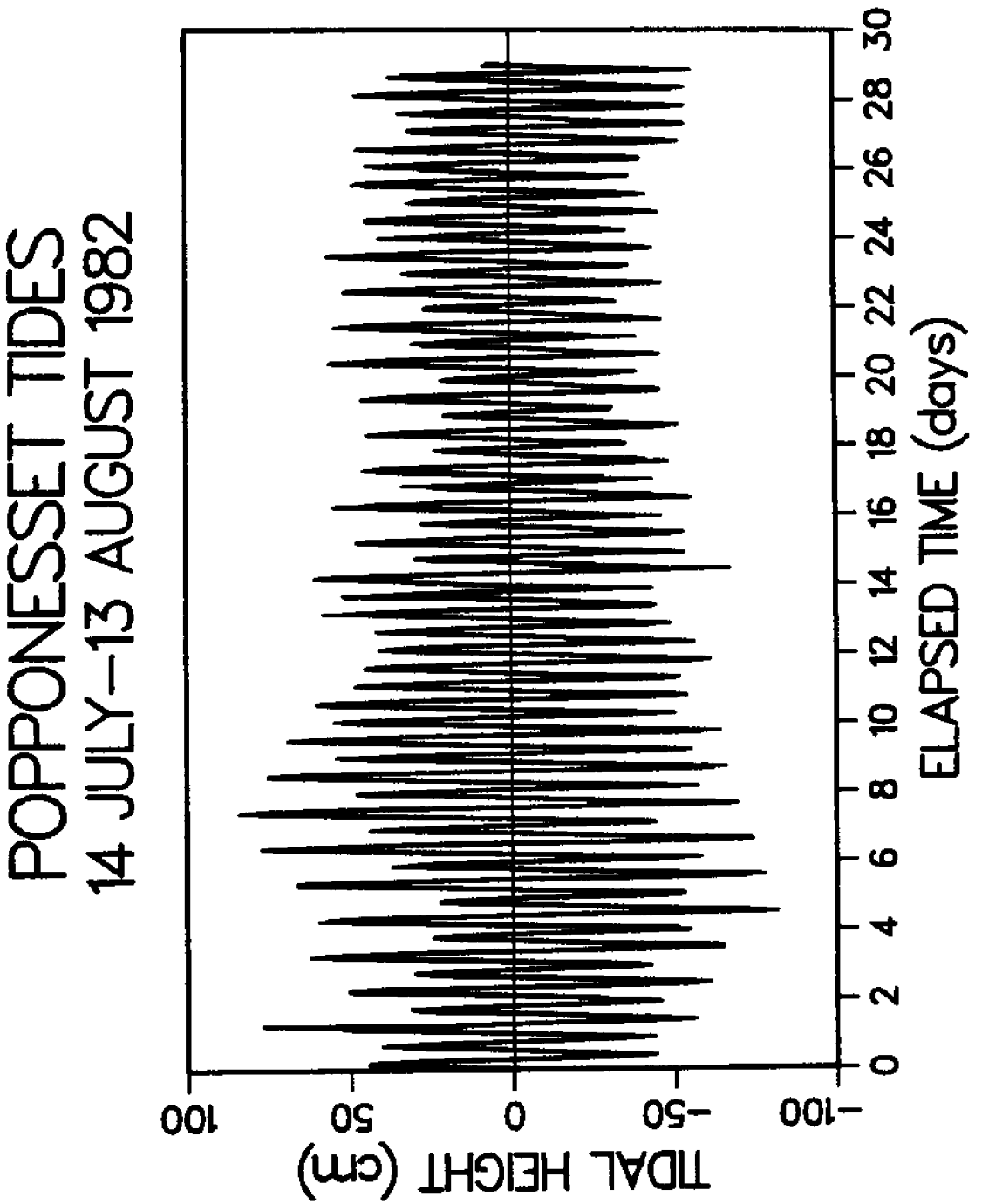

Figure 22. Record of tidal elevations at Cotuit Highland pier near Popponesset Beach. Datum is arbitrary. Measured with a Sea Data TDR1-A. Sampling at 10 minutes (internally averaging).

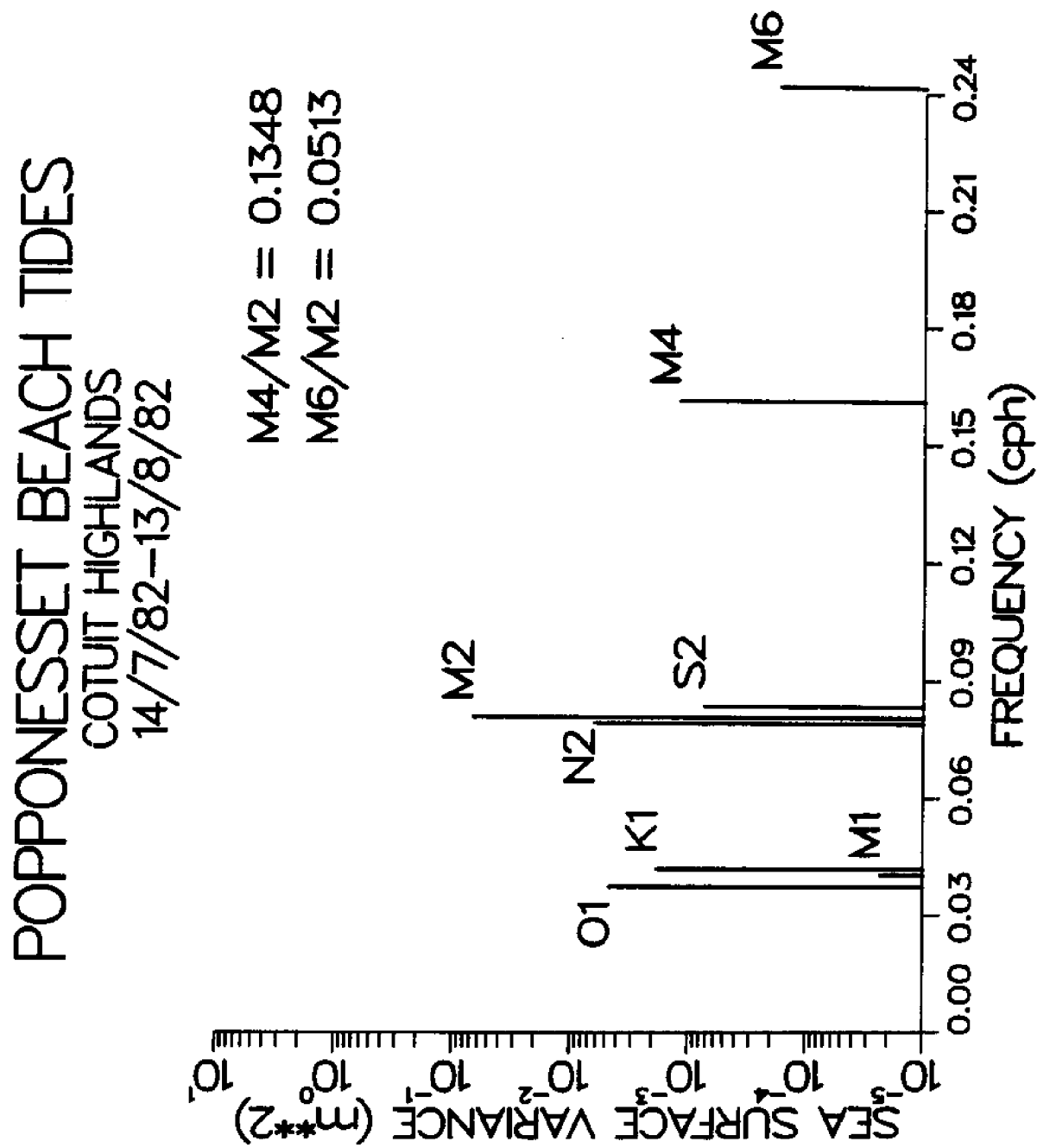

Figure 23. Harmonic constituents of 29-day tidal record shown in figure 22.

TABLE 5 TIDAL CONSTITUENTS FOR POPPONESSET BEACH

STATION: Cotuit Highlands LATITUDE: 41.6°N LONGITUDE: 70.4°W
DATE: 14 July - 13 August 1982

CONSTITUENT	AMPLITUDE (M)	(deg.)	G (deg.)
M_2	0.367	108	292
S_2	0.039	275	185
N_2	0.113	4	48
K_1	0.061	90	226
M_4	0.050	316	323
O_1	0.097	311	3
M_6	0.019	277	108
NU_2	0.014	102	341
MU_2	0.019	-61	38
2N2	0.010	-218	46
M1	0.007	-244	114
Q1	0.019	252	-20
P1	0.020	83	210
L2	0.010	87	235
K2	0.010	83	177

Recorded variance (m^2) 0.0865

Residual variance (m^2) 0.0024

tides, and suggest a net preferred direction of sand transport in the area to the southwest. Results from this analysis (table 5) can be used to predict astronomical tides at this location over the next century using a harmonic analysis prediction formula (e.g., Schureman, 1971).

The root-mean-square tidal range for the Cotuit Highlands station is 0.82 m. This compares to a mean range of 0.76 m presented in the National Ocean Survey tide tables (U.S. Dept. of Commerce, 1982). The difference is likely due to the location of the tide measurements; the NOS gage was probably located closer to Cotuit Bay, where the tide range is lower.

H) Wave Climate

Because of the importance of surface wave activity to nearshore sediment transport, this study included a task on measurement of directional wave characteristics (including heights, periods and directions of wave approach). A number of trade-offs must be considered when measuring directional waves. Besides sampling considerations (rate and length of burst wave sampling), water depth for a bottom-mounted instrument must be selected based on a trade-off between wave non-linearity and signal-to-noise ratio due to a varying ratio of wavelength to water depth. Since linear wave theory is used to correct bottom-mounted instrument data to surface conditions, the shoreward increasing non-linearity places a constraint on accuracy of wave estimates. For these reasons, the wave gage was placed in water deeper than 4 meters. From the standpoint of signal-to-noise, in order to measure waves of 3 second period and longer, the wave gage had to be in a water depth of 7 meters or less. A convenient compromise was to place the gage in a water depth of 6.5 m, within the channel separating the platform from Succonnesset Shoal.

Another consideration was whether to take measurements far offshore representing deep water incident wave energy, or closer to the study area for

a more local view. The former approach is more useful for applying measurements to adjacent areas of Nantucket and Vineyard Sounds. The latter approach is more directly applicable to the immediate area inshore of the gage. Because of the complex bottom topography (including convoluted shoals) and the consequent difficulty of numerically predicting the shoaling of deeper water waves past these shoals to obtain local wave conditions at Popponesset, we opted for local measurements, locating the gage inside Succonnesset Shoals.

The instrument used for wave measurements was a Sea Data Corporation 635-12. Its burst sampling capabilities permit measurement of waves as well as mean flows. More complete theory of operation and error analysis are contained in Aubrey (1980) and Grosskopf, Aubrey and Mattie (1983). For the present study, waves were sampled once every four hours (six times a day) for thirty-four minutes, acquiring a measurement of pressure and two horizontal velocity components once a second. Spectral estimates from these data were ensemble-averaged over 16 data subsets, yielding 32 degrees of freedom, with a frequency resolution of 0.0078 hz. The instrument was deployed with the pressure sensor 1.38 m above the sand bottom and the current meter 1.98 m above the bottom, directly above the pressure sensor.

Besides wave measurements, we obtained hourly meteorological observations from Otis Air Force Base, Hyannis, Chatham, Nantucket and Martha's Vineyard. These observations were collected to assess the predictability of local waves from local wind fields.

Over the month of deployment, wave energy was low, averaging only 61 cm^2 in variance (see Appendix III, figure 24). Variance ($\langle \eta^2 \rangle$) is defined by

$$E = \rho g \langle \eta^2 \rangle \qquad (1)$$

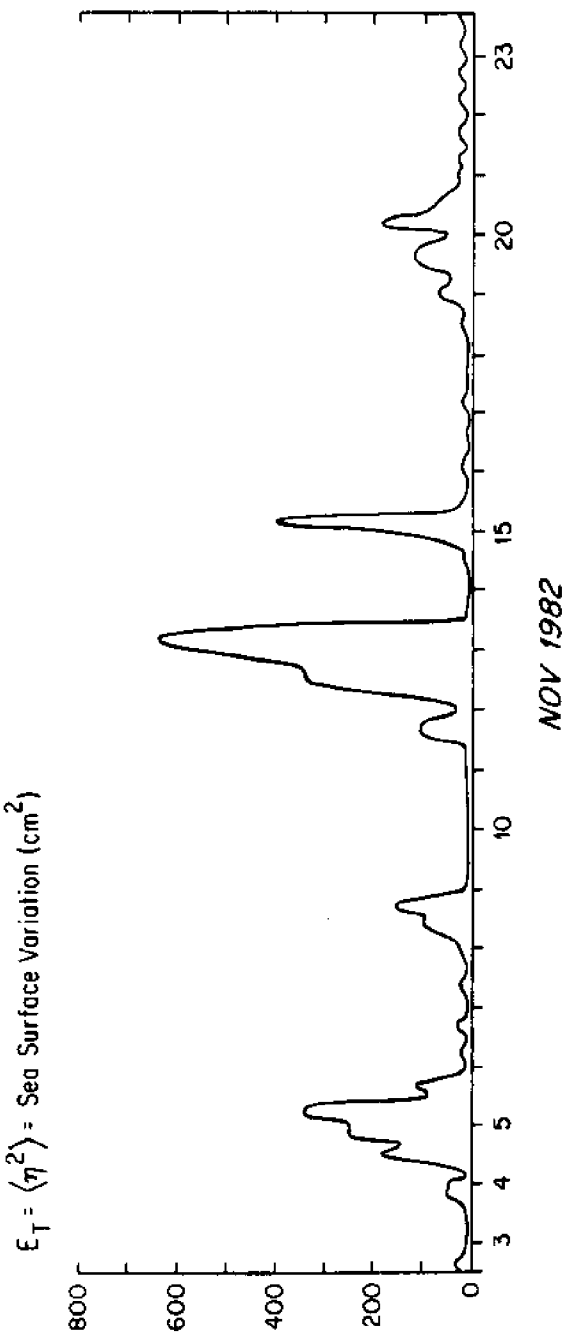

Figure 24. Sea surface variance measured by Sea Data 635-12 at a four-hour increment for a duration of 34 minutes/sample.

where E is the total wave energy, ρ is density of water, and g is the gravitational acceleration. Variance therefore is a direct function of the wave energy. Besides wave variance, another useful parameter representing wave energy is the significant wave height, $H_{1/3}$, where:

$$H_{1/3} \simeq 4 \sqrt{\langle n^2 \rangle} \qquad (2)$$

This wave height is close to the wave height one would estimate visually from a random wave field.

For the period of study, the mean significant wave height was only 0.24 m. The mean peak wave period over the duration of study was between 3 and 4 seconds. The longest peak period measured was 4.3 seconds. Because the analysis was cut off at 3.0 seconds, periods less than this were not measured. Generally there is ample 2 second wave activity in Nantucket Sound, but it is generally of negligible importance for sand transport because of its high frequency and low maximum wave height (limited by a breaking wave steepness). Storm events generate waves with maximum energies at periods higher than 3 seconds in Nantucket Sound.

Surface waves respond directly to local winds at Popponesset Beach, as shown by a comparison of wind stress (related to the square of the wind speed) and wave height or energy variance (figure 25, Appendix III). Over the duration of study, there were four periods when waves exceeded a 0.5 m significant wave height (4-5 November, 12-13 November, 15 November and 20 November). These were all periods when the wind stress exceeded 10 dynes/cm^2, generally with a southerly component (figure 25). When winds had a strong northerly component, wave energy dampened considerably. For example, at 0824 on 13 November 1982 winds at Otis AFB were 19 knots gusting to 29, from the south (190°TN). Four

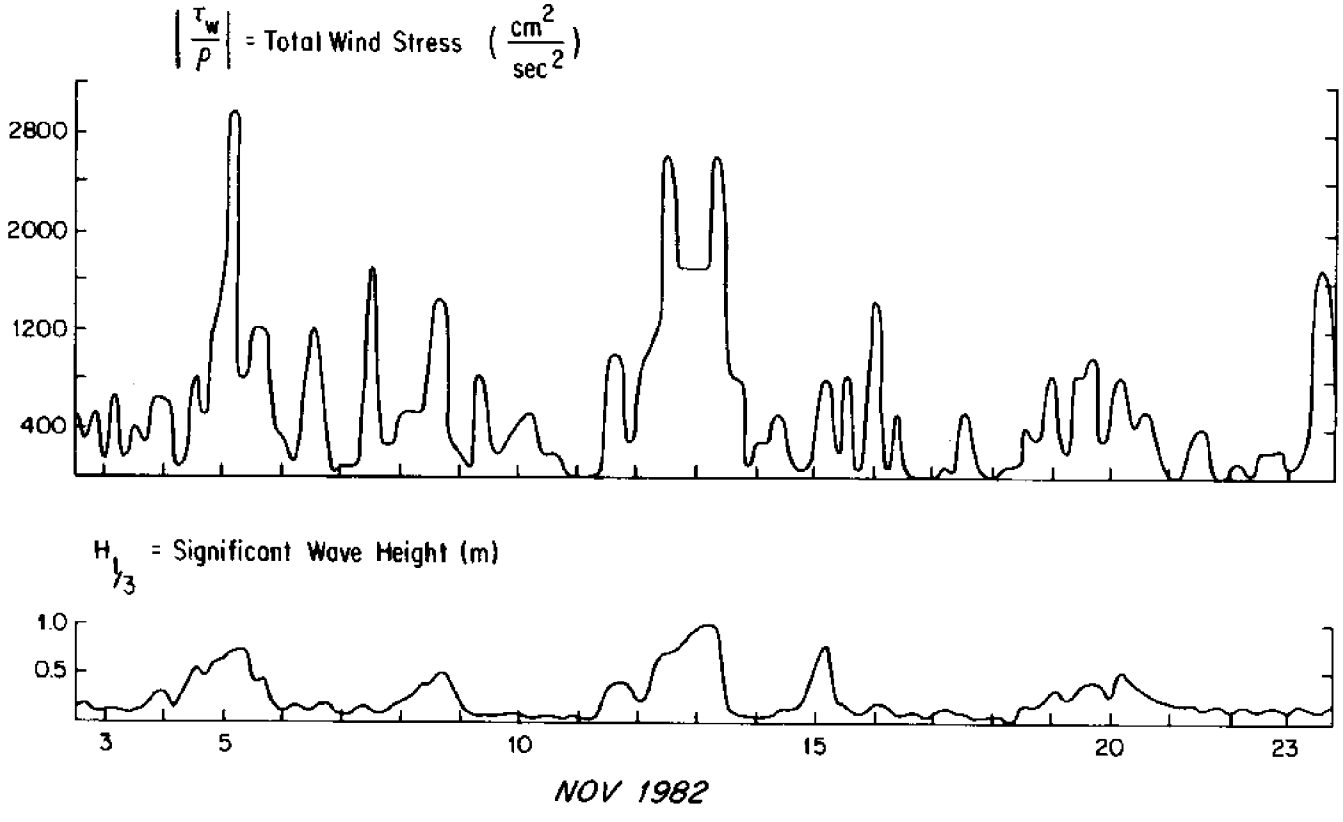

Figure 25. Time series of significant wave height ($H_{1/3}$) and wind stress (τ_w/ρ).

hours later, the winds had shifted to 310° at a speed of 12 knots, while the significant wave height decreased from 0.92 m to 0.14 m. The northerly shift of the wind quickly reduced the incident wave height.

As another indication of the wave response to local winds, the peak direction of the incident waves responded quickly to changes in wind direction (figure 26). Easterly wind stress components created waves traveling to the west, while westerly wind stresses created waves traveling to the east. This local response was pervasive through the period of study; at no time was there any significant low frequency energy propagating into the area from the straits between Nantucket Island and Martha's Vineyard, or Nantucket Island and Monomoy Island. Thus wave prediction for high wind conditions not observed during the study period is possible without considering contamination by distantly generated seas or swell.

I) Aerial Photography

Aerial photographs covering the study area were obtained on 5 dates from August 1981 - October 1982. Four of these sets, taken on 19 August 1981, 21 September 1981, 22 August 1982, and 20 October 1982, are map quality, stereo, vertical photographs. The fifth set, taken 2 July 1982, is a series of 35 mm oblique photos, both black-and-white and color.

The sets of vertical photos for each date include three series of overlapping shots at a scale of 1:18,000. There is more than 1 1/2 inches of overlap on each photo, so that edge distortion is not a problem. Features as small as 1 m can be distinguished on the photos. In addition, the 19 August and 21 September sets include a series of photos covering Popponesset Spit at a scale of 1:6,000.

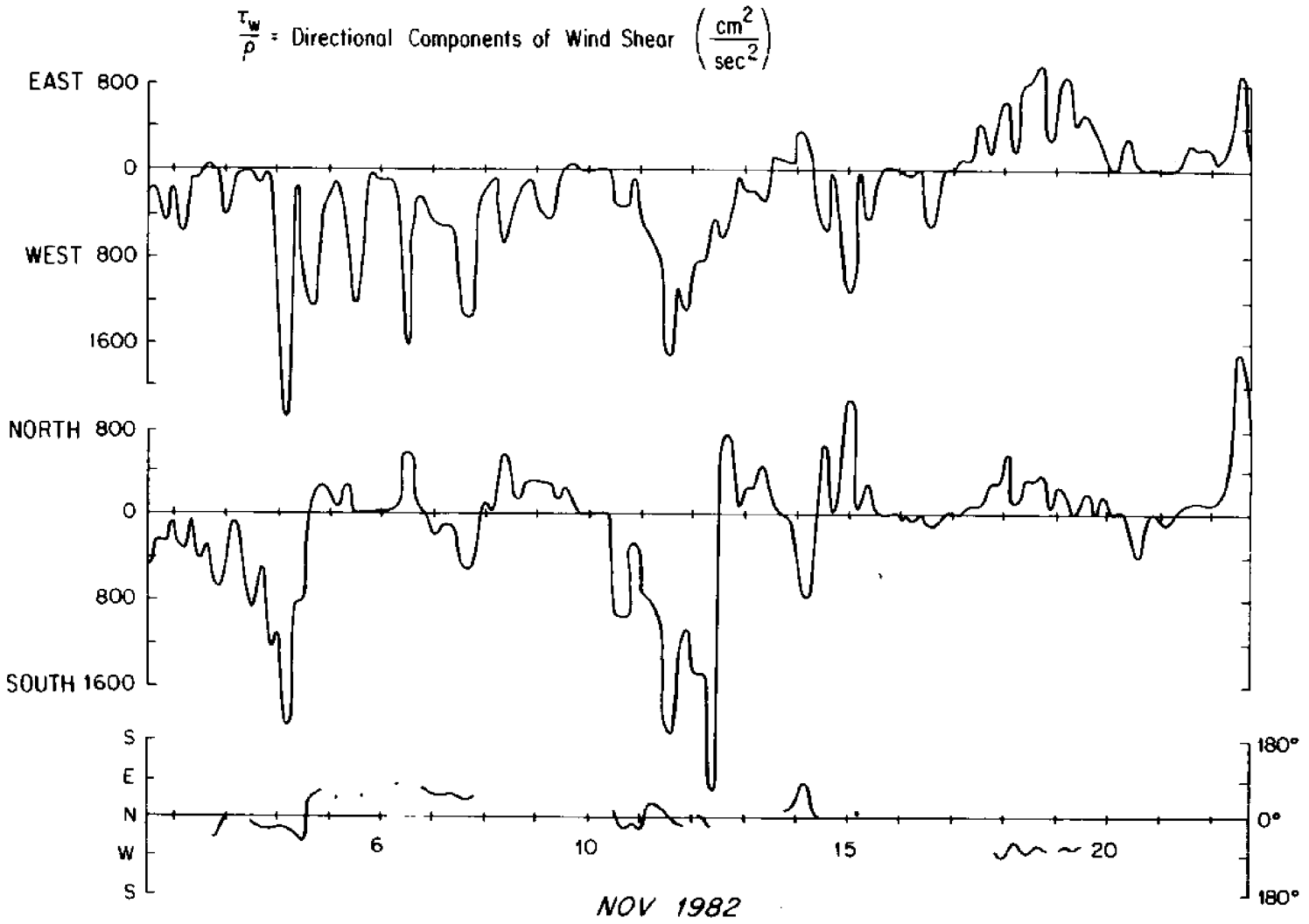

Figure 26. Time series of wave direction (α_o) and wind stress (τ_w/ρ). Wave direction is calculated only for wave heights exceeding 0.25 m.

The vertical photos clearly show both beach features (such as beach widths and engineering structures) and sand waves on the shallow platform. The sand wave migration calculations are based on these vertical photographs. The oblique photos are useful for illustrating changes in shoreline configuration, but not for making quantitative estimates of the changes. Because of their limited usefulness in this regard, a planned bi-monthly collection of oblique aerial photos was cancelled. In addition to the aerial photographs acquired during the study, 43 sets of photos dating from 1938-1979 are available from various sources (Appendix II in Aubrey and Gaines, 1982a), some of which were used for long term estimates of sand wave migration, as discussed below.

J) Shoreline Structures

The study area has many coastal engineering structures, including jetties, seawalls, revetments and groins. Nearly all perform their functions of protecting or enhancing the beaches and bluffs with minimal adverse side effects. A detailed survey of shoreline structures was performed as part of this study, and the results of that survey - including individual descriptions, evaluations and photographs of each structure - are presented in a companion report (Goud and Aubrey, 1983). The general locations and effects of the structures will be briefly discussed here.

The structures are spaced along the shoreline in groups, each group serving the same general protection purpose; each group was labelled as a station for our discussion (figure 27).

Station I consists of two jetties lining the entrance to Waquoit Bay. The channel requires no dredging, and sand build-up southwest of the jetty, while noticeable on aerial photos, overtops the jetty only during high winds. The

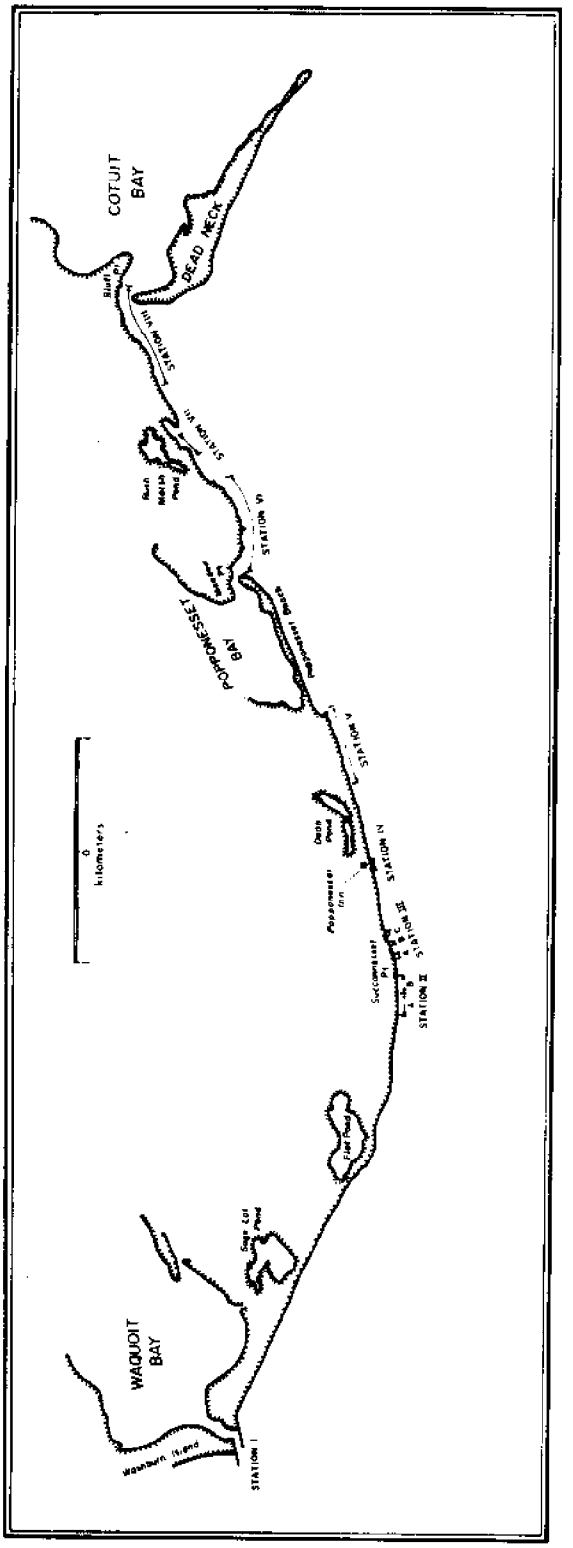

Figure 27. Locations of shoreline structure stations as referred to in text.

jetties, in combination with Succonnesset Shoal, which extends northeast from the end of the jetties, may have a profound effect on the sediment budget for the rest of the study area.

Stations II and III are seawalls designed to protect the exposed cliffs and bluffs (up to 10 m high) of Succonnesset Point. They appear to be effective; when compared with adjacent unprotected cliffs, the reinforced bluffs are decidedly less eroded. Beaches are nonetheless fairly wide (~12 m), indicating that the seawalls do not protect the cliffs at the expense of the beaches, at least under normal conditions.

Station IV is a series of low backshore groins whose purpose is dune stabilization. Their effect is minimal.

Station V consists of a set of groins once blamed for the disappearance of the northeast limb of the spit, with associated seawalls for protection. While beaches are fairly wide in this area (~18 m average), their width does not differ substantially from beaches further south, or even from the width of the spit. The prisms of sand (accretion fillets) captured by the groins change their orientation seasonally, sometimes collecting to the north of the groins, sometimes to the south. These features indicate that the effect of the groins is minor beyond their immediate vicinity (Aubrey and Gaines, 1982a). The groins are usually not filled to capacity.

Station VI is a continuous set of seawalls stretching around Meadow Point, with groins at regular intervals. The seawalls generally protect the bluff from erosion. At the center of the station this is accomplished at the expense of the beaches, however, and in this area very little sand is trapped by the groins due to the lack of sediment supply and constant wave stress. At the northern end of the station, where the shoreline curves away from direct attack by the waves, the groins are effective.

Station VII has received much of the onshore flux of sand from the abandoned spit, and the small embayment is a 3 m deep relic of the abandoned channel. The seawalls protecting a point of land jutting into the bay are crucial to protecting this point from eroding away; otherwise, structures in the area have been rendered obsolete by onshore sand migration.

Station VIII consists of 26 groins, some with seawalls between them. The structures vary in state of repair. In general, the groins which are large and in good shape are effective at preserving the beaches, while the stretches of unprotected shoreline have suffered.

DISCUSSION

A) General Outline of Nearshore Processes

Waves and tides produce different responses in each of the three morphological provinces of the study area: platform, channel and shoal. Each, however, is much more affected on a daily basis by tidal currents than wind-generated waves. The waves have a mean significant wave height of only 24 cm over the 3 weeks in late fall when they were measured and only 18 cm when winds are less than 7.5 m/sec. These waves may be strong enough to affect sediment transport during storm conditions, but can be discounted in calculations for non-storm transport. Tidal currents contain more energy in all environments, with root-mean-square velocities of 0.34 m/sec on the platform and 0.40 m/sec in the channel. Tidal currents in both platform and channel displayed asymmetries, with the stronger flows toward the southwest.

The platform, as discussed above in section F, displays a persistent set of low-amplitude, long-crested sand waves which migrate slowly to the southwest. These bedforms are slightly asymmetric, with their lee slopes oriented toward the southwest. The forms of these sand waves do not respond to daily

tidal fluctuations, though their slow migration results in part from the small tidal asymmetries. Small ripples formed on the flanks of and between the large waves reverse with the tidal flow. No major source of sand for the platform can be identified, since on/offshore exchange is minimal due to the low wave energy, jetties block littoral transport, and shoreline engineering structures prevent terrestrial input.

Patches of large sand waves (heights up to 2 m) are distributed on the channel floor. Despite stronger tidal flows in the channel, nearly all of these waves appear to be permanently oriented with their lee slopes to the southwest like the smaller waves on the platform. The waves are irregularly distributed on the channel floor, in some spots occuring in a regularly-spaced succession of crests, in others as isolated sequences of two or three waves. Their wavelength is characteristically 20 to 30 m. No general pattern of wave distribution is apparent, though the population appears denser in the southwest portion of the channel. Sub-bottom profiling shows the barren areas between sand wave patches as a strong reflector, continuous under the sand waves. The sand waves, therefore, appear as isolated patches of sand moving across a more resistant horizon. Since tidal asymmetry is directed toward the southwest in both the channel and the platform, sand waves migrate in that direction in both areas.

Sand wave heights on the flanks of the shoal are equal to those on the channel floor. The waves are oriented obliquely to the shoal, with their lee sides downslope. Succonnesset Shoal receives sand from tidal bypassing of littoral material at the Waquoit jetties, and the sand waves may provide a mechanism for transferring sand from the shoal to the deeper waters on its flanks.

Storm waves can be hindcast quite simply given the restrictions imposed by local fetches. Measurements show that waves do not penetrate from the Atlantic Ocean into Nantucket and Vineyard Sounds to any appreciable degree. Dominant fetch for storm waves is from the southwest or southeast. Analysis of several years of surface meteorological observations yields a design storm for this area with winds at about 30 m/sec. This design storm will cause waves at Popponesset to reach a period of 5.5 seconds, with a maximum height of 2 meters. Such a storm is expected to reach the coast about once every ten years (note that the design storm requires southeast or southwest winds to build waves to their maximum height).

Since the design storm has an associated onshore wind stress component, the water level during the storm would be superelevated. This would allow the storm waves to pass unbroken over Succonnesset Shoal and over most of the platform. Storm waves could break very near to shore under these conditions.

B) Littoral Sand Transport

The movement of sand in the zone of breaking waves adjacent to a beach is termed littoral sand transport (or littoral drift). Since mechanisms causing sand transport are different between the immediate breaker zone and areas further offshore, it is important to distinguish between these two regions. For this study, littoral sand transport refers to that movement confined to within twenty meters of the subaerial beach. Movement farther offshore will be referred to as alongshore transport.

Littoral drift is caused by currents set up by a gradient in momentum flux resulting from wave breaking and subsequent decay adjacent to a beach (see Komar and Inman, 1971; Komar, 1976). To calculate this flux, offshore wave conditions and nearshore bathymetry must be accurately known. Several

approaches are available for making these transport calculations from offshore wave data. First, if bathymetric contours are straight and parallel, Snell's Law can be applied:

$$\frac{\sin\alpha}{C} = \text{constant} \qquad (3)$$

where α is the angle of approach of the waves relative to a contour, and C is the phase speed of a wave. If bathymetry is more complex, then refraction must be calculated either by graphic techniques or by using a computer. Each technique has its drawbacks. Because the goal of this study was to supply an estimate of sand transport, and the platform bathymetry off Popponesset Spit is relatively straight and parallel, we used a simple application of Snell's Law for water waves. As indicated from the wave data (Appendix III), the most energetic wind waves measured at the wave gage were heading towards 305° and 25°TN (degrees clockwise from true north). On 5 November 1982 storm waves approached at 330°. On 12 November 1982 storm waves initially approached 25°, swung to 340°, then back to 0°TN. On 15 November waves approached 305°. These three samples were used to calculate sand transport as follows.

Assuming wave energy flux is approximately conserved from the wave gage in to the point of wave breaking on the beach, the following identity holds:

$$ECn\cos\alpha = \text{constant}. \qquad (4)$$

where n is the ratio of the wave group velocity to phase speed, and E is the wave energy, defined in equation (1). Field measurements (see, for example, Komar, 1976) have shown that the immersed weight transport of sand I is given by the formula:

$$I = K(ECn\cos\alpha\sin\alpha)_b \qquad (5)$$

where K is a constant (≈0.77), and the subscript b refers to conditions at breaking. The "at rest" volume transport rate of sand (Q_ℓ) is related to the immersed weight transport rate by:

$$Q_\ell = {}^{I_\ell}/_{(\rho_s-\rho)g\ N_o} \tag{6}$$

where ρ_s is the density of sediment, ρ is the density of water, and N_o is the volume concentration of sand (usually set equal to 0.6 for well-sorted sand at rest). From the previous relations, we can express the immersed weight transport rate as:

$$I_\ell = K(ECn\ \cos\alpha)_o \sin\alpha_b \tag{7}$$

$$= K(ECn)_o \quad \frac{S_o}{S_b} \quad (\cos\alpha\sin\alpha)_b \tag{8}$$

where the subscript "o" refers to conditions at the observation station offshore, and the "s" refers to wave ray separations. We will use equation (7) for our calculations, where the strike of the beach is 37°TN (so a perpendicular is 307°TN).

Because wave data was acquired for one month of twelve, littoral sand transport calculations are made for representative and maximum wave conditions, then constrained from a knowledge of the mean annual wind field. Mean annual wind fields were taken from two sources: the Summary of Synoptic Meteorological Observations (SSMO) available from the National Climatic Center were compiled for the years of 1856-1971, and observations from Logan Airport and Nantucket Airport were compiled for four years from 1970-1974 (figure 28, from Miller and Aubrey, 1983). SSMO data was compiled for two offshore sectors (Quonset and Boston Marsden squares), which includes Nantucket Sound. Although these results are not specific to Nantucket Sound alone, they provide a good indication of wind activity, particularly from an historical perspective.

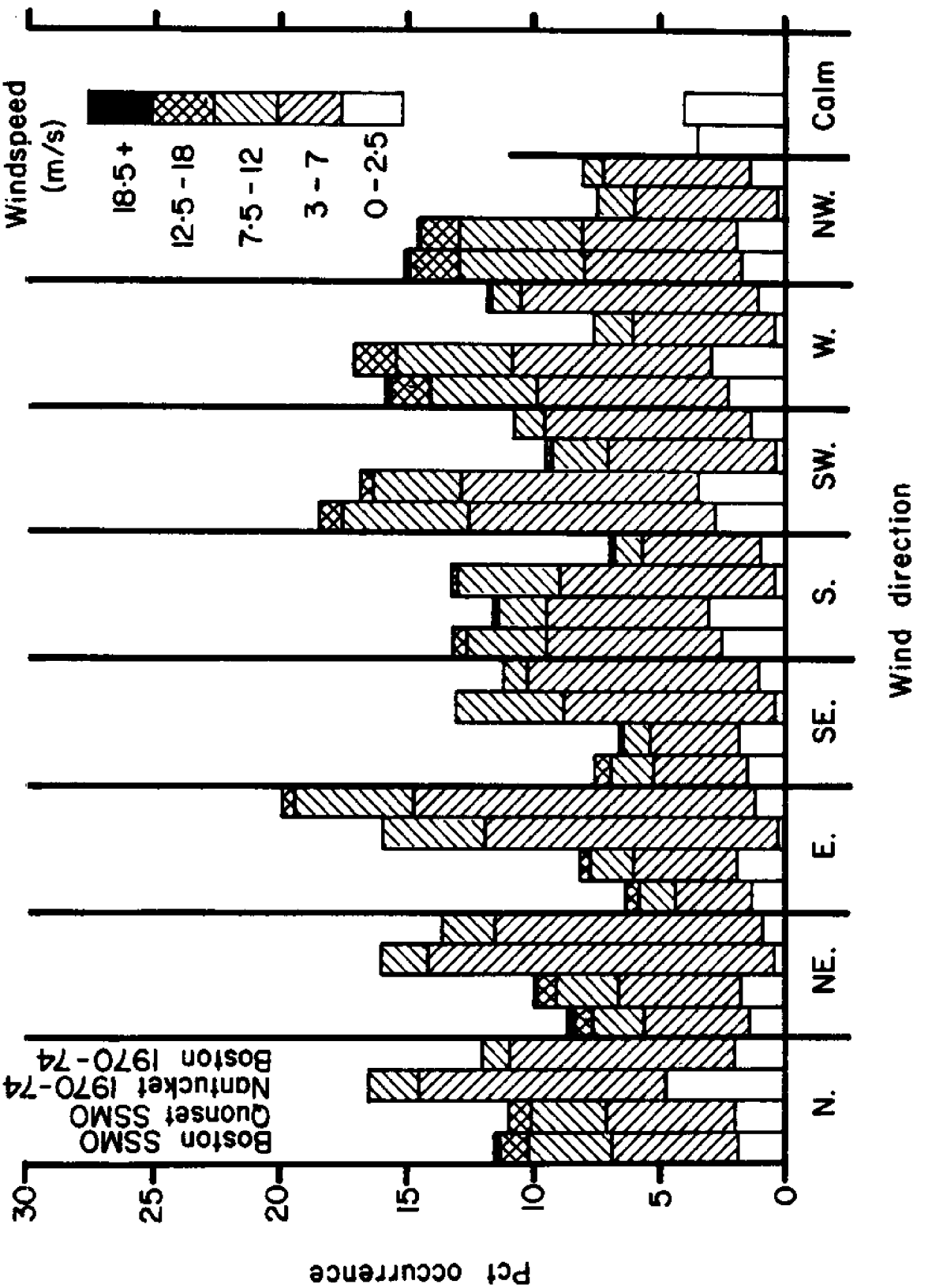

Figure 28. Comparison of average long-term (1874-1970) SSMO wind data from Marsden Square 12 (Boston) and 13 (Quonset) with winds recorded at Nantucket and Boston during the study period (1970-1974).

These data show the most frequently occurring winds are from the southwest, west and northwest, while the strongest winds are from the west, northwest, north or northeast. For the shorter periods of observation at Boston and Nantucket, however, the most frequent winds were from the southwest clockwise through the east.

Based on the SSMO observations, winds exceeded 12.5 m/sec about 8 percent of the time, and exceeded 18.5 m/sec less than 1 percent of the time. For these more energetic events, frequency of occurrence was nearly evenly split between winds with westerly components and winds with easterly components. We used this information to estimate littoral transport rates and net yearly littoral drift. Finally, these calculations were compared with observations and indirect estimates of longshore transport rates.

Maximum windspeeds with southerly components observed during the November, 1982, wave measurements were 10 m/sec. These winds generated waves with a significant height of about 1.0 meters, and a period of four seconds. For a 12.5 m/sec windspeed, maximum heights would be about 1.3 meters with a maximum period of 5 seconds and a maximum angle of approach in 6.5 m water depth of 250°TN (which is 78° from shore normal). If these waves occur 8 percent of the time as they did in October/November 1982, all coming from the same direction, maximum littoral sand transport would be about 53,000 m^3/year. Wind data (figure 28) shows these higher energy waves are more evenly distributed between easterly and westerly angles of approach, so the net transport is much less than the gross. In fact, winds with westerly components occur about twice as frequently as those from the east. Disregarding for the present moment any north/south components of the wind (which will affect the development of the wave field), maximum net storm transport would be less than 20,000 m^3/year to the northeast. Since northerly wind components reduce the energy of shoreward propagating waves

net transport is even less. If we examine only those winds from west, southwest, south, southeast and east, we find percent exceedance of 12.5 m/sec winds drops to four percent of the time. This lowers the estimate for maximum storm littoral transport to less than 10,000 m^3/year, to the northeast.

Finally, using a mean energy variance over the year of 0.0061 m^2, and a period of 3.5 seconds, we calculated the maximum gross littoral transport. Taking the $(\cos\alpha)_o(\sin\alpha)_b$ product to be near its maximum, we obtain an estimate of gross potential littoral transport of 110,000 m^3/year. Net transport is much less than this for two reasons: first, wave approach is nearly evenly distributed between east and west directions; second, there is inadequate sand available to support such a transport rate. Consequently, actual littoral transport is much less than potential transport when there is inadequate sand in the system. At Popponesset, parts of the beach are composed of cobbles, so the sand is certainly not available for transport at those locations.

These calculated net transport rates (order of 10,000 m^3/year) are in agreement with indirect observations made by Aubrey and Gaines (1982a), who noted a distinct seasonal trend in transport direction as shown by change in orientation of accretion fillets adjacent to groins. As evidence for small littoral transport rate along Popponesset, three observations were mentioned:

A) Stability of temporary breaches along Popponesset Spit without infilling;

B) Persistence of relicts of the 1954 inlet channel, which are still visible after nearly thirty years; and

C) The failure of the groin field just southwest of Popponesset Spit to either completely fill in or modify the updrift shoreline.

These calculations and observations therefore suggest a limited net littoral transport on the order of 10,000 m^3/year or less, which is superimposed on a transport with seasonal variability in magnitude and direction.

Although not studied in as much detail, littoral transport rates between the Waquoit jetties and Succonnesset Point, and from Cotuit inlet eastward to Osterville Point, have been considered. East of Waquoit jetties, historical evidence on winds and waves indicate transport to the east, opposite that suggested by Brownlow (1979) based on unknown evidence. Immediately adjacent to the eastern Waquoit jetty, there may be a local reversal in direction. Littoral transport in this area is considerably confused by the presence of a complex system of shoals immediately offshore. Succonnesset Shoal itself attaches to the mainland near this point, which may allow significant tidal transport in shallow waters. This net westward tidal transport may provide material for the nearshore shoals, and may help nourish the beaches immediately west of Succonnesset Point.

From Cotuit Harbor to Osterville Point, littoral drift has a net westward component. This drift has been interupted by jetties to West Bay which were constructed around 1900. Subsequent to the West Bay jetty construction, the beach to the east of the jetties has accreted, while those to the west (comprising Dead Neck) have eroded so that portions of Dead Neck are increasingly susceptible to overwash and breaching. Nourishment in the area immediately west of the West Bay jetties is strongly advised (and in fact was occurring at the time this report was written).

C) Alongshore Sand Transport

Alongshore transport in the Popponesset area results from the strong tidal flows in the area, augmented by the higher flows and wave action occurring during storms. Aerial photographs show sand waves migrating to the southwest

over periods of years. The measurements of tidal velocities in both platform and channel current meter deployments conform with these long-term observations, showing net tidal asymmetries toward the southwest. Having noted this qualitative agreement, more precise descriptions of sediment behavior are desirable.

The volume rate of sand transport can be calculated in two ways. With the first method, we determine the volume of sediment in a sand wave from bathymetric profiles, then calculate the net transport rate from sand wave migration distances. In the second, the rates are theoretically derived from current velocity measurements using fluid dynamic theory and semi-empirical formulas. The latter method provides estimates for both gross and net transport rates, for that portion of sand transport due to tidal asymmetry. The net migration is useful for general models of sediment behavior patterns, while the gross transport would be needed for forecasting dredging frequency, since sand would be transported into such a sink from both directions. The methods will be discussed separately, and the results compared.

As mentioned in the preceding section, this alongshore transport is to be distinguished from littoral transport. The latter results from oblique wave action on the shoreline, and is confined to the immediate nearshore. Alongshore transport is caused by steady or quasi-steady action of currents and waves in deeper water farther from shore. In the Popponesset area, however, non-storm wave energy is so minor that it has been ignored in transport calculations.

1) Sand wave migration

Maximum and minimum volume transport rates were determined from the bathymetric and photographic data. The minimum estimate is based on the assumption that the sand wave volume is concentrated in the immediate vicinity

of the crest, forming in cross-section an isolated, asymmetric triangle which migrates across the flat platform. The maximum estimate adds to that volume a layer of "active sand" 15 cm thick across the interval between sand waves. This approach was taken because the aspect ratio (wave length/wave height) of the sand waves is so large that the stoss (updrift) slope of the wave appears flat a short distance from the crest, thus giving the impression of the isolated, migrating wave. Unless the waves are migrating across a hard-packed, shallow substrate, however (as is the case in the channel), sand movement is probably occurring across the entire length of the wave. The wave height averages about 50 cm, and bathymetric profiles of the platform allow a rough estimate of the average stoss slope. From these observations, an average thickness of 15 cm across the entire length of the wave, beyond the estimated sand wave volume, was determined to be the maximum expected transport volume per wavelength.

The volume of sand contained in a single sand wave was calculated using a V_E (volume/meter of crest length/wavelength) of 10.1 $m^3/m/\lambda$, determined from a series of closely-spaced lines across a single sand wave. The area across the sand wave was calculated on each line; each area was multiplied by a representative crest length; the volumes were added together, then divided by the total crest length to give an average volume/m of crest/wavelength. The volume must be divided by the wavelength to give an average for the platform since this model assumes all sand moves as waves.

Sand wave migration distances were determined for 1971-81 and 1981-82 using vertical aerial photographs, at a common scale. Migration distances range from 0-35 m in one year, and from 54 to 200 m in 10 years (figure 17 and 18; table 3). Because of finite crest widths and sun angle, the accuracy of the 1-year migration estimates is not less than 15 m. Errors in

transferring the 1971 photo scale and slight changes in wave orientation and shape over the longer period yield an uncertainty of about 35 m for the 10-year estimates. Within these limits, agreement between the 1-year and 10-year migration figures is good.

The transport calculations used the formula

$$V_S = V_O \, D/\lambda \qquad (9)$$

where V_S = volume transport rate in m^3/yr

V_O = volume/wavelength in m^3

D = crest migration distance in m/yr

λ = wavelength in m

The formula for V_O depends on whether the maximum or minimum value is being calculated.

$$V_{O\,min} = V_E \, L$$

$$V_{O\,max} = V_E L + H \, \lambda \, L \qquad (10)$$

where V_E = sand volume/meter of crest length/wavelength = 10.1 m^3

L = wave crest length in m

H = estimated thickness of "active layer" = 0.15 m

To normalize for differences in transport across the platform, V_S was divided by the wave crest length to give

V_N = volume transport/year/m crest length.

When, as was often the case, the wavelength or crest migration distance varied along a wave, the wave was segmented, and the volumes summed.

These calculations were done on several waves, with crest lengths varying from 100 to 435 m and volumes ranging from 727 m^3 $< V_S <$ 4394 m^3, minimum, and 1807 m^3 to 10,582 m^3, maximum. The normalized values had a more compact range, from 0.7 $< V_{N\,min} <$ 1.4 $m^3/yr/m$ crest length, and 2 $< V_{N\,max} <$ 3.3 $m^3/yr/m$ crest length.

Since V_N is normalized for the entire length and width of the platform, volume transport past any transect normal to shore on the platform can be calculated by multiplying V_N by the width of the platform. For example, for a point just off Popponesset Beach where the platform is approximately 1 km wide, estimates of total volume transport, V_T, fall in the range:

$$700\ m^3/yr < V_{T\ min} < 1400\ m^3/yr.$$

$$2000\ m^3/yr < V_{T\ max} < 3300\ m^3/yr.$$

2) Theoretical transport rate

Sediment transport occurs when the shear stress on the seafloor is strong enough to place sediment grains in motion. This shear stress is caused by the motion of the fluid above the bed, its strength determined by a complex interaction of currents, waves and seafloor topography. Hydrodynamic theory and empirical models of bedload transport have, in recent years, provided models which can be used with field observations to predict volume transport rates. Certain simplifying assumptions must be made with respect to the field data and uncertainties always exist when laboratory models are transferred to field situations, still, calculations using these models are reliable to within an order of magnitude (factor of 10).

The procedure used for the Popponesset data is outlined here, with references provided if more detail is desired, and a sample calculation provided in Appendix IV. Boundary shear stress was calculated from current velocity data using the Law of the Wall (logarithmic velocity profile-Schlicting, 1968). Small ripples were assumed to be the primary roughness elements, their height and wavelength determined by the median grain size (Yalin, 1972), their equivalent sand grain roughness calculated using a recent theory (Grant and Madsen, 1982). This total boundary shear was divided in to skin friction and form drag components using a drag partitioning scheme

(Engelund, 1966), and the skin friction value used to test for initiation of motion using the Shields criterion. If the Shields Paramater was greater than the critical value for the grain size, a transport rate was calculated using the Meyer-Peter and Müller bedload formula (Yalin, 1972). This procedure was followed 2048 timed (by computer), each velocity value representing a 640 second average, with the total record spanning 19 days in October/November 1982. The positive (northeast) and negative (southwest) values were summed separately to provide total transport in each direction, then the two were added to produce a net transport estimate.

The calculations were performed using a range of parameters to provide limits on the transport estimates. Variations in the critical Shields Parameter, the partitioning ratio and the roughness produced differences in net transport of less than a factor of three. A typical calculation, using an equivalent sand grain roughness of 10.5 cm, partitioning ratio of 0.6 (skin friction/total boundary shear stress) and critical Shields Parameter of 0.035, gave the following transport figures for a 1km wide stretch of platform:

Transport to the northeast=147 m^3/yr

Transport to the southwest=327 m^3/yr

Gross transport=475 m^3/yr

Net transport=180m^3/yr

These numbers are within an order of magnitude of the minimum sand wave migration calculations, but substantially lower than the maximum. The general uncertainties in the methods can account for much of the disparity. Other sources of uncertainty come from storm input: transport goes up rapidly with increased currant velocity and with wave strength. Much of the transport observed as sand wave migration is due to storm events. Storm waves are longer than the waves occurring during our field measurements; such waves

increase the sediment transport rate becouse of the high boundary shear stresses associated with surface waves. Consequently our theoretical transports are biased towards low wave action; theory and measurements would agree more closely if wave/current interaction were incorporated in our calculations.

In summary, both methods confirm our initial impression of low volume, current-dominated transport to the southwest. The figures can be used to place constraints on dredging frequency for offshore channels.

D) Shoreline Changes: Observed and Predicted

Most beaches in the study area have been stable, their widths varying little over the last several decades. Aerial photographic evidence for this is documented in Aubrey and Gaines (1982a), where they measure beach widths at 19 different stations from Waquoit to Rushy Marsh Pond over a period of 40 years. The exception to this stability is the northeast limb of Popponesset Spit and the stretch of Meadow Point which had been protected by the severed limb of the barrier beach. This section of the shoreline remains the only area seriously out of equilibrium with the forcing mechanisms, and therefore the area most likely to change substantially in the near future. The remainder of the coastline will change slowly, unless affected by a catastrophic event such as a major storm.

A breach in Popponesset Spit in 1954 at the site of the present inlet caused the abandonment of the northeast limb. Following the breach, the northeast limb of the spit moved shoreward. Seaward of Meadow Point the spit quickly filled its former channel, leaving the shoreline exposed to wave attack. Only seawall reinforcement along the most exposed headland of the Point deters retreat of the bluff, and the beaches retain little sand, despite a sequence of groins at regular intervals. North of the headland, where the

shore is protected from direct wave attack, sand from the spit has accumulated onshore after filling the former channel, creating a wide, stable beach. Near Rushy Marsh Pond, as much as 30 m of sandy beach has been added.

The major relic of the former elongated channel is the small embayment directly seaward of Rushy Marsh Pond. It reaches depths of 3 m (as compared with the average 1-2 m depths just outside the embayment), but it will continue to fill over the next 10 to 15 years. The embayment causes an erosion problem north of the Meadow Point headland, as a small, exposed point of land on its southwest side has been retreating by several feet per year in recent years. The point was reinforced in the winter of 1982 to retard erosion.

Land on both sides of the mouth of Popponesset Bay is likewise susceptible to change. Ebb tidal flows attack Meadow Point as they turn the corner from the channel parallel to Popponesset Spit and enter Nantucket Sound, resulting in bluff erosion roughly at the rate of 2 m/yr. This erosion will continue unless the bluff is reinforced. The northeast end of Popponesset Spit has been rotating toward Popponesset Bay, as a result of ebb flow curvature depositing sand on the inside of the bend.

The spit has been migrating shoreward since 1938 at a rate of about 0.2 to 1.5 m/year, the higher rate applying to the northeastern tip, as documented in Aubrey and Gaines (1982a). Major storms are responsible for nearly one-half of the shoreward migration rate of the tip of the spit, for a total of about 140 m there, and have caused nearly all of the migration of the shore-attached end (storm-related migration of 55 m total in 35 years). Despite efforts at planting grasses on the spit to increase its stability, its low elevation makes it susceptible to overwash during storms, and landward migration will probably continue. The width of the spit varies occasionally, tending to become temporarily narrower in the wake of large storms, but has been generally

stable. Since a channel was dredged between the spit and Popponesset Island in 1961, however, scouring by tidal currents has caused thinning of the barrier beach from the backside. This location is particularly susceptible, therefore, to overwash and breaching. Openings to the bay have occurred at this location in the past (figures 4-6), but the main tidal channel did not skirt the spit before the 1961 dredging. A breach, therefore, could evolve to become the stable inlet unless this is actively prevented in the near future.

Because there is no sand source for the area, sand which is removed is not naturally replaced, leaving the remainder of the beaches susceptible to slow attrition. Artificial nourishment of the beaches, therefore, will be advisable periodically.

MANAGEMENT STRATEGIES

Five aspects of coastal management are considered in this section: beach stability and nourishment of nearshore regions using imported sand; effectiveness of coastal engineering structures in mitigating erosion and protecting property; dredging of navigation channels within Popponesset Bay, Popponesset Inlet, and Nantucket Sound; offshore dredging for beach renourishment; and land use and shoreline property management. Options for management strategy are presented here, with selection of a single eventual strategy for implementation in part dependent upon local interests. All strategies are based on our scientific assessment of physical nearshore processes along the Nantucket Sound coast of Mashpee, treating biological and chemical processes only peripherally. These management options were formulated with the Massachusetts CZM regulatory and nonregulatory policies (State of Massachusetts, 1978) in mind.

These management guidelines in some instances include several options for alleviating particular coastal problems. Selection of a particular option must be made by the Town of Mashpee, in consultation with scientists, engineers and planners and in light of the potential impact of each of these strategies on its coastal resources. The authors do not address the political, legal, economic, cultural and aesthetic trade-offs. The strategies proposed here reflect a scientific bias which must be balanced by those other considerations. Since the management strategy may have long-lasting effects on future coastal development, considerable thought and discussion is warranted on the Town's part.

No engineering design for dredging or renourishment projects has been performed as part of this report. Such projects should be planned by competent, registered civil engineers familiar with coastal problems, in conjunction with physical scientists familiar with the region. Much scientific information required for such design has been included in this report.

Finally, management recommendations are centered on the beach and offshore regions, less so on the estuarine problems. This emphasis mirrors the emphasis of the study, which was directed at offshore processes.

A) BEACH STABILITY AND NOURISHMENT:

Assessment of the stability of beaches in the study area is based on both historical evidence and estimates of on/offshore and littoral sand transport rates and patterns. In general, beach nourishment appears to have a good potential for success, due to the following factors.

1. Littoral sand transport rates in the area are low, as determined by indirect estimates based on observations of inlet behavior and sand bar migration (see Aubrey and Gaines, 1982a, b) and calculations based on *in situ*

wave measurements. Both techniques suggest net littoral transport rates on the order of 10,000 m^3/year or less, an order of magnitude less than some have suggested. Actual transport rates may be even lower than potential rates in areas where there is no available sand-sized sediment. The large stretches of Popponesset beach composed of cobbles and pebbles, suggest an inadequate source of sand. The region from Succonnesset Point to the Popponesset barrier spit is probably starved of sediment input due to seawall construction removing seacliffs as a source of sediment for beaches. To the northeast, from Meadow Point to the north, longshore transport rates appear to be low, with no general loss of sand-sized material. However, after a large storm event during which large quantities of sand are moved offshore, the continuous line of structures in this region will prevent natural renewal of the beaches. In this case sand must be replenished from alternative sources (brought in from land or dredged from offshore); this replacement sand will then be relatively stable until a subsequent large storm.

2. On/offshore sand transport: Other than the normal seasonal onshore/offshore exchange of sediment, on/offshore sand transport appears to be limited, and local. Because of their low migration rates, small sand volumes and movement parallel to shore, the sand waves populating the offshore platform shown on aerial photography appear to be an insignificant factor in beach nourishment/erosion. Elsewhere, local effects dominate. The entrance channel to Waquoit Bay, with its two jetties, removes sand from the nearshore and funnel it into deeper water offshore, where it adds to the offshore shoal system. The sand moved offshore is then not immediately available to nourish downdrift (to the east/northeast) beaches. This probably accounts for the ample sand supply west of Succonnesset Point where the shoal joins the main-

land, and lack of it to the east. Such shoal bypassing has been observed elsewhere (Seymour and Aubrey, in prep.), with consequent severe impact on beach rejuvenation following large storms.

From Succonnesset Point northeast to Cotuit Highland, beach renourishment may be the only way to maintain a wide, nearly continuous recreational beach. To nourish the beach extending from Succonnesset Point northeastwards 3 km would require approximately 10,000 m^3 of sand. Considering the low net littoral transport rate in this area, such a magnitude of renourishment should maintain a recreational beach for at least five years after nourishment. This would replace the natural renourishment which historically has come partly from erosion of sea cliffs.

3. Grain size compatibility: The natural grain size along the beach is highly variable, with median size ranging from fine sand to cobbles. This variability reflects local source material, sand starvation and subsequent lag deposits, wind erosion, and, to a very small degree, longshore sorting processes. This large variability suggests that a grain size match for beach renourishment would be fairly easy, accepting whatever local sorting will certainly take place (e.g., through wind erosion along Popponesset barrier beach). Offshore sands are generally coarse, and would be a possible source for renourishment material. The gas deposits described in the sub-bottom profiling section pose the only known restriction to an offshore source for the sands, since the gas-soaked sands may be inappropriate for beach replenishment.

B) IMPACT OF COASTAL ENGINEERING STRUCTURES:

More than seventy-five coastal engineering structures have been placed along the Nantucket Sound shoreline of Mashpee in the past century. These are described in detail in a related technical report (Goud and Aubrey, 1983). These structures range from being extremely effective, to completely ineffective, at mitigating shoreline erosion and damage. This range in effectiveness reflects a number of factors, including structural integrity and local erosion/accretion patterns. Two regions define the study area from the standpoint of coastal structures. Region I, from Popponesset Spit south to Succonnesset Point, has a lower density of shoreline structures than Region II, extending from Meadow Point to Cotuit Highland. Future structural management for the two areas may be different.

Region I includes only a few groins and several seawalls. Groins have been locally useful for maintaining beach width, but from a historical perspective do not appear necessary. Long-term changes (over a 40-year period) in beach width, locally or on adjacent properties, do not appear to have been influenced by the groins. Their use in the future should be discouraged, both to minimize any interruption of littoral transport, and to reduce the safety hazard they introduce. Seawall construction in this region has increased rapidly as waterfront population density has risen. Because past zoning laws have not encouraged adequate set-back requirements, the slowly-eroding cliffs have encroached on this beach front property, particularly at Succonnesset Point and near Popponesset Spit. Owners have resorted to rip-rap, seawalls and revetments to deccelerate this process. This removes a source of sediment from the nearshore to nourish beaches; the narrower beaches provide even less protection from wave action, thereby increasing the need for structural

reinforcement. An alternative to protecting bluffs structurally is to increase beach width through renourishment, thereby increasing natural bluff protection. This renourishment would also increase the recreational use of the beach.

A nearly continuous string of seawalls and groins in its southern end; to the north, approaching Cotuit, there is also a high density of shoreline protection structures. In the middle there are few active shoreline structures because of the addition of large quantities of sand from the separated north link of the pre-1954 elongated barrier spit. The Meadow Point Coastline has been exposed since 1954 to waves which had been previously absorbed by the elongated spit. There is no simple alternative in the south part of Region II to structural protection, because of the high structural density already present. Renourishment would increase pocket beach width and help protect bluffs, but any such material is prone to removal during storms, necessitating additional nourishment. In the north part of Region II, erosion is caused in part by the Cotuit Bay Inlet. As Dead Neck has extended to the west (an occurrence which is common throughout the last 200 years) the tidal channel has encroached against Cotuit Highlands. With the slight channel curvature (concave to the east), bank erosion is accelerated. The only remedy for these homeowners is continual renourishment, or straightening of the tidal channel in a future dredging operation. In the past two hundred years, as Dead Neck lengthened, a breach has occurred separating most of Dead Neck from its isolated extension (known as Sampson's Island). Relicts of these former breaches still exist. If left to its natural evolution, a similar breach might occur over the next half century. Although this would alleviate erosion

at Cotuit Highlands, it would inhibit navigation unless the western (present) inlet were closed. Some community options for this eventuality should be formulated before such a breach occurs (e.g., dredge or no dredge; straighten channel or leave as is).

C) MAINTENANCE OF NAVIGABLE WATERWAYS:

For some time there has been concern for establishing and maintaining stable navigation channels within and external to Popponesset Bay. If such channel projects are to be continued in the future, the following elements need consideration.

A stable navigation system will depend on access to deeper waters within Nantucket Sound, a stable inlet (in both location and in depth), and navigable channels in Popponesset Bay. In order to be effective, a system must be designed with all elements in mind. The shallow depths over the offshore platform, the shallow depths with the limited embayment (Popponesset Bay), and the low tidal range in this region all combine to make stable navigation channels more difficult to maintain.

Options for waterways navigation include:

a) Continuing the status quo (no-change option): This is the option followed for the last decade or so, not necessarily because of intent. If nothing is done to change the situation, one can anticipate the following problems. Navigation from Popponesset Bay to the deeper waters of Nantucket Sound will only be possible near higher waters, because of bay and sound shoals. Even shallow draft vessels will have difficulty navigating. In particular, the rapid build-up of the flood tide delta within the bay will restrict navigation more than before (the construction of this feature is discussed later in this section). The inlet position will likely continue to

migrate to the northeast, at a relatively slow rate (1.5 m/yr), continuing to erode Meadow Point. A breach may develop along the barrier beach near Popponesset Island, as the barrier beach continues to migrate landward, encroaching on the primary navigation channel within the bay. A response to such a breach formation must be rapid, and based on a management scheme accepted by the Town of Mashpee. The implications of such a new breach are profound, in terms of patterns of erosion and flushing of the estuary/bay system. The southern end of Popponesset Island would be subject to erosion; bathing beaches in the bay would be lost, and private property would be at risk. If both inlet channels were to remain open for an extended period of time, neither inlet would be navigable except at the highest waters. Even then navigation would be treacherous. If the present inlet filled in, tidal flushing patterns would be altered. Tidal phase lags to different parts of the inlet would change, and tidal elevations could also change. Contrary to the report by CDM (1981) there are significant tidal differences between Nantucket Sound and the distant reaches of Popponesset Bay. With changes in circulation patterns would come changes in shoal locations, perhaps affecting shellfish resources. Changes in circulation could also cause local degradation of water quality, while improving it elsewhere. Such changes are difficult to quantify a priori, except for erosion along Popponesset Island which is certain to occur.

b) Improving navigation only within the bay/estuary. This option would provide for increased tidal flushing, with consequent increase in water quality within the bay. Some increase in inlet stability will result, with more consistent channel depths throughout the year. This option requires some management decisions. The optimal pattern for channel distribution through

the bay is dependent on its usage. Maintenance of two channels from the inlet (one to Popponesset Island, one to Mashpee Neck), as is now occurring, encourages more rapid sedimentation in the channels. A single channel has more potential to be self-scouring; two channels would almost certainly result in increased maintenance dredging requirements.

The present channel distribution could be improved by some simple rearrangements, resulting in better recreational conditions as well as water exchange. One simple option for dredging which would improve circulation and still remain viable if the Town opted for a southwesterly inlet (near Popponesset Island) involves a minor change from existing channel patterns (figure 29). The proposed channel configuration makes use of the present connector between the inlet and Popponesset Island. A new channel would connect this channel to the channel north of Popponesset Island, as indicated. Although this new arrangement would require a longer run from Mashpee Neck to the inlet, the channel should be more continuously navigable. The former dredged channel from the inlet to Mashpee Neck (indicated on figure 29) could be allowed to fill in naturally or could be a receptacle for dredge spoil disposal for material incompatible with barrier beach deposits (where the majority of dredge spoil should be placed).

This new channel alignment may require some relocation of shellfish resources, but overall should provide a better flushed, more navigable estuary for natural and anthropic use. Specific dredged channel depths, channel widths, etc. must be specified by a competent dredging engineer, in conjunction with scientific and management personnel. Rates of channel infill are not specifically known, since this study did not addres estuarine sediment transport. However most of the estuarine channels dredged in 1961 are still

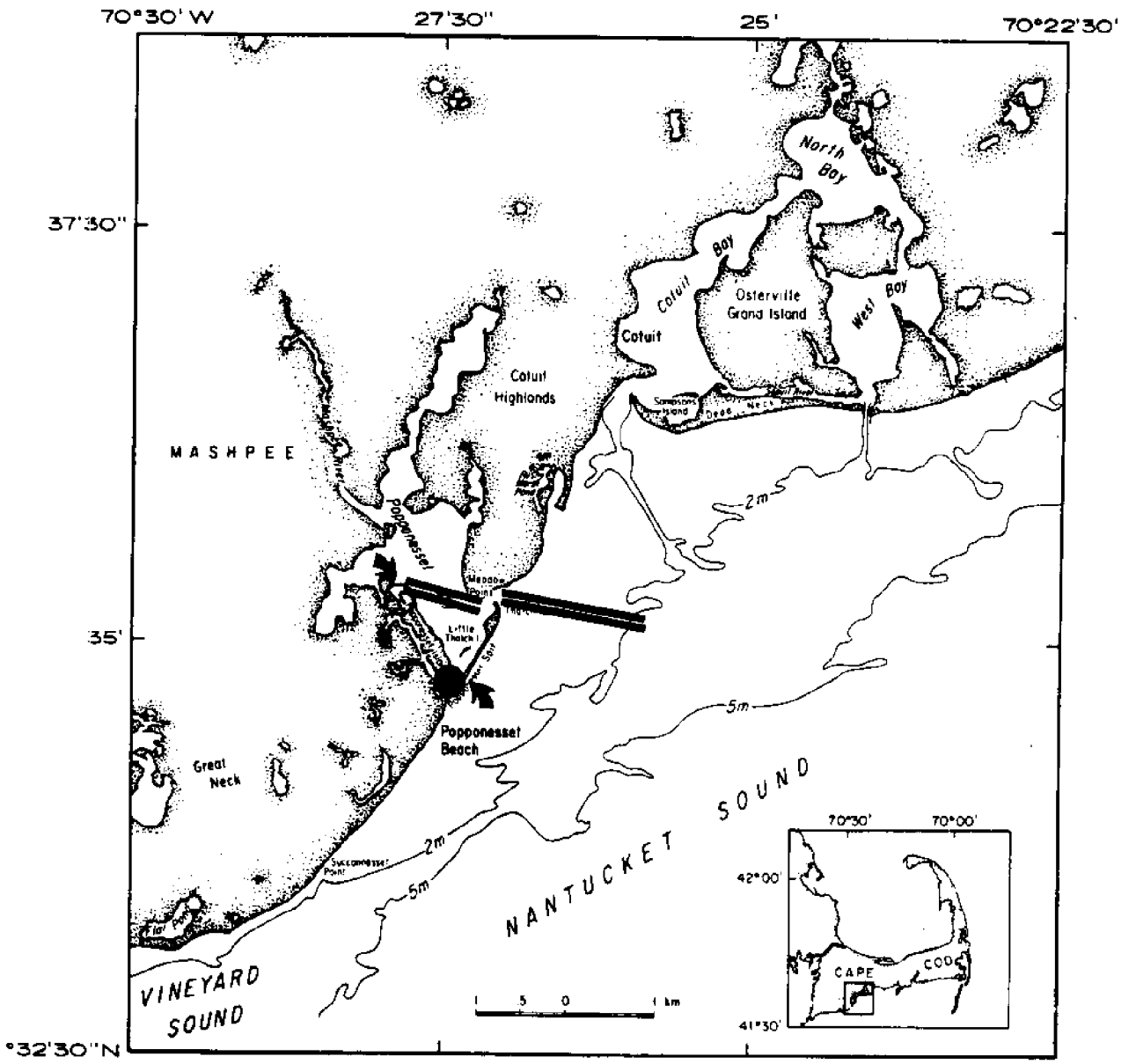

○ IMPROVE BRIDGE TO FACILITATE NAVIGATION.

● FILL IN EXISTING CHANNEL; INSERT SMALL CONDUIT FOR FLUSHING.

═ MOST DIRECT CHANNEL FOR PROPOSED DREDGING.

Figure 29. Schematic of existing and alternative navigation channel geometry for Popponesset Bay, inlet, and platform.

viable, suggesting that project duration should exceed 20 years, except for localized problem areas. One such localized problem area is the flood tide delta, built up considerably since the 1961 dredging operation. Unless a sand bypassing system is installed, this area will have to be periodically dredged, with the dredge spoil placed on the Spit.

The decision to maintain or otherwise manage the problem of breach formation near Popponesset Island was mentioned earlier; consideration for this possibility should be included in an assessment of dredging within the bay.

c) Improvement of navigation from deep waters of Nantucket Sound through the inlet into the bay system. The Nantucket Sound channel under such an option should connect with any channel passing over the offshore platform leading from Cotuit Bay into Nantucket Sound. A connecting channel would have a northeasterly bearing from the inlet serving Popponesset Bay. Navigation within the bay would have to be restructured to increase efficiency, as discussed in the previous section. Because of the expense of this particular option, some consideration must be given to the stability of the inlet and barrier beach to the southwest. As mentioned before, a breach near Popponesset Island could drastically affect the water exchange patterns within the bay. Structural control of the inlet passage between the bay and the sound is not feasible for economic reasons, as well as for sand transport reasons. Such structures would be ineffective over the long run if the barrier beach updrift were not stabilized at the same time. In summary, this option, which would still require maintenance dredging on a periodic basis, is the most expensive of the three, and not necessarily effective at realizing the goals of any navigation project.

D) OFFSHORE DREDGING FOR BEACH FILL MATERIAL:

One possibility for nourishing the beaches in the study area is to dredge material from offshore and transport it to the beaches. There is a large supply of sediment offshore which is compatible with beach materials on the shore. Areas of possible supply include Succonnesset Shoal and its adjacent shoals, and the shallow platform directly off the beach. The platform should not be altered to any significant degree, because it provides an important buffer to storm activity in its present configuration. There is inadequate sand available in the sand waves on the platform to justify using these for nourishment material. Consequently, the best option for offshore sources is removal from the offshore shoals, such as Succonnesset Shoal. The greater water depth, the presence of a relatively compacted, shallow substrate, large tidal velocities and the possibility of gas deposits combine to make the channel an unattractive source area for beach fill material.

E) LAND USE:

Management of beach-front property involves regulating construction in areas which are still undeveloped and controlling the proliferation of shoreline structures. Zoning and permitting procedures provide mechanisms for this type of management.

Set-back of structures from the beach is necessary for stability of the beach and protection of the structure, as well as being desirable esthetically. Minimum set-back requirements vary with location; history of bluff retreat dictates the proper local set-back. Shoreline segments with continuous structures will require less of a set-back than unstructured, sea-cliff segments. Set-back requirements for structured segments should conform with at least minimum local requirements, depending on the condition and geometry

of the adjacent structures. For shoreline segments with no structures in the immediate area, set-back should be based on historical rates of cliff recession. For a fifty-year planning period, and for the cliffed segments of the Mashpee/Cotuit shoreline which have a historical erosion rate of 0.25 meters/year, a set-back of 12.5 m is suggested. If a longer planning period is required, the set-back should be adjusted.

Passive buffers such as set-back and beach nourishment (as described in the nourishment section) should be encouraged over protection structures such as seawalls and revetments. The structures are acceptable for storm damage prevention of the bluffs, as described in the Massachusetts Coastal Zone Management Program, but only when their effect on adjacent beaches is minimal. Licensing must consider existing structures. While beach nourishment north of Succonnesset Point should be encouraged over seawall construction, local conditions may dictate structural measures. For instance, existance of near-continuous seawalls adjacent to the subject property makes the non-reinforced bluff more susceptible to erosion. Denial of a permit in this case would cause the beach-front property owner lacking structures to experience accelerated erosion; seawall construction may be the owner's only real alternative.

Attempts to structurally reinforce any barrier spits in the area should be denied since they could cause unacceptable beach changes. Popponesset Spit, in particular, is vulnerable to erosion induced by construction of seawalls and groins. Similarly shoreline protection structures should be discouraged in the undeveloped region in the southwestern part of the study area, from Succonnesset Point to Washburn Island. Construction of structures such as parking lots or bath-houses on the backshore or back beach should conform to set-bach requirements, based on historical data in this and companion reports.

ACKNOWLEDGEMENTS

This work was supported from a variety of sources. Primary impetus and initial funding for this study came from the Town of Mashpee. A Community Assistance Grant was provided through the Massachusetts Coastal Zone Management Program. A grant was provided through the Woods Hole Oceanographic Institution Sea Grant Program through grant number NA80AA-D-00077(RB-40). Finally, support came from ALCOA Foundation to complete synthesis of these data.

We would like to acknowledge the considerable efforts of Dr. Arthur G. Gaines of W.H.O.I. who helped initiate the study, and who has contributed significantly since. Mr. Steven Gegg of W.H.O.I. performed most of the field work in association with the second author, with some help from Mr. Wayne Spencer. Mr. Gegg developed analysis software for the bathymetric charts. Ms. Jean Thomas of Mashpee was our most interested contact with the Board of Selectmen; she helped focus our scientific findings to more immediate questions of coastal management in Mashpee. Preparation of this report was facilitated with the help of Ms. Pamela Barrows of W.H.O.I.

REFERENCES

Aubrey, D.G. and A.G. Gaines, 1982b. Rapid formation and degradation of barrier spits in areas with low rates of littoral drift. Marine Geology, 49, 257-278.

Aubrey, D.G. and P.E. Speer, 1983. Sediment Transport in a Tidal Inlet, Woods Hole Oceanographic Institution Tech. Report, WHOI-83-20, 130 pp.

Aubrey, D.G., 1981. Field evaluation of Sea Data directional wave gage (Model 635-9). Woods Hole Oceanogr. Inst. Tech. Rept. WHOI-81-28, 52 pp.

Aubrey, D.G., and A.G. Gaines, 1982a. Recent evolution of an active barrier beach complex: Popponesset Beach, Cape Cod, Massachusetts. Woods Hole Oceanogr. Inst. Tech. Rept., WHOI-82-3, 77 pp.

Benoit, J.R. and B.M. Donahoe, 1980. Improper resource management of the Popponesset Barrier Spit System, Cape Cod, Massachusetts. p. 384-388. In N. West (ed.), Resource Allocation Issues in the Coastal Environment, Proceedings of the Fifth Annual Conference of the Coastal Society, Nov. 6-8, 1979. 455 pp.

Brownlow, A.H. (ed.), 1979. Cape Cod Environmental Atlas. Department of Geology, Boston University, Boston, MA. 62 pp.

Bumpus, D.F., W.R. Wright and R.F. Vaccaro, 1971. Predicted effects of the proposed outfall. J. Boston Soc. Civil Engineers, 58(4):255-277.

Camp, Dresser and McKee, 1981. Environmental Review Record, Popponesset Barrier Beach Restoration. September 1980. Massachusetts Disaster Recovery Team, Boston, MA. 89 pp. plus appendices.

Dennis, R.E. and E.E. Long, 1971. "A Users Guide to Computer for Harmonic Analysis of Data at Tidal Frequencies", NOAA Tech. Rept. NOS-41, July.

Engelund, F., 1966. Hydraulic resistance of alluvial streams. J. Hydraulic Div. Am. Soc. Civ. Engrs., v. 92(HY2), p. 315-326.

Gonella, J., 1972. "A rotary-component method for analyzing meteorological and oceanographic vector time series", Deep-Sea Research, v. 19, p. 83-846.

Goud, M.R. and D.G. Aubrey, 1983. Survey of shoreline structures, Popponesset Beach, MA. Woods Hole Oceanogr. Inst. Tech. Rept. WHOI 83-14, 32 pp.

Grant, W.D. and O.S. Madsen, 1982. "Moveable bed roughness in unsteady oscillatory flow", Journal of Geophysical Research, v. 87, p. 469-481.

Grosskopf, W.G., D.G. Aubrey, and M.G. Mattie, 1983. Field intercomparison of nearshore directional wave sensors, in press, IEEE.

Inman, D., 1952. Measures for describing the size distribution of sediments. Journal of Sedimentary Petrology, v. 22, p. 152-145.

Komar, P.D. and D.L. Inman, 1971. Longshore sand transport on beaches. J. Geophys. Res., v. 75, p. 5914-5927.

Komar, P.D., 1976. Beach processes and sedimentation, Prentice-Hall, Inc., Englewood Cliffs, N.J., 429 pp.

Longuet-Higgens, M.S., 1952. On the Statistical Distribution of the Heights of Sea Waves, Jour. of Mar. Research, v. 11, p. 245-266.

Madsen, O.S. and W.D. Grant, 1976. "Sediment transport in the coastal environment", Ralph M. Parsons Laboratory Report no. 209, Mass. Inst. of Technology, 105 pp.

Miller, M.C. and D.G. Aubrey. Beach changes at Cape Cod, Massachusetts. U.S.A.C.E. Coastal Engineering Research Center, in press.

Oldale, R.N., 1975. Geologic Map of the Cotuit Quadrangle, Barnstable County, Cape Cod, Massachusetts. MAP GQ-121, U.S. Geological Survey, Reston, VA.

Redfield, A.C., 1980. The tides of the waters of New England and New York. William S. Sullwold Publishing, Inc., Taunton, MA. 108 pp.

Schlee, J., 1966. A Modified Woods Hole Rapid Sediment Analyzer, Jour. Sed. Petrology, v. 36, p. 403-413.

Schlicting, Herman, 1968. Boundary-Layer Theory. McGraw Hill Book Co., Inc. Verlag G. Braun (6th edition). 748 pp.

Schureman, P., 1971. "Manual of Harmonic Analysis and Prediction of Tides", U.S. Department of Commerce, Coast and Geodetic Survey, Special Publ. No. 98, Revised 1940 edition.

Seymour, R.J. and D.G. Aubrey. Beach morphology changes at Santa Barbara, California, submitted.

State of Massachusetts, 1978. Massachusetts Coastal Zone Management Program, Coastal Zone Management, Boston, MA, 439 pp.

U.S. Department of Commerce, 1983. Tide Tables 1983, East Coast of North and South America. NOAA, National Ocean Survey, 285 pp.

Woodworth, J.B. and E. Wigglesworth, 1934. Geography and Geology of the Region Including Cape Cod, The Elizabeth Islands, Nantucket, Martha's Vineyard, No Man's Land and Block Island. Vol. LII, Memoirs of the Museum of Comparative Zoology, Harvard University, Cambridge, MA. 322 pp.

Yalin, M.S., 1972. Mechanics of Sediment Transport. Pergamon Press. 290pp.

APPENDIX I

Survey notes, including detailed location drawings, from the benchmark survey performed by engineering firm Holmes and McGrath. General locations are shown in Figure 8.

holmes and mcgrath, inc.
civil engineers & land surveyors
301 main street
falmouth, ma 02540
phone 548-3564

JOB TOWN OF MASHPEE
SHEET NO. 1 OF 3
CALCULATED BY MES DATE 9/17/21
DRAWN MBM
CHECKED BY DATE 9/17/21
SCALE NONE

STATION: DISK A & TARGET IRON PIPE in PILING

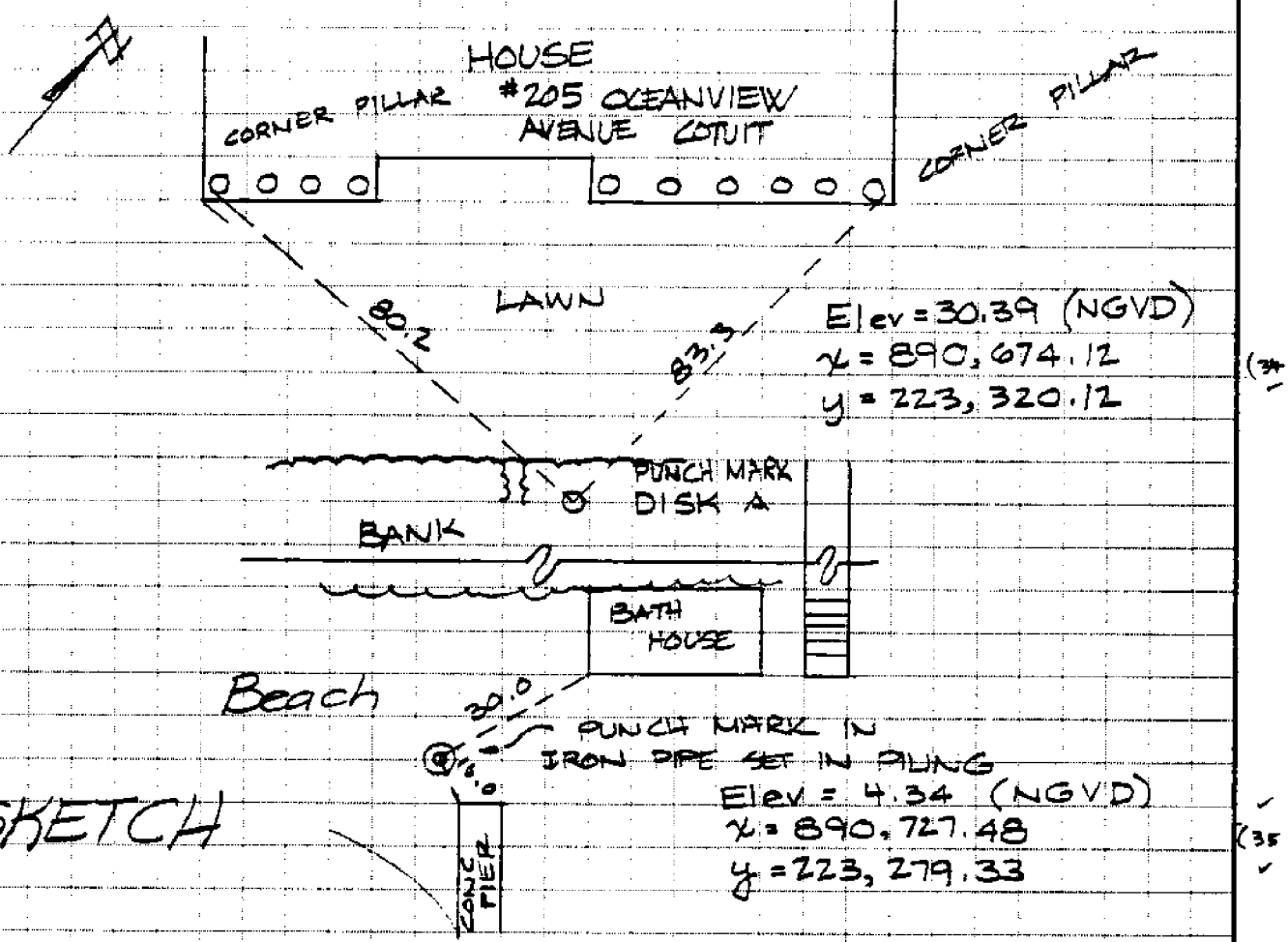

Disk A is a brass disk set in a concrete-filled pipe located at the rear of #205 Oceanview Avenue Cotuit. The disk is just below the surface and is just over the bank.
The iron pipe was set on the beach as the target for the aerial photographs. Disk A was unsuitable due to the owners insistence that it be placed on the bank. The iron pipe was driven into a piling that has its surface flush with the beach.

holmes and mcgrath, inc.
civil engineers & land surveyors
301 main street
falmouth, ma 02540
phone 548-3564

JOB TOWN OF MASHPEE
SHEET NO. 2 OF 3
CALCULATED BY MEJ DATE 9/17/81
CHECKED BY MBM DATE 9/17/81
SCALE NONE

STATION DISK B

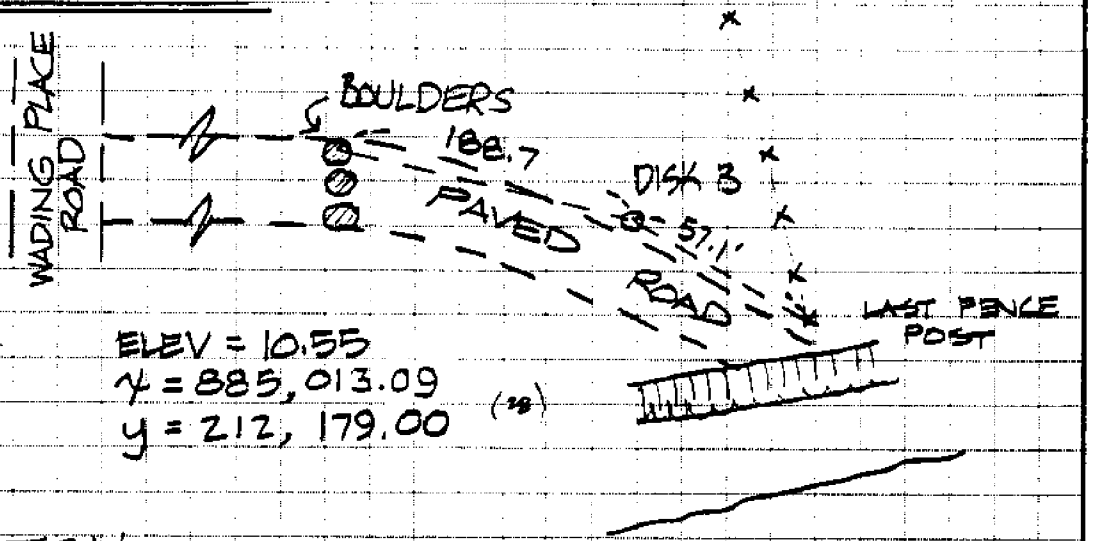

SKETCH

NANTUCKET SOUND

Disk B is a brass disk set in a concrete-filled pipe located at the west end of the popponesset spit The brass disk was set about one inch below the earth's surface at the edge of the pavement

holmes and mcgrath, inc.
civil engineers & land surveyors
301 main street
falmouth, ma 02540
phone 548-3564

JOB TOWN OF MASHPEE
SHEET NO. 3 OF 3
CALCULATED BY MES DATE 9/17/81
CHECKED BY MBM DATE 9/17/81
SCALE NONE

DISK C

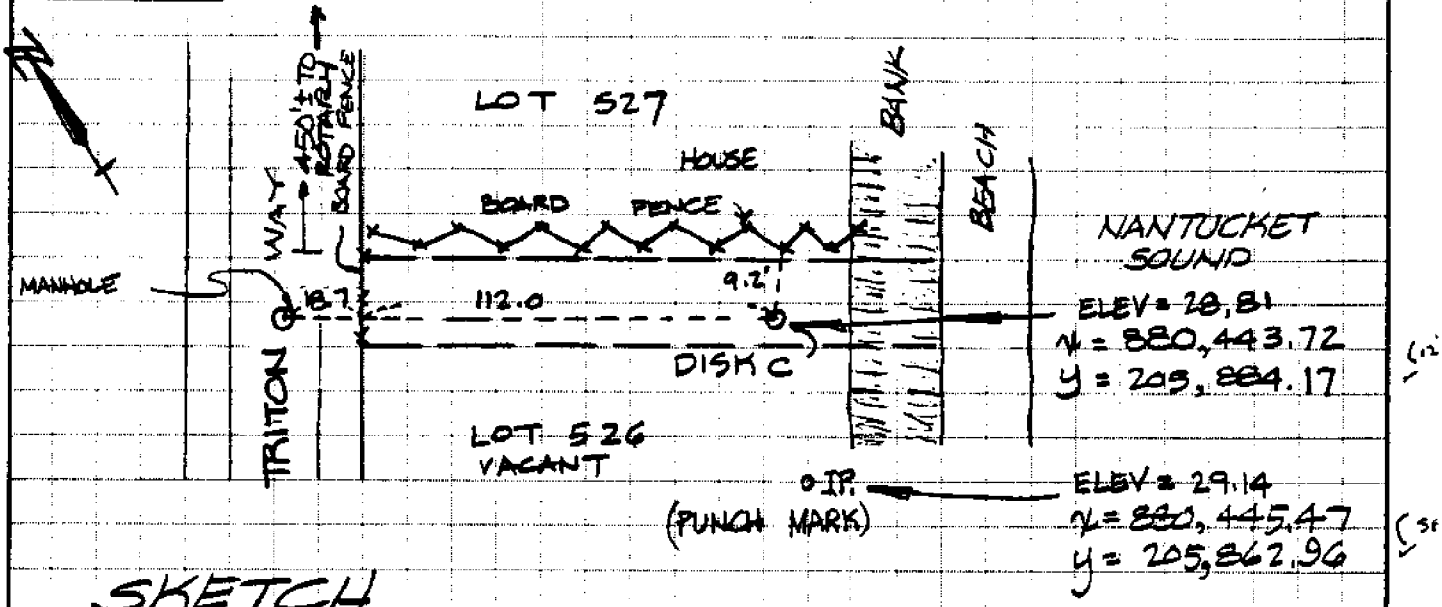

SKETCH

Disk C is a brass disk set in a concrete filled pipe located in a Right-of-Way off Triton Way in New Seabury. The Right-of-Way is described as Reserved Area R-2, and is 450 feet from the Rotary called Triton Sound Circle. The disk is set within ½" of the surface. When we set the disk, the owner of Lot 527 asked us to move the disk back from the top of the bank. The iron pipe was provided for the instrumentation of W.H.O.I. as the disk has limited visibility to the east.

	HI		ELEV.	
	45.87		44.180	M28 SA
		6.33 6.07	39.54	TP
	42.29			I.V.
		9.69 3.20 7.11	32.89	I.V.S. at Library
	35.16			
		0.93 0.21 0.72	34.33	
	44.77			
		5.80 5.57 6.45	38.20	M28SC (38.22 given)
			38.22	HELD
	39.01			
		1.97 1.65 1.21	37.36	

Town of Mashpee — Aug. 25, 1981 — Bunker Hood — 1

Cotuit Levels — Mist — 65°

11.42 1.05 0.62	48.41		
		10.87	37.26
0.31 0.21 0.12	37.47		
		5.58 5.42 5.27	32.05
2.98 2.80 2.22	34.65		
		9.91 9.56 9.22	25.09
6.12 5.92 5.52	30.91		
		1.27 1.05 0.83	29.86
11.39 11.14 10.69	41.00		
		3.04 2.80 2.56	38.20

5.79 5.59 5.29	43.74	10.02 9.71 9.48	38.20 33.95		8.12 8.08 8.25	14.07			
5.64 5.56 5.49	40.64				5.64 5.56 5.49	9.91	9.61	4.35	PIPE
		4.49 3.98 3.97	36.66		11.08 11.06 11.04	20.51	0.49 0.46 0.44	9.45	
3.69 3.48 3.26	40.14				12.79 12.76 12.74	32.73	0.56 0.54 0.52	19.97	
		9.95 9.75 9.56	30.39	MON. DISC A	5.94 5.90 5.85	37.96		32.06	
7.11 7.02 6.93	37.44				9.74 9.52 9.30	39.94	7.54 7.50 7.46	30.41 30.39	(+0.02 HOLD UP & DOWN STAIRS OK MON. DISC A
		10.77 10.74 10.71	26.70		4.29 3.90 3.50	40.57	3.47 3.27 3.05	36.67	
0.11 0.10 0.09	26.80				6.58 6.17 5.76	40.78	6.31 5.96 5.62	34.61	
		12.84 12.81 12.79	13.99		2.34 2.07 1.80	40.27	2.96 2.52 1.10	38.20	

						BS	HI	FS	ELEV	DESC	
2.91 1.91 1.41	29.91	12.[illegible] 11.88	28.10			4.29 3.14 2.39	32.46		28.62	114 E	MDPW
3.55 4.16 3.05	33.70	0.96 0.66 0.36	29.25			12.15 11.76 11.34	38.37	5.35 5.95 5.35	26.61		
[illegible] 12.15	45.92	0.69 0.44 0.18	33.26			9.74 9.39 9.04	47.52	0.37 0.24 0.11	38.13		
11.90 ~~11.69~~ 11.67 11.37	44.74	13.37 ~~12.84~~ 12.85 12.41	33.07			13.34 14.07 12.84	52.57	8.39 5.60 7.59	39.48		
		6.65 6.33 6.41	38.21	-0.01 M23SC	OK	0.48 0.30 0.12	50.99	2.13 1.22 1.68	50.69		
						9.91 9.64 9.36	51.57	9.25 9.06 8.87	41.93		
						2.22 8.06 1.90	48.98	4.89 4.65 4.41	46.92	TP STONE	
						2.00 1.75 1.50	42.06	8.87 8.67 8.48	40.31	NW CORNER TRITON WAY	C. BASIN TRANS FOR CIRCLE
						2.60 2.50 2.40	35.81	9.04 8.75 8.47	33.31		
						5.96 5.91 5.96	34.72	7.10 7.00 6.91	28.81	DISC C	

BS	HI	FS	ELEV	DESC
5.92 5.84 5.76	34.98	5.66 5.58 5.52	29.14	IRON PIPE
6.47 6.41 6.35	35.23	6.21 6.14 6.11	28.82	DISC C
12.14 11.76 11.39	44.93	2.18 2.06 1.94	33.17	
8.81 8.61 8.41	48.92	4.70 4.62 4.44	40.31	CATCH BASIN
4.83 4.57 2.36	51.51	2.15 2.00	46.92	TP SHORE
12.84 12.56 12.27	54.59	9.86 9.58 9.30	41.93	
1.02 0.89 0.76	50.96	4.67 4.43 4.18	50.06	
8.52 8.11 7.70	48.68	10.53 10.38 10.22	40.57	
0.55 0.41 0.27	38.54	10.87 10.56 10.22	38.13	
6.25 5.75 5.25	32.37	12.33 11.92 11.52	26.62 ~~50.00~~	

BS	HI	FS	ELEV	DESC
4.40 3.95 3.50	32.57	4.20 3.75 3.30	28.62	OK (0.00) 11AE NGPW
3.55 3.85 3.33	31.45 ~~32.00~~ ~~31.45~~	4.87 4.51 4.15	28.06 ~~28.06~~	
0.67 0.56 0.45	19.10	13.05 12.91 12.76	18.54	
3.69 3.36 3.03	13.06	9.53 9.40 9.27	9.70	
5.43 5.19 4.94	13.03	5.65 5.21 4.87	7.85	
5.69 6+10 S20 4.73	11.35	7.33 6.85 6.43	6.15	
4.78 4.85 4.93	11.30	4.82 4.40 3.97 L95	6.95	TP POLE A
5.23 5.01 4.31	15.32	1.53 1.05 0.57	10.25	4 PT SB SHORE ROAD BETWEEN DEAD E HOLLOW & SQUARE LANE
4.09 3.73 3.37	16.41 8.	2.80 2.64 2.45	12.68	
6.87 6.61 6.34	11.74	11.58 11.21 10.84	5.20	

B.S	HI	F.S	ELEV	DESC
12.58 57 12.29 38 12.19	19.77	4.72 4.35 3.98	7.39	SW CORNER C. WASH E. SHOCK ROAD BENCHMARK ELEVATION IS ASSUMED
6 0.37 6 0.23 6 0.09	14.36	5.86 5.64 6.41	14.13	
12 5.98 11 5.80 11 5.62	13.27	7.06 6.89 6.72	7.47	
8 12.56 8 12.44 8 12.31	23.18	2.70 2.53 2.36	10.74	
4 7.82 4 7.42 4 7.02	29.44	1.28 1.16 1.04	22.02	
12 2.34 12 2.26 12 2.17	23.19	7.85 8.85 8.51 8.16	20.93	
5.30 5 5.02 4 4.74	14.42	8.87 8.79 8.72	14.40	
5.59 5.38 4.99	19.68			
8 1.51 8 1.39 7 1.27	16.09	3.33 3.98 4.63	14.70	
6.03 6.13 5.78 5.43	16.33	5.71 5.54 5.37	10.55	DISC B
5.23 5.53 5.23 4.93	19.41	2.42 2.15 1.87	14.18	

B.S	HI	F.S	ELEV	DESC
7.39 7.33 7.27	26.00	0.83 0.74 0.65	18.67	
7.39 3.02 1.46	27.49	0.87 0.55 0.37	25.47	
0.53 0.44 0.36	18.56	9.73 9.37 9.01	18.12	
10.15 9.65 9.15	18.05	10.34 10.16 9.98	8.40	
1.59 1.31 1.03	13.38	6.28 5.99 5.68	12.07	
7.60 7.10 6.61	13.56	7.23 7.02 6.41	6.46	
2.32 1.92 1.52	14.96	0.96 0.63 0.09	13.04	
4.99 4.60 4.22	11.21	8.76 8.35 7.95	6.61	
3.83 3.48 3.09	10.97	4.01 3.68 3.29	7.53	TP POLE B
5.07 4.68 4.29	13.43	2.62 2.22 1.82	8.75	

B.S	HI	FS	ELEV	DESC.	
5.56 ~~5.04~~ 5.30 5.04	13.04	6.08 5.69 5.30	7.74	TP SHED	
6 12.58 6 12.32 6 12.06	20.55	5.08 4.81 4.55	8.23	TP SHED	
1 11.90 1 11.47 1 11.04	~~31.55~~ ~~32.49~~	0.53 0.49 0.40	20.08 ~~2.02~~	TP SHED	
8 4.82 8 4.53 8 4.24	31.60 ~~32.54~~	4.84 4.48 4.12	27.07 ~~28.01~~	TP BEAM	
4 4 4		3.13 2.98 2.84	28.62	OK 114 E	MIDAW
4.42	11.95		7.53	TP POLE	B
		5.00	6.95	OK TP POLE	A

0-00-14	29	0-00-15	27		
180-00-34		180-00-39			
87-03-45	01	272-56-50	55		
267-04-17		92-57-01			
87-03-37		92-56-28			
				(86)	
114A → 114B		114A →		114A → 84	
90-13-48		90-02-42		90-01-42	
269-17-59		269-57-10		269-58-57	
1003.41				2112.58	
1008.41				2112.58	
307.365				643.917	
307.365				643.915	
0-00-12	21	0-00-09	15	0-00-04	
180-00-31		180-00-22		180-00-47	
84-02-13	19	275-58-07	16	182-42-44	
264-02-26		95-58-25		2-43-10	
84-09-50		275-58-01			
0-00-04	15	0-00-07	20	0-00-01	16.5
180-00-27		180-00-33		180-00-32	
182-42-28	41	177-17-45	56	178-12-37	59
2-42-59		357-17-09		358-13-21	
182-42-26		177-17-36		178-12-43.5	
(36) → (35)					
ST → 32				90-00-07	15.5
90-01-14				180-00-24	
269-59-04				181-47-20	
1870.10				01-47-39	29.5
1870.10				181-47-14	
570.008					
570.008					

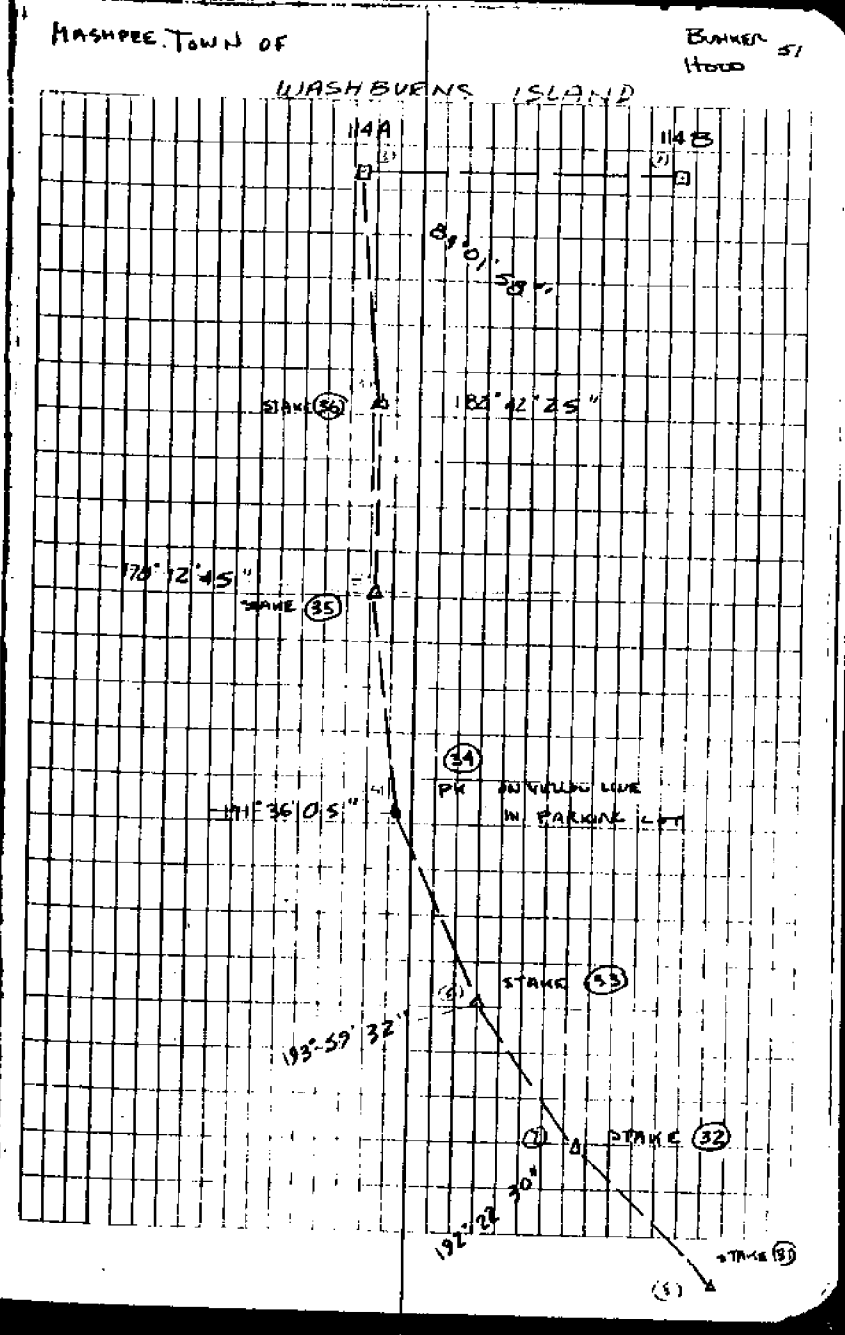

0-00-11		0-00-07		0-00-13	
180-00-35	/ 23	180-00-35	/ 21	180-00-00	/ 26
356-44-10		2-15-15		244-30-47	
176-44-58	/ 49	183-16-03	/ 59	64-31-10	/ 59
356-44-26		3-15-33		244-30-33	
0-00-00		0-00-05		0-00-09	
180-00-15	/ 7	180-00-23	/ 19	180-00-29	/ 19
115-29-14		61-14-59		86-35-19	
295-29-35	/ 24	291-15-15	/ 07	266-35-30	/ 21
115-29-17		61-14-53		86-35-07	
0-00-10		0-00-07		0-00-01	
180-00-32	/ 21	180-00-32	/ 19	180-00-11	/ 06
212-10-16		271-23-05		88-36-22	
32-10-39	/ 25	91-23-27	/ 16	268-37-07	/ 01
212-10-04		271-22-57		88-36-55	
disc A - dh 9		04.61		S-S 6-7	
91-28-20		88.29		90-13-39	
268-32-07		172.90		269-46-26	
1066.48				1169.48	
1066.50				1169.49	
325.065				356-459	
325.069				356.462	
0-00-06		0-00-00		0-00-13	
180-00-00	/ 08	180-00-17	/ 08	180-00-35	/ 29
271-22-49		271-22-50		88-37-24	
91-23-19	/ 04	91-23-17	/ 03	268-37-41	/ 32
271-22-56		271-22-55		88-37-08	
0-00-07		0-00-09		0-00-07	
180-11-31	/ 18	180-00-50	/ 29	180-00-29	/ 17
176-16-26		183-44-15		183-43-15	
356-16-10	/ 33	3-44-36	/ 25	3-44-03	/ 54
176-16-15		183-43-56		183-43-37	

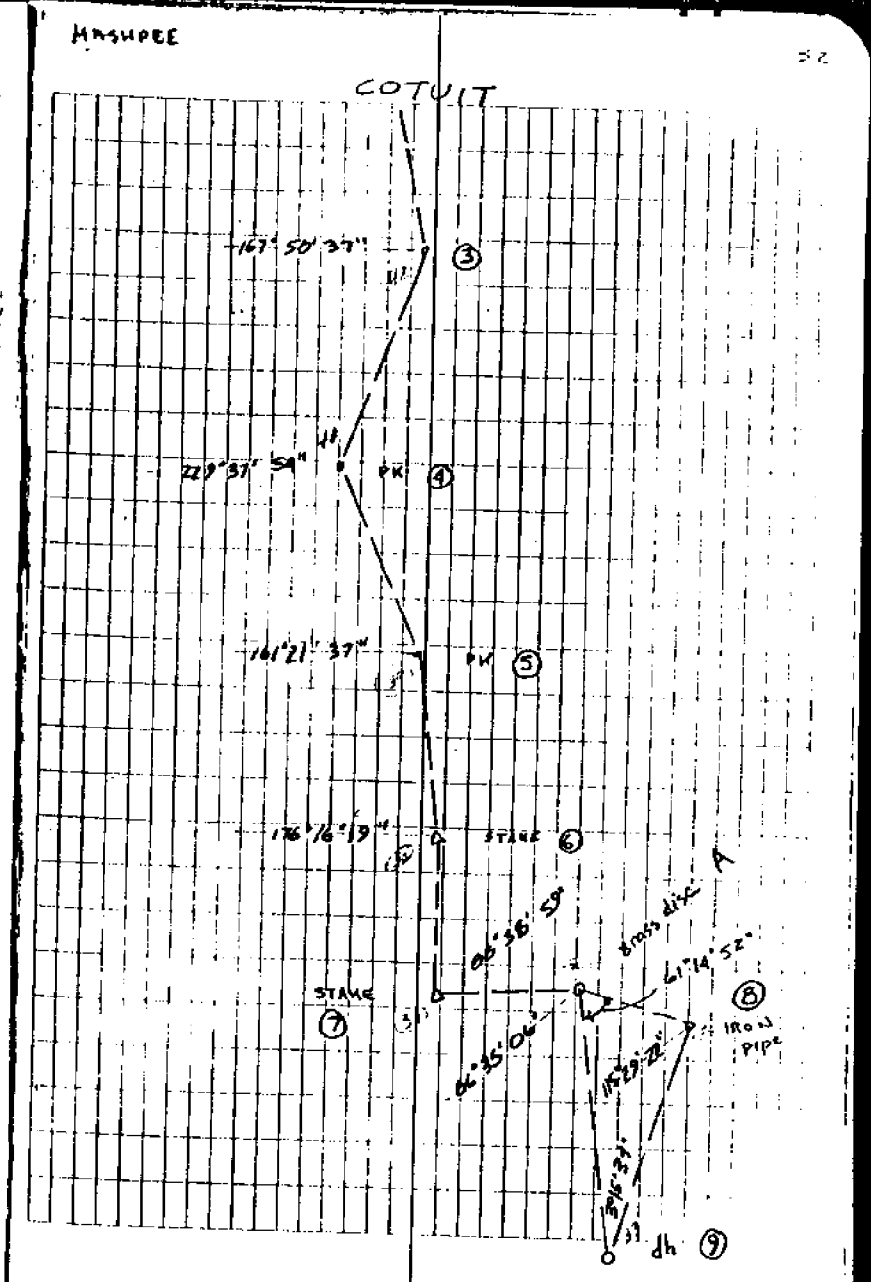

0-00-01	/15	0-00-05	/13	0-00-01	/18
180-00-29		180-00-22		180-00-28	
197-48-39	/47	162-11-39	/40	163-45-05	/13
17-48-56		342-11-52		343-45-22	
197-48-32		162-11-27		163-44-55	
d-p		d-s		s-j	
9-8		9-10		10-11	
89-56-28		89-54-12		90-03-01	
270-03-38		270-05-51		269-57-27	
1035.43		2097.32		3053.43	
BT 1035.49		2097.22		3053.43	
315.619		639.236		930.687	
315.618		639236		930.687	
0-00-03	/12	0-00-03	/54	0-00-10	/16
180-00-21		119-59-15		180-00-23	
190-15-03	/12	169-44-57	/49	190-15-05	/18
10-15-22		349-44-42		10-15-28	
190-15-00		169-44-54		190-15-02	
0-00-06	/15	0-00-01	/09	0-00-05	/16
180-00-25		180-00-18		180-00-25	
192-23-10	/17	167-36-59	/08	180-38-13	/22
12-23-25		347-37-18		0-38-31	
192-23-02		167-36-59		180-38-07	
d-t		t-s		13 disc B	
11-12		12-13			
89-53-34		90-00-16		89-55-08	
270-06-49		269-59-59		270-05-03	
762.74		2863.52		2768.19	
762.75 (d)		2863.53		2760.19	
232.485		872.749		813.733	
232.488		872.745		813.732	
0-00-06	/14	0-00-02	/14	0-00-06	/19
180-00-23		180-00-26		180-00-23	
179-21-52	/09	180-31-33	/43	179-28-39	/45
359-22-13		0-31-54		359-28-56	
179-21-50		180-31-29		179-28-31	

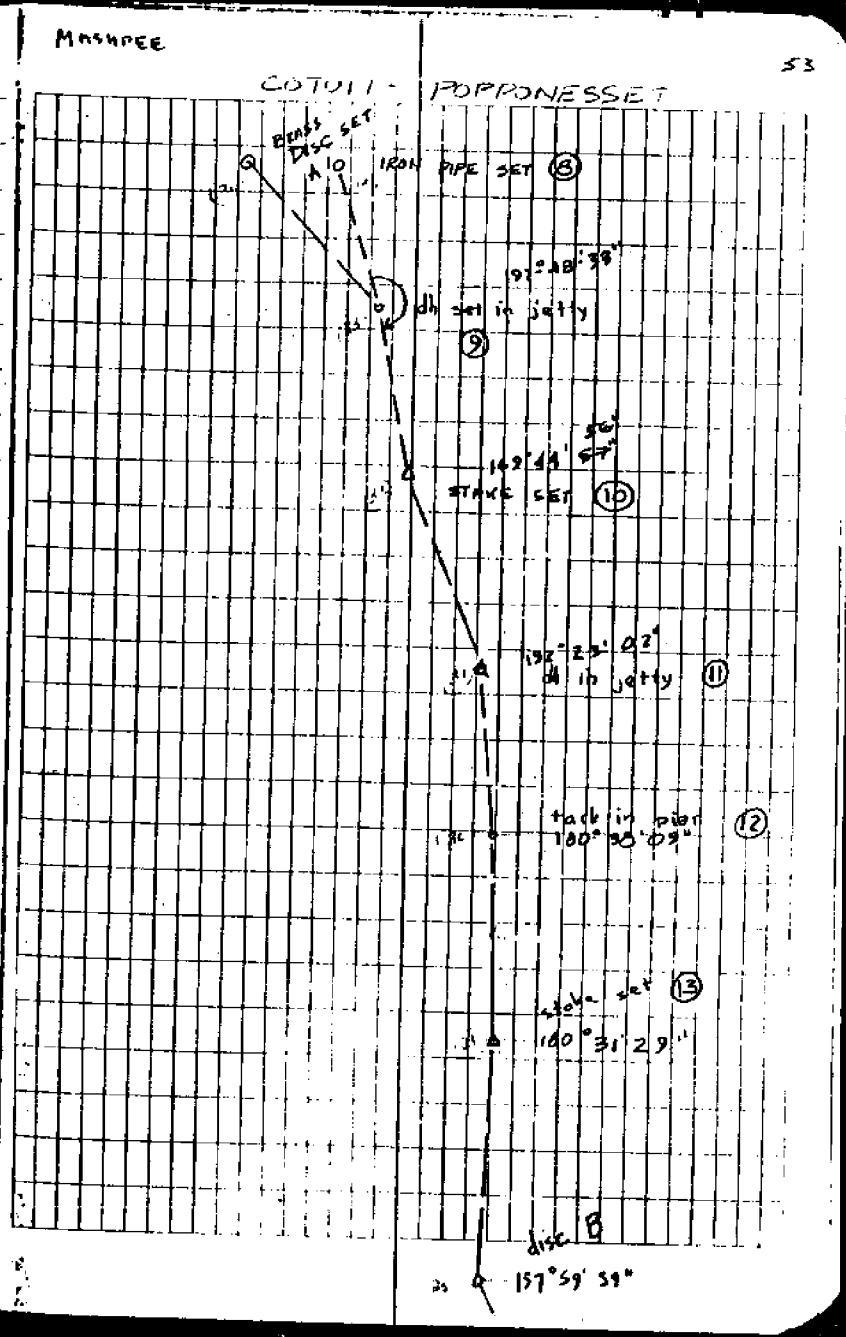

MASHPEE

0-00-04		0-00-02		0-00-04	
180-00-01	/12	180-00-20	/11	180-00-20	/12
157-59-34		202-00-24		198-41-50	
337-59-59	/49	22-00-42	/34	18-41-51	/40
157-59-32		202-00-23		198-41-28	
disc B - 14		14-15		15-16	
89-12-00		90-53-09		89-19-01	
270-98-10		263-07-18		270-10-31	
117.93		1154.78		1769.77	
117.92		1154.78		1769.77	
218.825		351.979		539.429	
218.824		351.979		539.426	
0-00-06		0-00-07		0-00-08	
180-00-27	/17	180-00-33	/20	180-00-25	/16
161-18-29		141-18-38		198-41-37	
341-18-52	/40	341-18-56	/45	18-41-56	/46
161-18-23		161-18-25		198-41-30	
0-00-07		0-00-03		0-00-03	
180-00-56	/22	180-00-21	/15	180-00-20	/11
191-03-08		168-57-15		191-48-55	
11-03-27	/17	348-57-35	/25	11-49-16	/05
191-02-56		168-57-10		191-48-54	
0-00-04		0-00-08		0-00-08	
180-00-15	/09	180-00-27	/17	180-00-25	/16
168-11-06		175-43-42		184-16-20	
348-11-26	/16	355-43-03	/52	4-16-40	/30
168-11-07		175-43-35		184-16-19	
17→16		17→18			
89-45-26		89-56-52			
270-14-44		270-03-19			
365.43		808.06			
365.43		808.05			
172.343		246.298			
172.343		246.295			

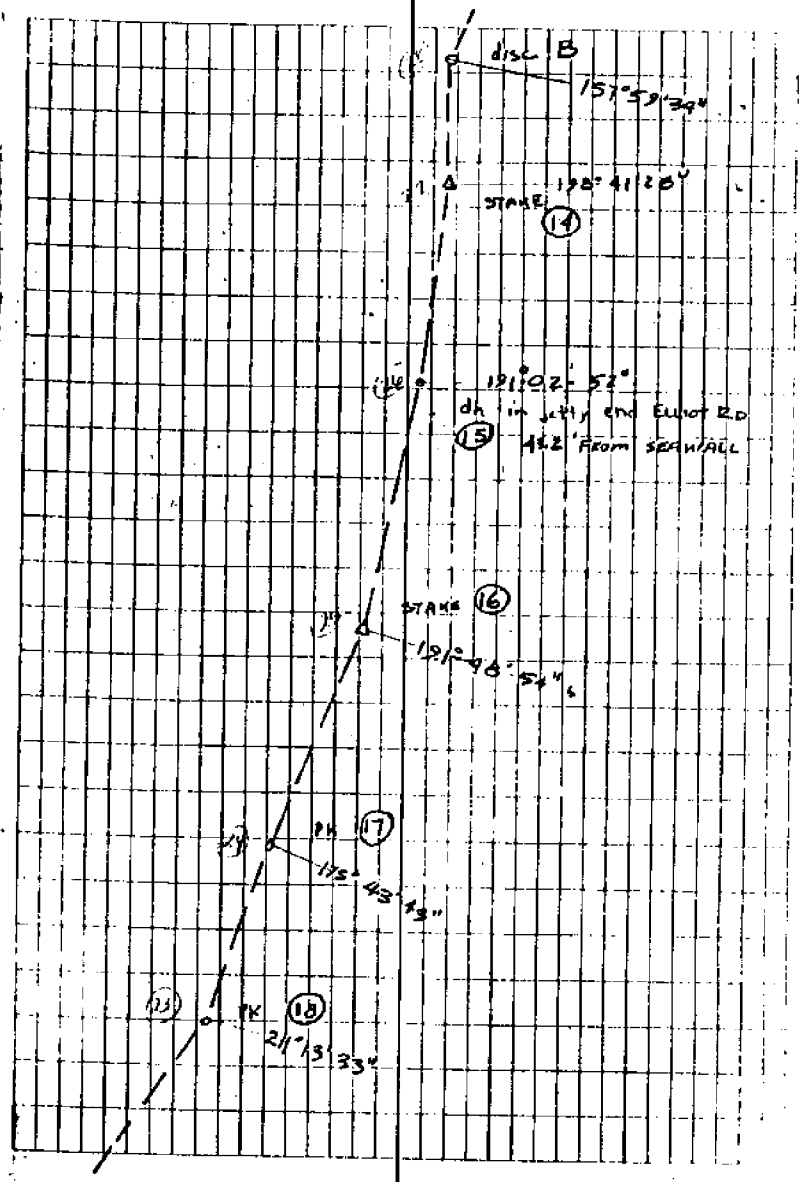

6→5		From 4 to 5		4→3	
91·29·35		91·09·50		89·09·39	
268·29·50		268·36·36		270·19·30	
58 133		305.27		601.34	
584.33		505.26		601.35	
178 105		154.007		185.290	
178.105		154.005		185.291	
0-00-12		0-00-08		0-00-07	
180-00-35	/23	180-00-25	/14	180-00-30	/18
176·16·22		161·21·36		198·38·31	
356·16·51	/42	341·22·00	/48	18·38·45	/38
176·16·19		161·21·34		198·38·20	
0·00·07		0-00-01		0-00-11	
180·00·30	/18	180·00·28	/14	180-00-19	/15
179·38·22		229·38·00		130·21·56	
18·38·49	/57	49·38·20	/10	310·22·19	/07
138·38·19		229·38·56		130·21·52	
0-00-02		0-00-06		0-00-05	
180·00·19	/10	180·00·20	/13	180·00·23	/14
130·22·08		167·58·46		192·01·22	
310·22·14	/16	347·58·53	/52	12·01·58	/30
130·22·06		167·58·39		192·01·16	
0·00·03		0-00-03		0-00-06	
180·00·36	/22	180·00·36	/22	180·00·26	/16
166·41·20		130·33·20		193·19·02	
346·41·17	/33	10·33·37	/28	13·19·18	/10
166·41·11		130·33·06		193·10·51	
2→3		2→1		1→M28SA	
89·25·40		90·03·22		89·11·02	
270·34·12		269·56·29		270·40·40	
415.12		687.97		523.93	
415.13		687.96		523.93	
126.530		209.540		159.691	
126.531		209.537		159.693	

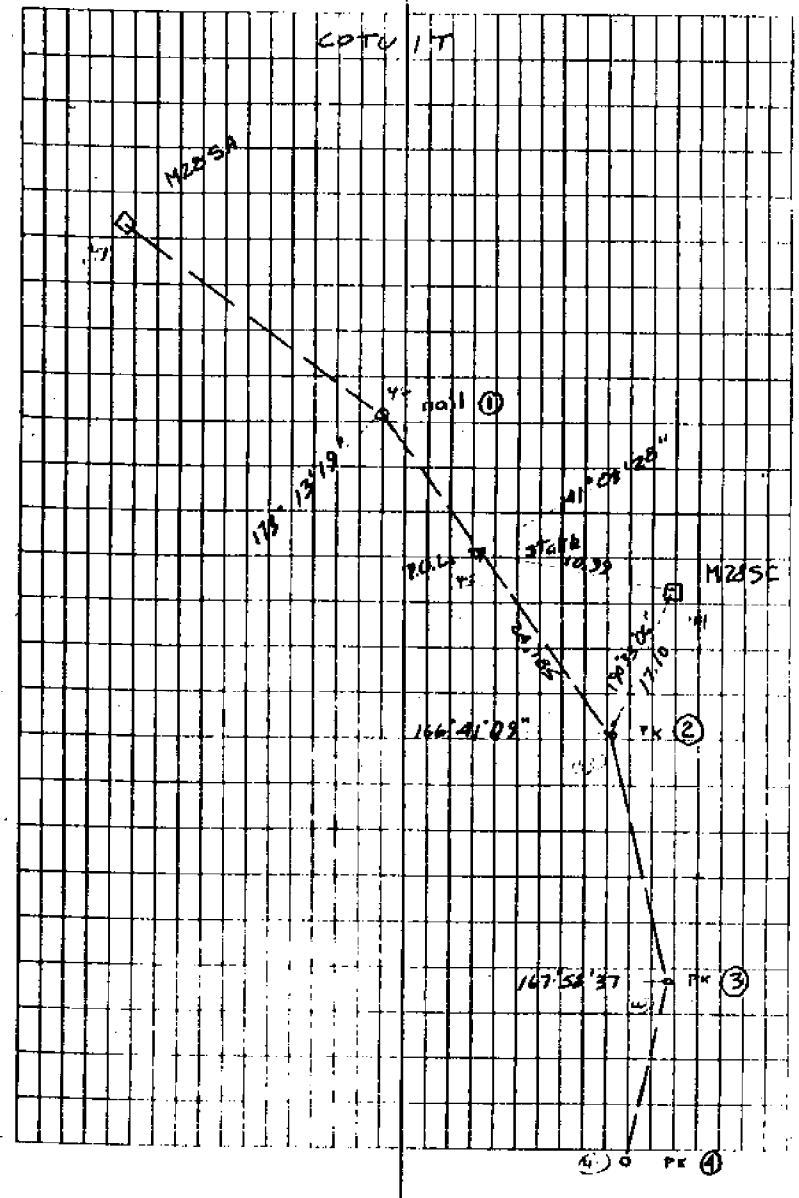

COTUIT

0-00-11		0-00-09		0-00-17	
180-00-27	/19	180-00-29	/19	180-00-13	/30
141-03-56		173-13-26		186-46-58	
321-04-00	/47	353-18-45	/56	6-47-06	/02
141-03-28		173-13-17		186-46-32	
0-00-05		0-00-06			
180-00-10	/07	180-00-20	/14		
186-46-21		186-46-44			
6-47-49	/35	6-47-02	/53		
186-46-28		186-46-39			

POPPONESSET

0-00-03		0-00-01		0-00-08	
180-00-22	/15	180-00-24	/12	180-00-25	/16
189-16-23		175-43-15		169-02-56	
4-16-39	/31	355-44-04	/54	349-03-09	/01
189-16-16		175-43-43		169-02-45	
0-00-01		0-00-05		0-00-03	
180-00-21	/11	180-00-26	/15	180-00-17	/10
211-13-35		148-46-51		195-57-15	
31-13-55	/44	328-46-56	/43	15-57-31	/23
211-13-33		148-46-28		195-57-13	
19→18		19→20			
92-16-13		89-30-48		127-46-54	
247-43-54		270-29-16		150-59-24	
436.97		363.16		81-13-57	
436.98		363.16		359-59-55	
133.138		110.692			
133.193		110.692			
03					
0-00-19		0-00-23		0-00-01	
180-00-46	/25	180-00-40	/31	180-00-15	/08
~~232-13-25~~		121-46-59		150-59-23	
127-47-08	/4	331-47-12	/05	330-59-47	/32
307-47-20					
46 / 127-46-49		127-46-34		150-59-24	

MASHPEE

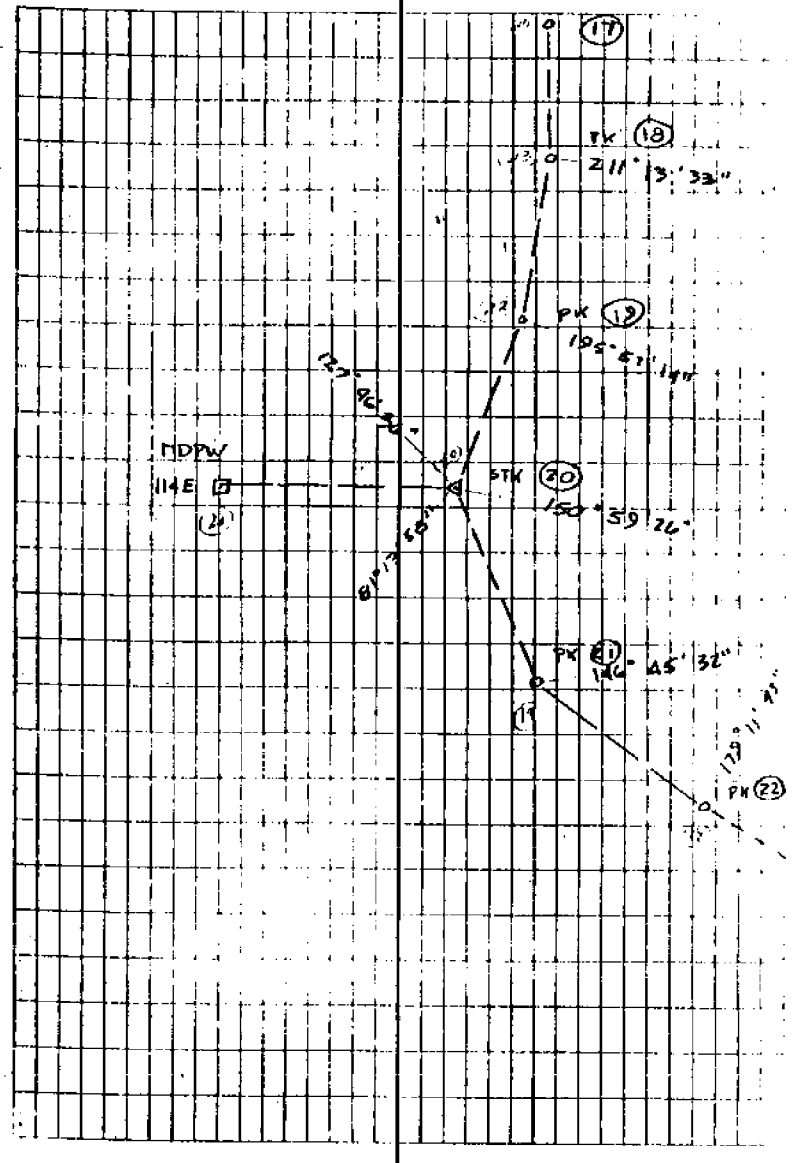

0-00-06		0-00-08		0-00-05	
180-00-18	/12	180-00-18	/11	180-00-26	/15
81-14-00		146-45-50		213-14-29	
261-14-16	/09	326-45-42	/36	53-44-54	/11
81-13-57		146-45-25		213-14-26	
20 → 21		20 → LINE		24 → 25	
90-09-37		89-50-24		89-01-53	
269-59-57	✓	270-09-24		270-58-04	
327.15		303.52		221.52	
327.15		303.52		221.53	
99.715		92.514		67.520	
99.715		92.514		67.522	
0-00-07		0-00-01		0-00-01	
180-00-24	/15	180-00-22	/11	180-00-20	/10
213-14-30		146-45-32		179-11-46	
33-19-52	/41	226-45-50	/41	359-12-01	/53
213-14-26		146-45-30		179-11-43	
22 → 21		22 → 23		24 → 23	
48-07-55		89-23-48		89-23-46	
267-52-08		270-28-22	✓	270-36-08	
488.62		505.19		482.71	
488.63		505.19		482.70	
148.933		153.382		147.130	
148.934		153.382		147.127	
0-00-07		0-00-08		0-00-15	
179-59-52	/57	180-00-21	/14	180-00-28	/21
180-47-48		180-48-25		150-07-31	
0-48-03	/55	0-48-36	/30	330-07-47	/39
180-47-58		180-48-16		150-07-18	
0-00-09		0-00-03		0-00-10	
180-00-31	/20	180-00-25	/14	180-00-24	/17
209-52-45		196-08-54		163-51-22	
29-53-11	/58	16-09-12	/03	343-51-46	/3331
209-52-30		196-08-49		163-51-46	
				14	

MASHPEE

57

POPPONESSET — NEW SEABURT

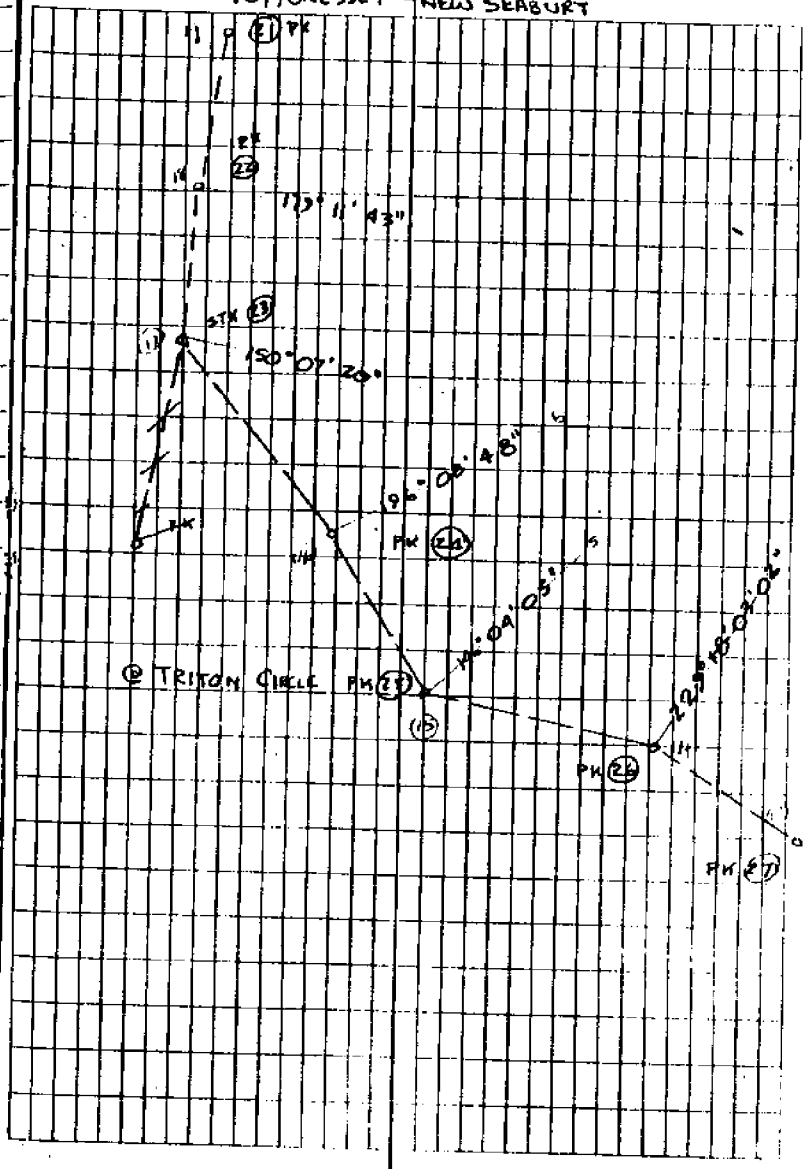

0-00-09		0-00-03		0-00-01	
180-00-18	/06	180-00-17	/10	180-00-23	/12
146-04-09		213-55-41		146-04-13	
326-09-16	/10	33-55-57	/49	326-04-26	/13
146-04-04		213-55-39		146-04-07	
0-00-11		0-00-05		0-00-02	
180-00-21	/16	180-00-13	/09	180-00-16	/08
213-55-54		146-04-06		213-55-51	
33-56-13	/03	326-09-16	/12	33-56-09	/02
213-55-47		146-04-03		213-55-59	
0-00-06		0-00-07		0-00-02	
180-00-25	/14	180-00-22	/14	180-00-14	/08
229-15-15		229-03-07		130-56-58	
49-03-23		49-03-20	/13	310-57-12	/02
		229-02-59		130-56-54	
26-25		26-27		71.15	
88-45-36		91-27-29		47.47	
271-14-15		268-32-49		120.92	@70'
399.15		235.84		13.67	
399.16		235.84			
121.662		71.884			
121.664		71.883			
0-00-01		0-00-03		0-00-06	
180-00-29	/15	180-00-19	/08	180-00-27	/16
97-07-00		262-53-01		256-23-22	
277-07-27	/13	82-53-21	/11	76-23-35	/28
97-06-58		262-53-03		256-23-12	
0-00-05		0-00-08		0-00-05	
180-00-27	/16	180-00-18	/13	180-00-29	/14
103-37-01		199-44-04		60-11-05	
283-37-13	/07	19-43-21	/12	340-11-21	/13
103-36-53		179-48-59		160-10-51	

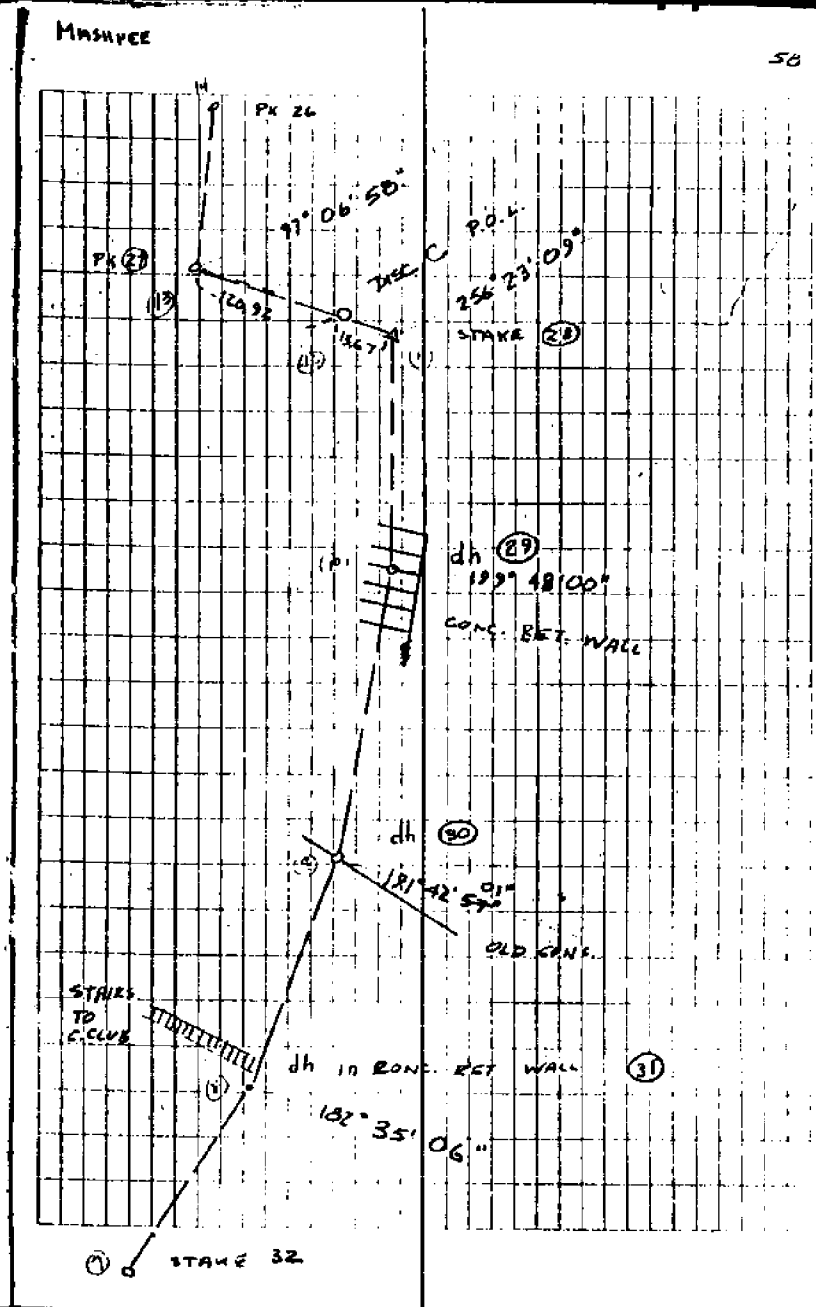

29-28		29-30		31-30	
81-24-58 272-35-45		90-29-04 269-31-37		90-31-56 269-28-A	
409.06 409.04		838.42 838.92		541.14 541.14	
124681 121675		278.84 273.939		1641.933 1641.939	
0-00-06 191-42-~~06~~	0-00-06 180-00-18 / 12			0-00-10 180-00-24	/ 17
~~191-42-05~~	191-42-06 11-42-21 / 13			168-18-06 348-18-21	/ 13
	191-41-59			168-17-56	
0-00-~~10~~ 07 180-00-~~32~~	/ 19	0-00-17 180-00-30	/ 28	0-00-04 180-00-22	/ 13
~~182-35-29~~ 02-35-38	/ 33	182-35-23 02-34-42	/ 32	177-24-59 357-25-10	/ 69
182-35-14		182-35-09		177-24-56	
31-32		32-33		33-34	
89-52-35 270-08-25		90-02-29 269-58-01		90-08-44 269-51-49	
2354.57 2359.58		2419.71 2419.72		1880.11 1880.10	
726.880 726.822		737.530 737.532		573.068 573.056	
0-00-08 180-00-31	/ 19	0-00-03 180-00-19	/ 11	0-00-05 180-00-14	/ 9
192-22-41 12-23-01	/ 51	167-37-37 347-37-49	/ 42	193-59-32 13-59-24	/ 43
[illegible] 32		167-37-32		193-59-32	
0-00-04 180-00-25	/ 14	0-00-07 180-00-23	/ 15	0-00-10 180-00-26	/ 18
166-00-36 346-00-47	/ 41	171-36-11 351-36-28	/ 19	188-24-03 08-24-20	/ 11
166-00-27		171-36-04		168-23-53	

MASHPEE

59

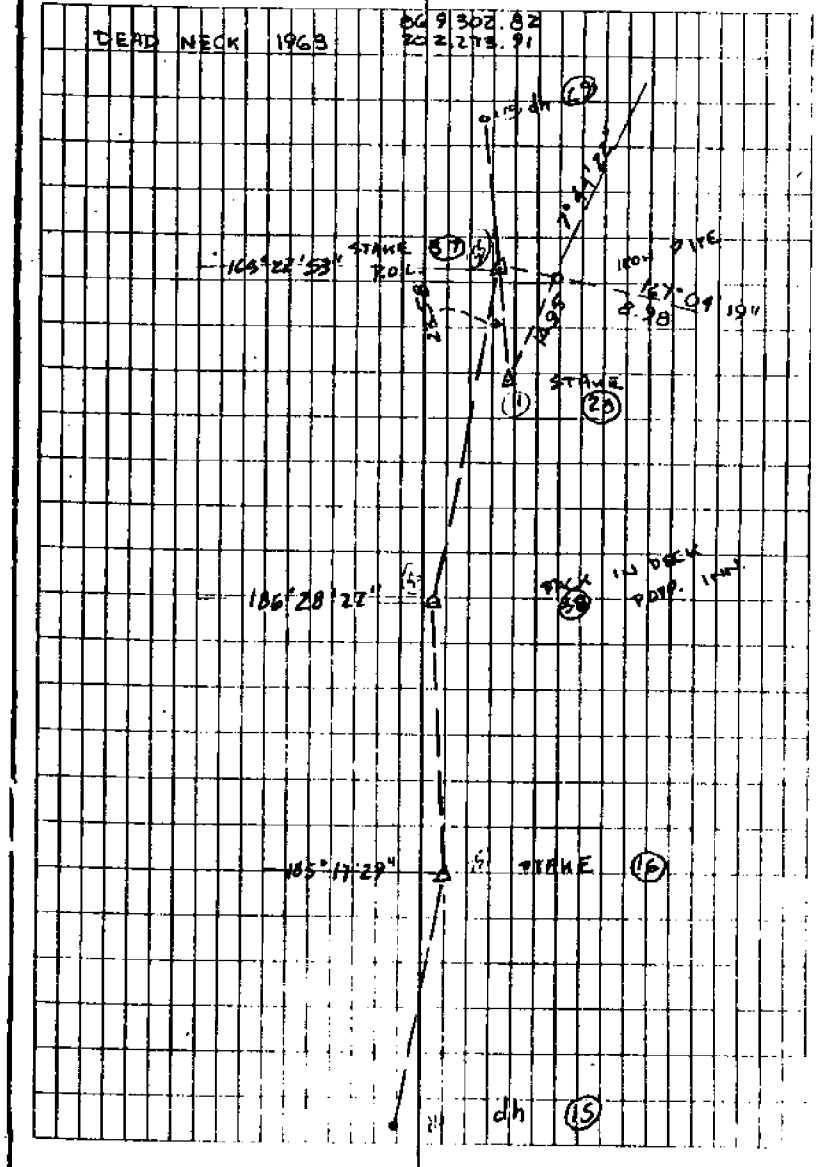

24-35 89-59-17 270-01-08 3401.79 3401.78 036.869 036.865		0-00-03 / 180-00-08 / 07-44-10 / 167-44-44	27		
P.P. 00-00-03 167-44-16		0-00-03 195-17-16		~~90-23-18~~	
00-00-03 180-00-21 167-04-21 347-12-03	12	00-00-03 180-00-21 194-37-17 14-43-29	12	57-38	832.72 273.06 ~~832.80~~
00-00-06 180-00-23 167-04-31 347-04-27 167-04 19.5	14.5 34	00-00-06 180-00-23 194-37-04 14-37-21 194-37 02	14.5 12.5	269-37-27 90-23-18	273.06 832.126
		00-00-03 165-22-22	00-00-02 180-00-16 165-22-47 345-23-10 165-22-~~37~~ 49.2 00-00-05 180-00-18 165-22-36 345-23-10 165-22-35	9 ~~58.5~~ 58.2 11.5 63	
		00-00-02 180-00-18 194-37-68 14-37-22 194-37 06	10 16	0-00-03 / 180-00-25 / 186-28-26 06-28-50 / 38 186-28-24	
0-00-07 180-00-20 / 13 173-31-44 / 54 353-32 04 173-31-41					

NAHUEE

60

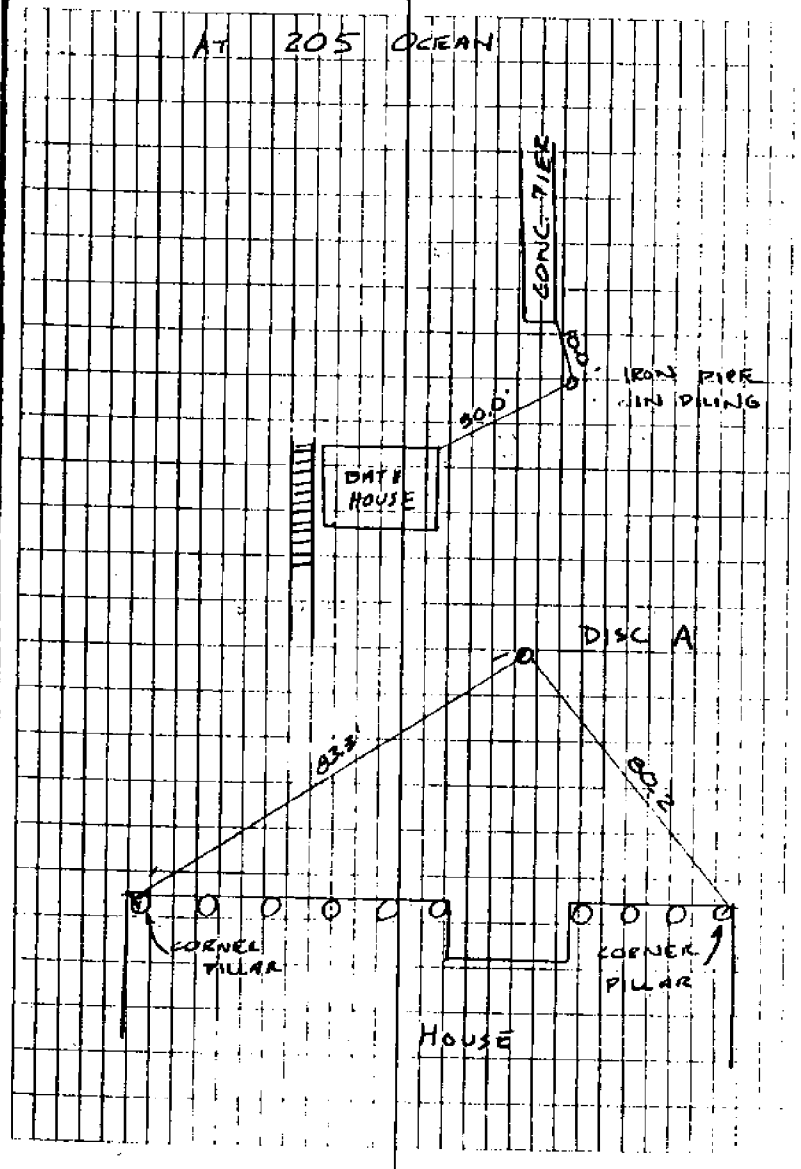

APPENDIX II

Empirical Eigenfunction Analysis

Empirical eigenfunction analysis is a statistical technique for efficiently representing the variability in an array of data. The method is useful for examining interrelationships within a data set, with the aim of finding natural groupings which can be related to some physical process. Eigenfunctions are extracted from the data by numerically solving sum of squares and cross product (SSCP) matrices. For more information on eigenfunction analysis (also called characteristic function analysis, or multivarient factor analysis) see Aubrey (1978), Davis (1976) or Joreskog, Klovan and Reyment (1976). In this section we present the results of eigenanalysis of grain size data, describing the analysis methods only as much as necessary to interpret the results. The data consisted of sediment samples from 45 offshore stations. Each sample was analyzed in an electronic settling tube to determine the weight percent of sediment in each of 10 size classes, spaced at $\frac{1}{2}$ phi (ϕ) intervals from -1.0 ϕ (2 mm) to 3.5 ϕ (0.088 mm). These weight percentages form the data matrix. The purpose of the eigenanalysis was to determine whether the variation in grain size distribution followed any discernable pattern across the platform.

The method produces three sets of functions: eigenvalues (λ), phi-dependent eigenfunctions ($C(\phi)$), and spatial eigenfunctions ($e(x)$). Eigenvalues are weighting functions indicating what portion of the total variation in the data set is attributable to that function. There are as many eigenvalues as the smaller dimension of the data matrix, in this case ten. The eigenvalues are listed in descending order in Table A1. As shown on that table, the first 3 eigenfunctions account for 94 percent of the variance in the data set. We will discuss only these three information-rich functions.

Phi-dependent eigenfunctions indicate how much variance in the data set is clustered around each phi size class. Most of the variation is centered around 1.5 ϕ; that is, 1.5 ϕ is the mean grain size for all samples (figure A1a). The first eigenfunction accounts for 74 percent of the total variation, so the 1.5 ϕ size class dominates the sample set.

The second eigenfunction (figure A1b), which accounts for 13 percent of the total variation, has two primary contributions: around 0.5 ϕ and 2.0 ϕ; the third accounts for 6.4 percent of the variation, mostly at 0.0 ϕ and 1.0 ϕ.

The spatial eigenfunctions (Table 2; figures A3, A4, A5) indicate the importance of each of the three most energetic phi-dependent eigenfunction curves (figure A1) on the total grain size distribution for that station. This effect is most easily demonstrated by comparing reconstructed grain size curves (from summing eigenfunctions) to the original data (figure A2). Comparisons are presented for 3 samples, where the reconstructed data ($h(x,\phi)$) is represented by

$$h(x,\phi) = \sum_{\ell=1}^{N} C_\ell(\phi)\, e_\ell(x)(\lambda_\ell N_x N_\phi)^{1/2}$$

where $C_\ell(\phi)$ = the ℓ^{th} phi-dependent eigenfunction

$e_\ell(x)$ = the ℓ^{th} spatial eigenfunction; in this case we compute the grain size distributions for x - stations 3, 13, 19.

λ_ℓ = the ℓ^{th} eigenvalue, used here with N_x and N_ϕ as scaling factors

N_x, N_ϕ = number of stations and grain size categories; in this case 47, 10.

TABLE A1

Eigenvalues of grain size distributions

Offshore samples: Popponesset Beach, MA

Eigenvalue	Percent of Total Sum of Squares
182.7	74.1%
33.4	13.6%
16.5	6.7%
7.5	3.0%
4.2	1.7%
1.4	.6%
.3	.1%
.2	.08%
.1	.06%
.095	.004%
Total 246.4	100 %

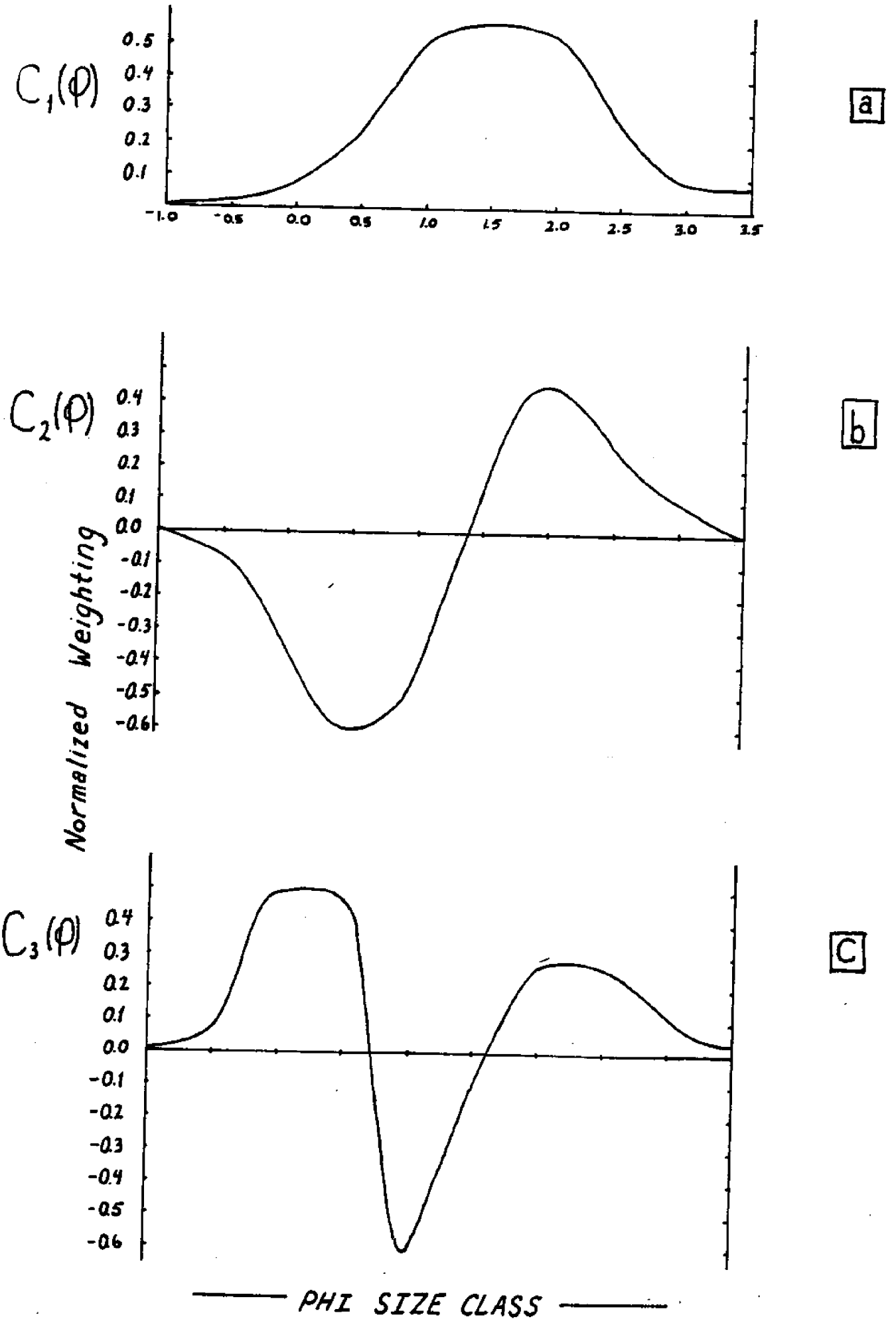

Figure A1. Three most energetic phi-dependent eigenvectors for Popponesset Beach offshore sand samples.

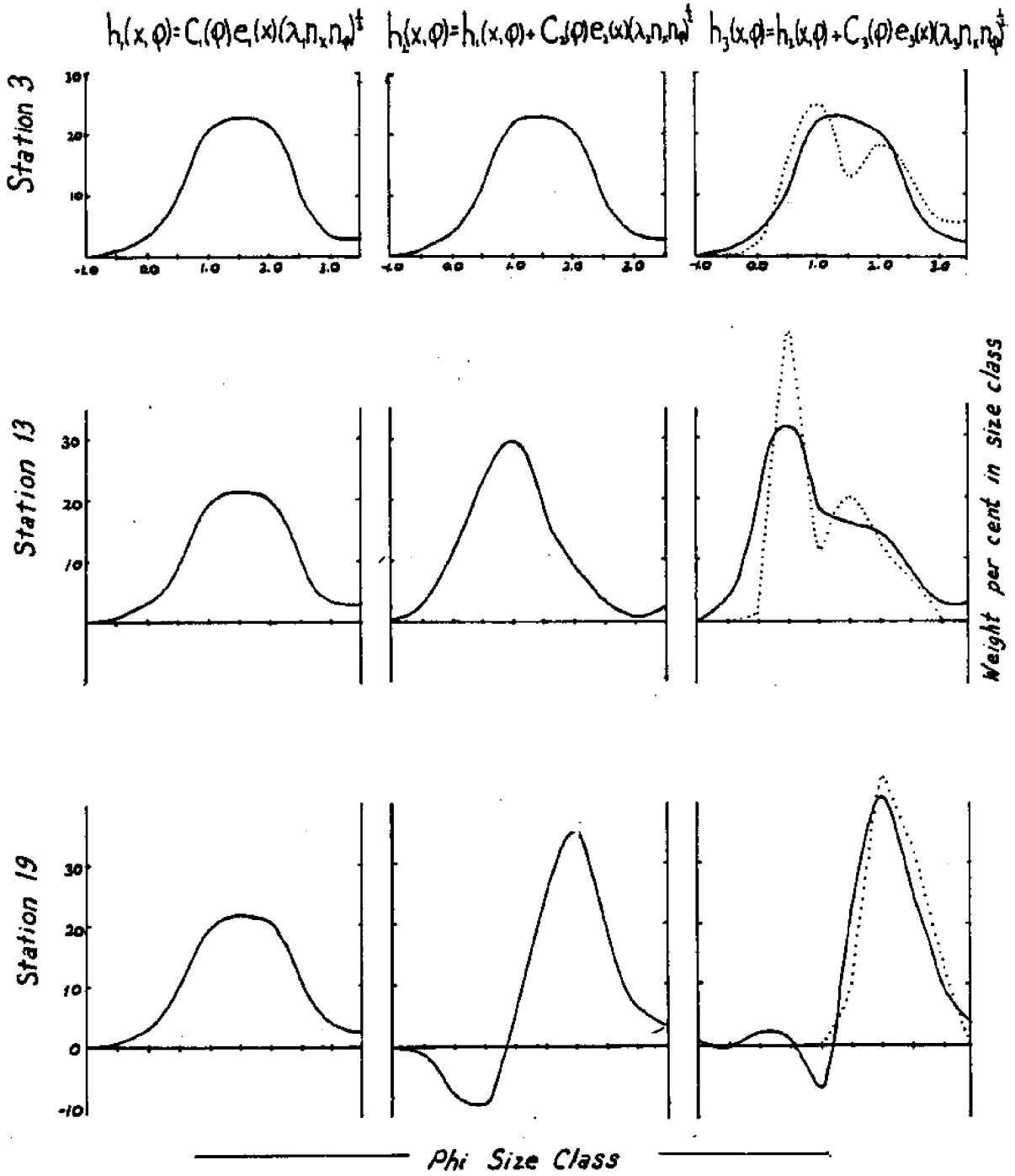

Figure A2. Reconstructions of grain size curves for three sample stations using results from eigenanalysis. Each station forms a row. Left-hand panels represent reconstruction using only the first eigenfunctions; middle panels use the first two eigenfunctions; and right-hand panels use the three most energetic eigenvectors. Right-hand panels also have plots of actual grain size distributions shown as dotted lines.

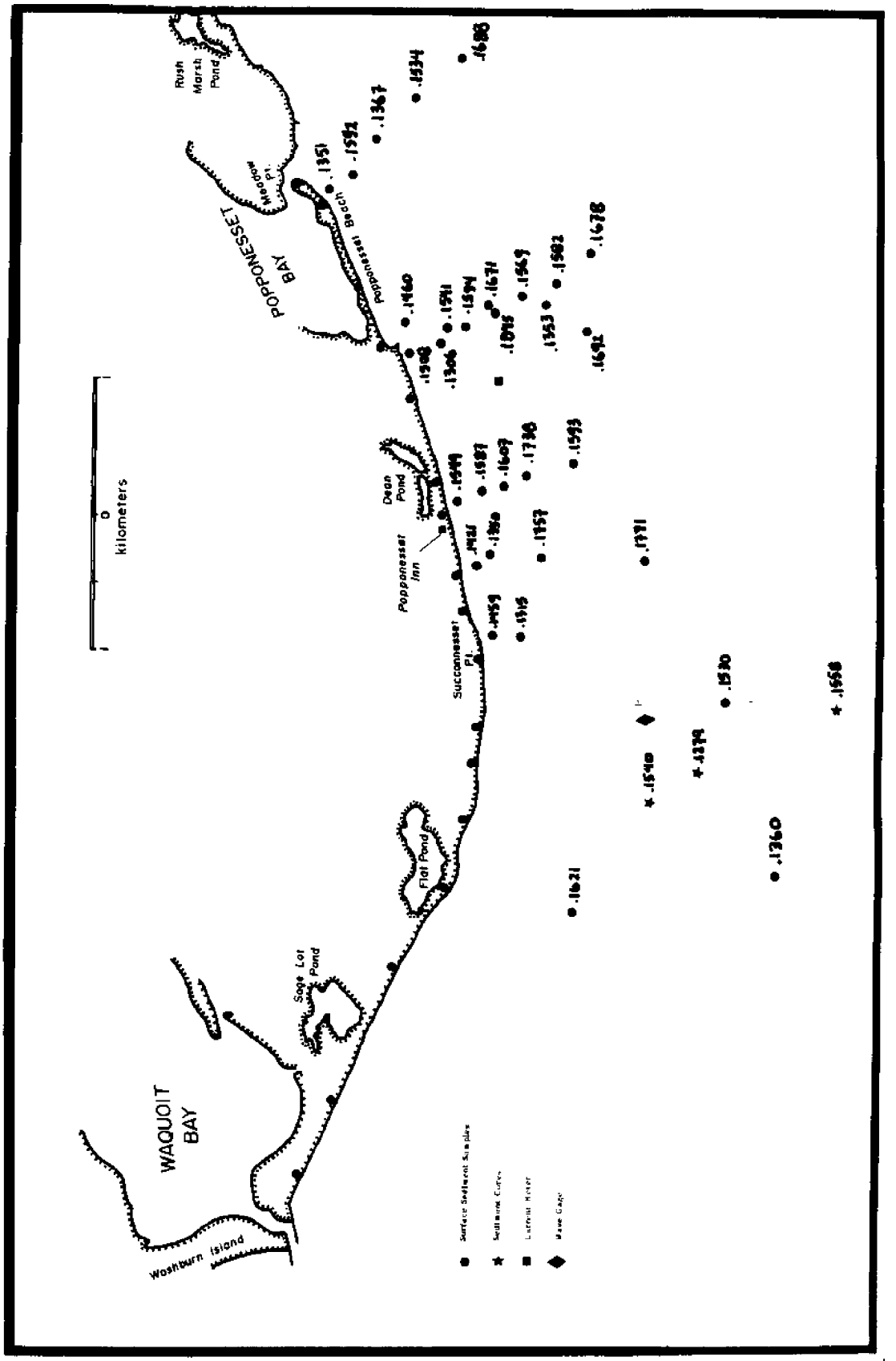

Figure A3. First spatial eigenfunction ($e_1(x)$) for Popponesset Beach

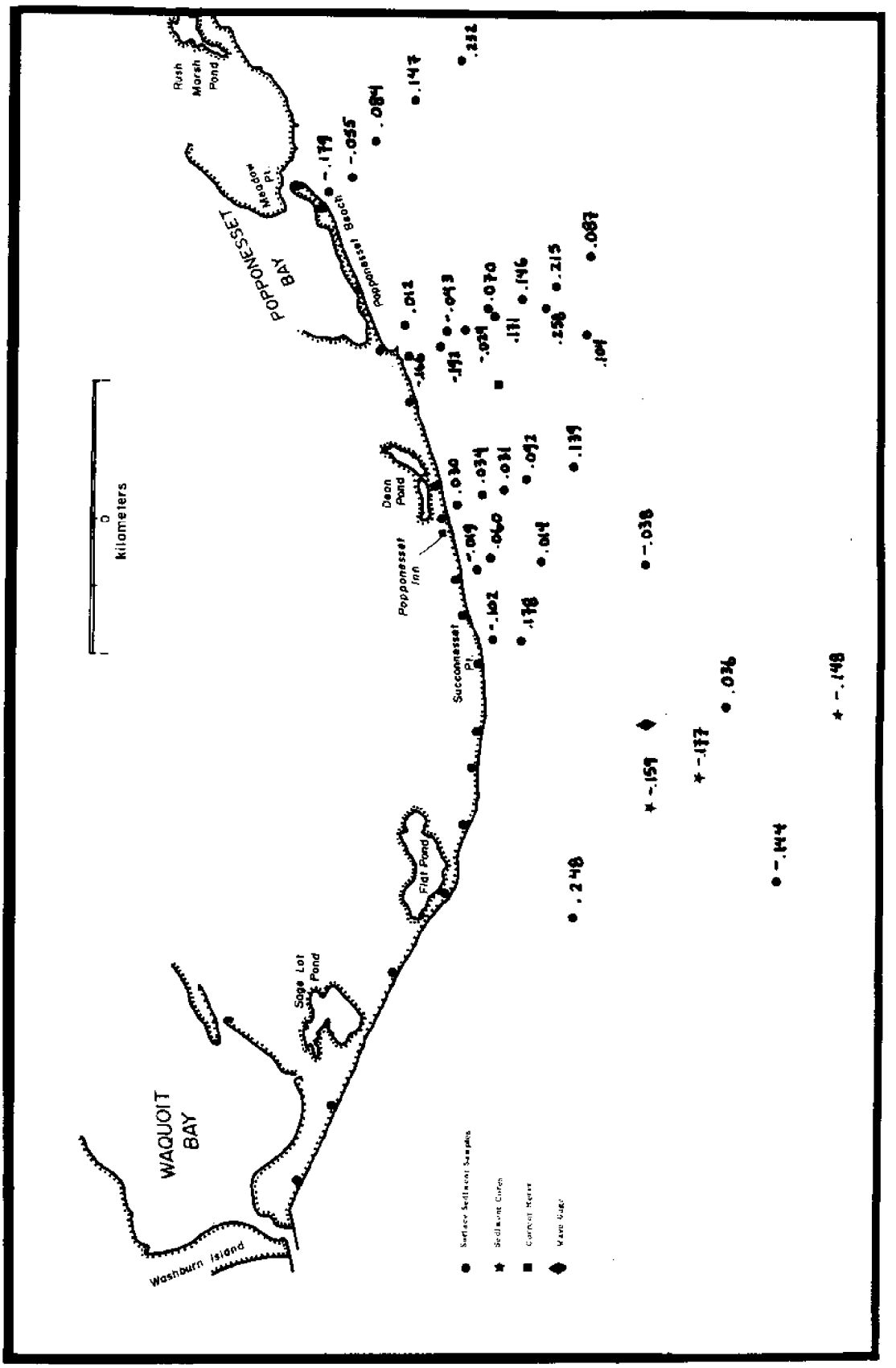

Figure A4. Second spatial eigenfunction ($e_2(x)$) for Popponesset Beach offshore sand samples.

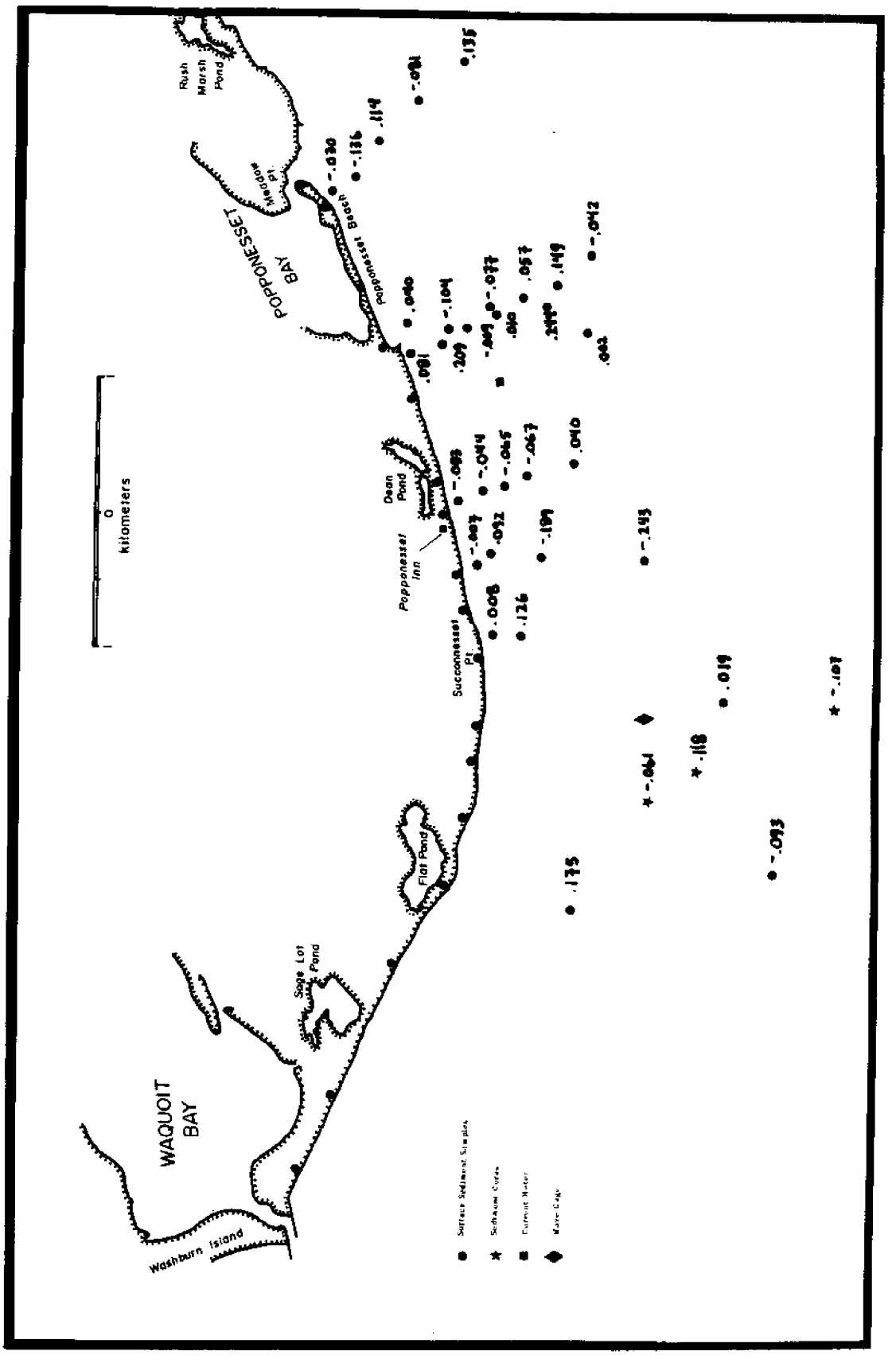

Figure A5. Third spatial eigenfunction ($e_3(x)$) for Popponesset Beach offshore sand samples.

The graphs in Figure A2 show the influence of a large $e_2(x)$, both positive (figure A2c) and negative (A2b) on the distribution curve. Figure A3a shows the effect of small second and third eigenfunction coefficients; that is, the grain size curve is primarily represented by the first eigenfunction. Comparisons of reconstructions based on three eigenfunctions with the original grain size data show how each additional eigenfunction brings the result closer to the actual values.

The first, second and third spatial eigenfunctions are plotted on Figures A3 through A5. If the values fall into natural groups, then grain size may be related to a physical process causing sorting of sand grains. Such groupings or trends are weak on the platform. The most dominant trend is a gradual offshore fining, as discussed previously. Lack of obvious alongshore trends implies either that alongshore sorting does not take place, or more local variations disguise larger scale trends. For instance, grain size variability across a single sand wave may exceed larger scale variability.

In summary, eigenanalysis provided an objective method of examining large scale trends in grain size variation. Other than a general fining offshore, no major trends are detectable.

REFERENCES

Aubrey, D.G., 1978. Statistical and Dynamical Prediction of Changes in Natural Sand Beaches. Ph.D. dissertation, University of California, San Diego, 194 pp.

Davis, R.E., 1976. Predictability of sea surface temperature and sea level pressure anomalies over the North Pacific Ocean. Journal of Physical Oceanography, v. 6, no. 3, p. 249-266.

Joreskog, K.G., J.E. Klovan, and R.A. Reyment, 1976. Geological Factor Analysis. Elsevier: Amsterdam, 178 pp.

APPENDIX III

Analysis of the 21-day wave/tide record, measured in the channel with a Sea Data 635-12. Values are recorded at 4 hour intervals for the following parameters:

Peak = peak wave frequency (sec^{-1})

Period = peak wave period = $\frac{1}{\text{peak wave frequency}}$

E_T = total energy variance in wave (cm^2)
This parameter is proportional to the amount of energy in the wave.

E_p = energy in peak frequency variance (cm^2)

α_o = direction of wave propagation, measured in degrees clockwise from true north.

$P(\alpha_o)$ = angular spread of direction of propagation of the wave field.

$H_{1/3}$ = significant wave height (m)
This parameter is derived directly from E_T

$\bar{h}$ = mean water depth (m).

U, V = components of current velocity (m/sec); U is positive to the north, V is positive to the east.

V ,θ = wind velocity and direction measured at Otis Air Force Base, Cape Cod, MA (knots, degrees from true north). These measurements were used to calculate the wind stress values referred to in the text.

Dashes in the wave data indicates absence of significant wave peaks at periods greater than 3 seconds.

RUN	PEAK	PERIOD (sec)	BW (Hz)	E_T (cm^2)	E_p (cm^2)	a_0	$P(a_0)$%
2Nov82-04	—	—	—	13(36)	—	—	—
-05	0.3203	3.1		26(35)	6	13	33
-06	—	—		6(20)	—	—	—
3Nov82-01	—	—		8(23)	—	—	—
-02	—	—		7(12)	—	—	—
-03	—	—		4(24)	—	—	—
-04	—	—		7(25)	—	—	—
-05	—	—		—(19)	—	—	—
-06	0.3047	3.3		52(63)	7	315	42
4Nov82-01	>0.33	<3.0		47(51)	10	356	33
-02	—	—		9(20)	—	—	—
-03	—	—		—(75)	—	—	—
-04	0.2891	3.5		180(190)	26	347	32
	0.2561	3.9			26	334	39
-05	0.2813	3.6		136(158)	20	335	42
-06	0.2734	3.7		248(224)		330	43
	0.2891	3.5				352	42
5Nov82-01	0.2813	3.6		245(256)	28	332	52
-02	0.2500	4.0		339(335)	41	328	42
-03	0.2500	4.0		342(302)	35	323	39

RUN	PEAK	PERIOD (sec)	BW (Hz)	E_T (cm^2)	E_p (cm^2)	a_0	$P(a_0)$%
5Nov82-04	0.2422	4.1		84 (95)	6	301	43
	0.3203	3.1			6	344	48
-05	0.2344	4.3		110 (154)	13	47	33
-06	0.3125	3.2		28 (38)	3	58	29
6Nov82-01	—	—		8 (18)	—	—	—
-02	0.3047	3.3		19 (43)	3	43	50
-03	—	—		11 (19)	—	—	—
-04	—	—		8 (19)	—	—	—
-05	0.2891	3.5		26 (58)	4	48	43
-06	—	—		5 (9)	—	—	—
7Nov82-01	—	—		2 (5)	—	—	—
-02	—	—		4 (17)	—	—	—
-03	0.3047	3.3		23 (38)	3	71	43
-04	—	—		5 (18)	—	—	—
-05	—	—		- (2)	—	—	—
-06	0.3125	3.2		15 (27)	2	61	44
8Nov82-01	0.3125	3.2		26 (41)	3	49	37
-02	0.3203	3.1		43 (54)	7	44	24
-03	0.3203	3.1		91 (112)	10	50	27

RUN	PEAK	PERIOD (sec)	BW (Hz)	E_T (cm^2)	E_p (cm^2)	a_0	$P(a_0)$%
2NOV82-04	0.3203	3.1		85 (95)	13	45	32
-05	0.2891	3.5		158 (161)	17	31	52
-06	0.2734	3.7		83 (114)	8	41	33
9NOV82-01	—	—		8 (21)	—	—	—
-02	—	—		4 (8)	—	—	—
-03	—	—		4 (21)	—	—	—
-04	—	—		4 (13)	—	—	—
-05	—	—		3 (10)	—	—	—
-06	—	—		2 (20)	—	—	—
10NOV82-01	—	—		3 (9)	—	—	—
-02	—	—		1 (11)	—	—	—
-03	—	—		2 (20)	—	—	—
-04	—	—		4 (7)	—	—	—
-05	—	—		1 (13)	—	—	—
-06	—	—		5 (24)	—	—	—
11NOV82-01	—	—		2 (6)	—	—	—
-02	—	—		1 (13)	—	—	—
-03	—	—		3 (17)	—	—	—
-04	0.3203	3.1		93 (100)	17	10	41

RUN	PEAK	PERIOD (sec)	BW (Hz)	E_T (cm^2)	E_p (cm^2)	a_0	$P(a_0)$%
11Nov82-05	0.3047	3.3		104 (98)	15	33	52
-06	0.3125	3.2		81 (87)	13	341	34
12Nov82-01	0.3203	3.1		29 (35)	6	327	44
-02	0.3281	3.0		86 (74)	23	25	39
-03	0.2969	3.4		240 (255)	29	25	36
-04	0.2422	4.1		336 (332)	44	6	32
-05	0.2500	4.0		340 (305)	43	346	31
-06	0.2656	3.8		427 (415)	66	334	30
13Nov82-01				—			
-02	0.2344	4.3		636 (599)	99	0	39
-03	0.2188	4.6		530 (493)	69	330	33
-04	—	—		12 (33)	—	—	—
-05	—	—		8 (21)	—	—	—
-06	—	—		4 (11)	—	—	—
14Nov82-01	—	—		4 (21)	—	—	—
-02	—	—		4 (16)	—	—	—
-03	—	—		4 (13)	—	—	—
-04	—	—		11 (31)	—	—	—
-05	—	—		11 (18)	—	—	—

RUN	PEAK	PERIOD (sec)	BW (Hz)	E_T (cm^2)	E_p (cm^2)	a_0	$P(a_0)$%
14 Nov 82-06	0.3203	3.1		65 (75)	13	305	44
15 Nov 82-01	0.2734	3.7		161 (165)	21	338	49
-02	0.2422	4.1		390 (378)	76	304	34
-03	0.2344	4.3		29 (47)	2	312	55
-04	—	—	BROAD	16 (39)	—	—	—
-05	—	—		5 (10)	—	—	—
-06	—	—		6 (18)	—	—	—
16 Nov 82-01	—	—	BROAD	22 (42)	—	—	—
-02	0.3203	3.1		17 (23)	2	54	42
-03	—	—		3 (20)	—	—	—
-04	—	—		6 (23)	—	—	—
-05	—	—		3 (8)	—	—	—
-06	—	—		1 (15)	—	—	—
17 Nov 82-01	—	—		8 (15)	—	—	—
-02	—	—		19 (26)	—	—	—
-03	—	—		9 (24)	—	—	—
-04	—	—		7 (20)	—	—	—
-05	—	—		2 (11)	—	—	—
-06	—	—		2 (18)	—	—	—

RUN	PEAK	PERIOD (sec)	BW (Hz)	E_T (cm^2)	E_p (cm^2)	α_0	$P(\alpha_0)$%
18NOV82-01	—	—		3(8)	—	—	—
-02	—	—		1(12)	—	—	—
-03	—	—		—	—	—	—
-04	—	—	BROAD	20(28)	—	—	—
-05	—	—	BROAD	14(26)	—	—	—
-06	0.2969	3.4		23(43)	2	271	33
19NOV82-01	0.3125	3.2	BROAD	64(75)	6	263	42
-02	0.2969	3.4		47(65)	5	295	38
-03	0.2969	3.4		49(65)	5	279	37
-04	0.2969	3.4		103(120)	10	271	26
-05	0.2969	3.4		115(116)	13	288	49
-06	0.2578	3.9		88(108)	7	279	37
	0.2891	3.5			7	283	45
20NOV82-01	—	—	BROAD	45(59)	—	—	—
-02	0.2734	3.7		180(178)	20	286	35
-03	0.2734	3.7		106(127)	10	275	27
-04	0.2734	3.7	BROAD	65(8)	6	290	35
-05	—	—	BROAD	53(64)	—	—	—
-06	—	—	BROAD	28(39)	—	—	—

RUN	PEAK	PERIOD (sec)	BW (Hz)	E_T (cm^2)	E_p (cm^2)	α_0	$P(\alpha_0)$%
21Nov82-01	—	—		28(43)	—	—	—
-02	—	—		20 (36)	—	—	—
-03	—	—		23(28)	—	—	—
-04	—	—		10(24)	—	—	—
-05	—	—		21(37)	—	—	—
-06	—	—		16 (26)	—	—	—
22Nov82-01	—	—		8(19)	—	—	—
-02	—	—		21(31)	—	—	—
-03	—	—		20(29)	—	—	—
-04	—	—		9(21)	—	—	—
-05	—	—		20(32)	—	—	—
-06	—	—		17(23)	—	—	—
23Nov82-01	—	—		8(18)	—	—	—
-02	—	—		20(31)	—	—	—
-03	—	—		19(26)	—	—	—
-04	—	—		13(28)	—	—	—
-05	—	—		—(23)	—	—	—

DATE	RUN No.	E_T (cm²)	$\overline{h}$ (m)	$\overline{U}$ (m/sec)	$\overline{V}$ (m/sec)	$H_{1/3}$ (m)	OTIS U_w (Knots)	OTIS TN θ_w
2Nov82	04	13	6.99	-0.53	-0.46	0.14	10	210
	05	26	6.13	-0.19	-0.16	0.20	8	220
	06	6	6.42	0.38	0.28	0.10	10	240
3Nov82	01	8	6.84	-0.44	-0.39	0.11	6	240
	02	7	6.33	-0.24	-0.19	0.11	11	240
	03	4	6.69	0.42	0.30	0.08	5	220
	04	7	7.14	-0.44	-0.37	0.11	9	190
	05	19	6.39	-0.41	-0.34	0.17	8	170
	06	52	6.32	0.45	0.33	0.29	11	180
4Nov82	01	47	6.78	-0.20	-0.17	0.27	11	220
	02	9	6.47	-0.41	-0.35	0.12	5	220
	03	75	—	0.39	0.26	0.35	7	190
	04	180	7.07	-0.19	-0.15	0.54	12	180
	05	136	6.60	-0.51	-0.42	0.47	10	190
	06	248	6.11	0.44	0.34	0.63	14	180
5Nov82	01	245	6.62	0.10	0.10	0.63	16	230
	02	339	6.62	-0.48	-0.41	0.74	20	230
	03	342	6.32	0.41	0.32	0.74	12G17	190
	04	84	6.88	0.12	0.11	0.37	14	230
	05	110	6.71	-0.51	-0.45	0.42	14	270
	06	28	5.78	0.30	0.25	0.21	10	300
6Nov82	01	8	6.32	0.27	0.21	0.11	8	310
	02	19	6.58	-0.49	-0.43	0.17	6	310
	03	11	6.08	0.21	0.17	0.13	10	310
	04	8	6.64	0.28	0.21	0.11	14	270
	05	26	6.87	-0.54	-0.45	0.20	10	270
	06	5	5.91	-0.03	-0.04	0.09	4	330
7Nov82	01	2	6.27	0.34	0.24	0.06	5	290
	02	4	6.71	-0.39	-0.34	0.08	5	300
	03	23	6.18	-0.11	-0.11	0.19	8	290
	04	5	6.49	0.35	0.25	0.09	16	290
	05	2	—	-0.38	-0.33	0.06	8	300
	06	15	6.14	-0.28	-0.24	0.15	8	270

DATE	RUN No.	cm^2 E_T	m $\overline{h}$	m/sec $\overline{U}$	m/sec $\overline{V}$	m $H_{1/3}$	OTIS (knots) W_w	TN θ_w
8NOV82	01	26	6.15	0.39	0.29	0.20	10	250
	02	43	6.65	-0.08	-0.05	0.26	10	260
	03	91	6.32	-0.25	-0.22	0.30	10	260
	04	85	6.23	0.38	0.27	0.37	14G24	250
	05	158	6.77	-0.02	0.01	0.50	15G20	250
	06	83	6.34	-0.39	-0.34	0.36	9	260
9NOV82	01	8	5.94	0.35	0.26	0.11	7	300
	02	4	6.47	0.06	0.05	0.08	5	300
	03	4	6.53	-0.45	-0.40	0.08	12	310
	04	4	6.21	0.24	0.20	0.08	9	290
	05	3	6.78	0.13	0.10	0.07	7	310
	06	2	6.75	-0.50	-0.43	0.06	8	340
10NOV82	01	3	6.03	0.17	0.15	0.07	9	310
	02	1	6.54	0.26	0.19	0.04	10	310
	03	2	6.80	-0.45	-0.39	0.06	7	310
	04	4	6.19	-0.02	-0.02	0.08	7	350
	05	1	6.61	0.26	0.19	0.04	6	020
	06	5	6.86	-0.46	-0.39	0.09	0	0
11NOV82	01	2	6.20	-0.13	-0.12	0.06	0	0
	02	1	6.51	0.31	0.23	0.04	0	0
	03	3	6.96	-0.38	-0.34	0.07	0	0
	04	93	6.33	-0.24	-0.21	0.39	13	200
	05	104	6.47	0.36	0.29	0.41	13	200
	06	81	6.82	-0.30	-0.27	0.36	8	190
12NOV82	01	29	6.34	-0.29	-0.26	0.22	12	210
	02	86	6.35	0.36	0.29	0.37	13G20	220
	03	240	6.85	-0.09	-0.06	0.62	14G21	220
	04	336	6.43	-0.31	-0.27	0.73	19G25	220
	05	340	6.23	0.42	0.33	0.74	16G23	220
	06	427	6.71	-0.01	0	0.83	16G23	230
13NOV82	01	—	—	-0.37	-0.31		16G24	210
	02	636	6.30	0.46	0.38	1.01	16G27	210
	03	530	6.87	0.12	0.12	0.92	19G28	190

DATE	RUN NO.	E_T (cm²)	$\overline{h}$ (m)	$\overline{U}$ (m/sec)	$\overline{V}$ (m/sec)	$H_{1/3}$ (m)	OTIS U_W (Knots)	OTIS θ_W TN
13Nov82	04	12	6.46	-0.55	-0.49	0.14	12	310
	05	8	5.99	0.33	0.25	0.11	12	330
	06	4	6.49	0.17	0.13	0.08	5	330
14Nov82	01	4	6.49	-0.50	-0.44	0.08	8	320
	02	4	6.22	0.33	0.26	0.08	8	320
	03	4	6.87	0.19	0.16	0.08	10	330
	04	11	6.84	-0.57	-0.49	0.13	7	030
	05	11	6.23	0.14	0.13	0.13	5	080
	06	65	6.63	0.24	0.22	0.32	5	140
15Nov82	01	161	6.84	-0.50	-0.44	0.51	10	140
	02	390	6.44	0	0	0.79	12	160
	03	29	6.81	0.26	0.23	0.22	7	280
	04	16	6.81	-0.54	-0.49	0.16	12	320
	05	5	6.07	0	0	0.09	4	290
	06	6	6.21	0.27	0.26	0.10	12	310
16Nov82	01	22	6.60	-0.35	-0.34	0.19	15	310
	02	17	6.16	-0.05	-0.07	0.16	5	330
	03	3	6.61	0.32	0.29	0.07	10	310
	04	6	6.85	-0.39	-0.38	0.10	4	300
	05	3	6.13	-0.17	-0.18	0.07	2	190
	06	1	6.29	0.30	0.27	0.04	0	0
17Nov82	01	8	6.65	-0.26	-0.28	0.11	3	220
	02	19	6.40	-0.22	-0.23	0.17	5	220
	03	9	6.62	0.30	0.28	0.12	4	250
	04	7	6.97	-0.31	-0.33	0.11	10	260
	05	2	6.45	-0.28	-0.28	0.06	6	240
	06	2	6.31	+0.32	0.27	0.06	0	0
18Nov82	01	3	6.66	-0.11	-0.11	0.07	0	0
	02	1	6.52	-0.33	-0.32	0.04	5	080
	03	—	—	0.27	0.25	—	5	050
	04	20	6.92	-0.17	-0.18	0.18	9	080
	05	14	6.60	-0.38	-0.39	0.15	8	030

DATE	RUN No	cm^2 E_T	m $\bar{h}$	m/sec $\bar{U}$	m/sec $\bar{V}$	m $H_{1/3}$	knots U_W	OTS / TN θ_W
19Nov82	01	64	6.57	0.03	0.03	0.32	12G19	050
	02	47	6.64	-0.34	-0.34	0.27	7	060
	03	49	6.55	0.20	0.19	0.28	12G18	070
	04	103	6.98	-0.05	-0.06	0.41	12G18	070
	05	115	6.87	-0.41	-0.44	0.43	13	070
	06	88	6.36	0.18	0.18	0.38	8	070
20Nov82	01	45	6.65	0.11	0.11	0.27	11	070
	02	180	6.81	-0.31	-0.33	0.54	12	080
	03	106	6.52	0.12	0.14	0.41	9	090
	04	65	6.81	0.09	0.09	0.32	10	070
	05	53	6.85	-0.36	-0.40	0.29	9	090
	06	28	6.22	0.07	0.08	0.21	6	010
21Nov82	01	28	6.44	0.19	0.18	0.21	0	0
	02	20	6.69	-0.28	-0.31	0.18	0	0
	03	23	6.36	0.01	0.02	0.19	8	110
	04	10	6.57	0.18	0.17	0.13	9	170
	05	21	6.81	-0.37	-0.37	0.18	5	180
	06	18	6.19	-0.10	-0.11	0.17	0	0
22Nov82	01	8	6.31	0.22	0.20	0.11	5	190
	02	21	6.67	-0.22	-0.24	0.18	5	210
	03	20	6.40	-0.11	-0.11	0.18	3	090
	04	9	6.47	0.21	0.18	0.12	7	080
	05	20	6.82	-0.26	-0.28	0.18	7	060
	06	17	6.33	-0.19	-0.19	0.16	7	060
23Nov82	01	8	6.29	0.26	0.22	0.11	5	030
	02	20	6.69	-0.11	-0.13	0.18	7	030
	03	19	6.56	-0.24	-0.24	0.17	10	030
	04	13	6.51	0.23	0.20	0.14	16	030
	05	23	—	-0.11	-0.14	0.19	12	010
	06	—						
MEAN		61	6.51m	-0.048	-0.055	0.24		
S.D.		109	0.28	0.31	0.27	0.21		

TD ≡ 2G m

APPENDIX IV

Sample Calculation of Sediment Transport using Method Outlined in Discussion Section C-2.

Given a velocity measurement U = 34 cm/sec the Law of the Wall defines the velocity profile

$$\frac{U}{U_*} = \frac{1}{\kappa} \ln \frac{z}{z_0} \qquad \text{A4-1}$$

where U_* = shear velocity = $(\frac{\tau_0}{\rho})^{1/2}$

τ_0 = total boundary shear stress

ρ = density of water ~1.0 gm/cm^3

κ = von Karman's constant = 0.4

z = height of velocity measurement above boundary = 148 cm

z_0 = bottom roughness felt by flow.

The two unknowns at this point are U_* and z_0. We take the ripple height h and length L to be defined by the median grain size D = 0.035 cm, so that L = 1000 D = 35 cm and h = 0.1L = 3.5 cm. We insert these values into the equivalent sand grain roughness formula

$$k_b \sim 30\ h\ (\frac{h}{L}) = 10.5 \text{ cm} \qquad \text{A4-2}$$

If we assume rough turbulent flow we obtain a roughness, based on Nikuradse's work,

$$z_0 = \frac{ks}{30} = 0.35 \qquad \text{A4-3}$$

The Law of the Wall then produces a shear velocity

$$U_* = 2.25 \text{ cm/sec.} \qquad \text{A4-4}$$

Drag partitioning gives us a typical ratio of skin friction/total boundary shear stress of 0.6. Since $U_* \sim \sqrt{\tau_o}$, we multiply: $\sqrt{0.6}\, U_{*tot} = U_{*skin} =$ 1.74 cm/sec. Now we determine if this is greater than the critical boundary shear stress, using Shields Parameter ψ, where

$$\psi = \frac{\tau_o}{(S-1)\rho g D} = 5.3 \times 10^{-2} \qquad \text{A4-5}$$

where $S-1 = 1.65$ = relative density of quartz particles

$g = 980$ cm/sec^2 = gravitational acceleration

ψ_{crit} is determined from the Shields Diagram (figure A6), as a function of

$$S_* = \frac{D}{4\nu}\sqrt{(S-1)gD} = 6.58$$

As shown on Figure A6, this yields a critical Shields Parameter of

$$\psi_{crit} = 3.5 \times 10^{-2} \qquad \text{A4-6}$$

Since we have exceeded the critical Shields Parameter, we calculate a transport rate q_{SB} using the Meyer-Peter and Muller bedload formula:

$$q_{SB} = 12(D\sqrt{(S-1)\, gD})\, (\psi - \psi_{crit})^{3/2} = 7.63 \times 10^{-3}\ \text{cm}^3/\text{sec}$$

Sums of numbers of this magnitude yield the estimates listed in the transport section.

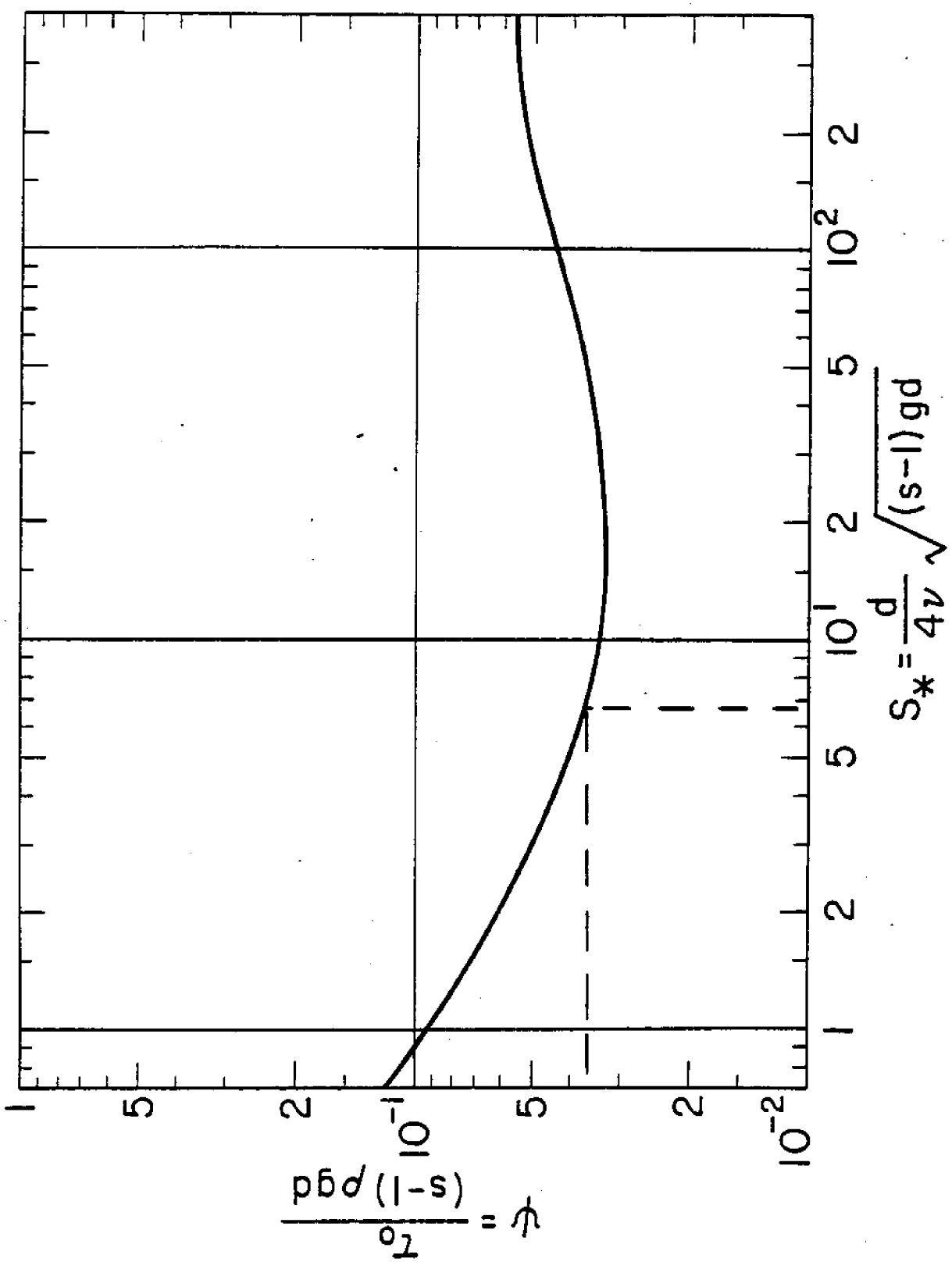

Figure A6. Modified Shields Diagram for the initiation of motion for cohesionless sediments (from Madsen and Grant, 1976).

50272-101

REPORT DOCUMENTATION PAGE	1. REPORT NO. WHOI-83-26	2.	3. Recipient's Accession No.

4. Title and Subtitle

Coastal Sediment Transport
Popponesset Beach, MA

5. Report Date
Ausut 1983

6.

7. Author(s)
David G. Aubrey and Margaret R. Goud

8. Performing Organization Rept. No.

9. Performing Organization Name and Address

Woods Hole Oceanographic Institution

10. Project/Task/Work Unit No.

11. Contract(C) or Grant(G) No.
(C)
(G)

12. Sponsoring Organization Name and Address

Alcoa Foundation

13. Type of Report & Period Covered
Technical

14.

15. Supplementary Notes

This report should be cited as: Woods Hole Oceanog. Inst. Tech. Rept. WHOI-83-26.

16. Abstract (Limit: 200 words)

Pathways and rates of near-bed sediment transport near Popponesset Beach, MA, were calculated using several distinct techniques. For the nearshore platform, sand transport in the form of sand waves was determined from vertical aerial photography spanning periods of four decades. In addition, calculations based on theoretical and empirical equations for near-bed sediment transport were made using field measurements of wind waves and tidal currents. Net sediment transport to the southwest inferred from these two techniques differed by about a factor of five. The higher net transport rate predicted in the aerial photographic method is a result of lack of wave measurements during storm conditions. Storm waves increase the net transport through a local increase in bed shear stress. Net transport to the southwest across the platform is between 700 and 3300 m^3/yr.

Littoral sand transport along Popponesset Beach was calculated from one month of directional wave measurements, extrapolated to a yearly value using long-term meteorological observations. Littoral transport from these calculations is 10,000 m^3/yr to the northeast, opposite the sense of alongshore transport in the shallow nearshore.

Patterns of shoreline change are discussed from a historical perspective, and using the transport calculations discussed above. Several management alternatives for coping with predicted shoreline change are presented for consideration by the Town of Mashpee.

17. Document Analysis a. Descriptors

1. Sediment Transport
2. Bedforms
3. Waves
4. Tides

b. Identifiers/Open-Ended Terms

c. COSATI Field/Group

18. Availability Statement	19. Security Class (This Report) Unclassified	21. No. of Pages 132
	20. Security Class (This Page)	22. Price

May 1982

DISTRIBUTION FOR SEA GRANT REPORTS

No. of Copies	Address
3	National Sea Grant Depository Pell Marine Science Library University of Rhode Island Kingston, RI 02881
5	Communications Specialist NOAA, Office of Sea Grant 6010 Executive Blvd. Rockville, MD 20852
25	NOAA Environmental Data & Info. Serv., ESIC D812 11400 Rockville Pike Rockville, MD 20852
1	Sea Grant Today Editor, Food Science and Technology VPI & SU Blacksburg, VA 24061